INVESTIGATION OF RESISTANCE MECHANISMS IN RESPONSE TO PIK3CA INHIBITION IN BREAST CANCER

A THESIS SUBMITTED TO

THE GRADUATE SCHOOL OF ENGINEERING AND SCIENCE

OF BILKENT UNIVERSITY

IN PARTIAL FULFILLMENT OF THE REQUIREMENTS FOR

THE DEGREE OF

MASTER OF SCIENCE

IN

MOLECULAR BIOLOGY AND GENETICS

By

İbrahim Oğuzhan Tarman

December 2020

INVESTIGATION OF RESISTANCE MECHANISMS IN RESPONSE TO PIK3CA INHIBITION IN BREAST CANCER

By İbrahim Oğuzhan Tarman

December 2020

We certify that we have read this dissertation and that in our opinion it is fully adequate in scope and in quality, as a thesis for the degree of Master of Science.

Onur Çizmecioğlu
(Advisor)

Özgür Şahin
(Co-advisor)

Serkan İsmail Göktuna

Ayşe Elif Erson Bensan

Approved for Graduate School of Engineering and Science

Ezhan Karaşan
Director of the Graduate School of Engineering and Science

ABSTRACT

INVESTIGATION OF RESISTANCE MECHANISMS IN RESPONSE TO PIK3CA INHIBITION IN BREAST CANCER

İbrahim Oğuzhan Tarman
M.S. in Molecular Biology and Genetics
Advisor: Onur Çizmecioğlu
Co-advisor: Özgür Şahin

December 2020

Breast cancer is the most frequently diagnosed cancer type, accounting for 25% of total cancer cases. PI3K pathway is the most deregulated pathway in breast cancer. Therefore, many inhibitors have been developed for druggable pathway constituents. PIK3CA, which codes for p110α catalytic domain of PI3K, is often found to be mutated in breast cancer patients, resulting in overactivation of PI3K signaling. Recent FDA approval of Alpelisib (BYL719), a p110α-specific small molecule inhibitor, has proven to be effective in hormone receptor positive advanced or metastatic breast cancer patients with activating PIK3CA mutations. Despite its superior efficacy compared to pan-PI3K inhibitors, therapy resistance is still the major problem. AKT has been viewed as the main kinase that relays oncogenic PI3K signal further downstream. Recent studies have revealed readily known kinases that function independent of AKT to be involved in PIK3CA resistance in a PI3K-dependent manner. In this study, we aimed to identify novel molecular targets within the PI3K pathway, but signal in an AKT-independent manner that can confer resistance to PIK3CA inhibition. Our bioinformatical analyses identified STK10 as a potential

candidate. STK10 knockdown was able to sensitize breast cancer cells to BYL-719 and induce cell growth in untransformed cell. Moreover, we developed BYL-719 resistant Luminal A subtype breast cancer cell lines to further study additional mechanisms of resistance. Our resistant cell line models had sustained AKT, S6 and 4EBP1 phosphorylation compared to wild-type counterparts under BYL-719 inhibition. Future transcriptomic and proteomic analyses to be performed on these cell lines will provide new insights on BYL-719 resistance mechanisms and help identify novel molecular targets for new therapeutic approaches in combatting BYL-719 resistance in patients.

Keywords: Breast cancer, PIK3CA, alpelisib, BYL-719, drug resistance

ÖZET

MEME KANSERİNDE PIK3CA İNHİBİSYONUNA KARŞI DİRENÇ MEKANİZMALARININ İNCELENMESİ

İbrahim Oğuzhan Tarman
Moleküler Biyoloji ve Genetik, Yüksek Lisans
Tez Danışmanı: Onur Çizmecioğlu
İkinci Tez Danışmanı: Özgür Şahin

Aralık 2020

Meme kanseri en çok tanı koyulan kanser türüdür ve toplam tanıların %25'ini oluşturmaktadır. PI3K yolağı meme kanserinde en çok değişime uğrayan yolaktır. Bu nedenle, PI3K yolağının hedeflenebilir üyelerine karşı pek çok inhibitor geliştirilmiştir. p110α katalitik alt birimini kodlayan PIK3CA geni meme kanseri hastalarında yüksek sıklıkla mutasyona uğrar, bu da yüksek PI3K yolak etkinliğine neden olur. Amerikan FDA kuruluşunun PIK3CA mutasyonu olan ileri düzey veya metastatik hormon reseptörü pozitif meme kanseri hastalarında kullanımına onay verdiği p110α spesifik küçük molekül inhibitörü Alpelisib (BYL-719) oldukça etkili sonuçlar vermiştir. Alpelisib, Tüm PI3K izoformlarını hedefleyen inhibitörlerden daha üstün olmasına karşın, terapi direnci halen büyük bir sorun teşkil etmektedir. PI3K yolağı elemanlarından AKT, onkojen PI3K sinyalinin iletilmesinden sorumlu ana kinaz olarak görülmektedir. Ancak, yakın zamanlı çalışmalar PI3K yolağında yer alan birtakım kinazların da AKT'den bağımsız şekilde sinyal iletimi yaparak PIK3CA inhibisyonuna karşı gelişen dirençte rolü olduğunu göstermiştir. Bu çalışmada da benzer şekilde PI3K yolağında yer alıp AKT'den bağımsız şekilde sinyal iletimi

yaparak PIK3CA direncinde rol alan yeni moleküler hedefleri bulmayı amaçladık. Biyoinformatik analizlerimiz STK10'u bu kriterlere uyan potansiyel bir aday olarak belirlemiştir. STK10 ifadesinin siRNA yoluyla düşürülmesi meme kanseri hücrelerini BYL-719 tedavisine hassas hale getirmiştir ve transforme olmamış hücrelerde büyüme hızına pozitif katkı sağlamıştır. Buna ek olarak sonradan kazanılmış BYL-719 direncine sahip Luminal A alt tipine sahip meme kanseri hücre hatları geliştirdik. Dirençli modellerimizde AKT, S6 ve 4EBP1 fosforilasyon düzeyleri yabanıl tip hücrelere oranla BYL-719 etkisi altında daha yüksek oranda korunmaktadır. Dirençli hatlarımızda gerçekleştirilebilinecek olan transkriptomik ve proteomik analizler yeni BYL-719 direnç mekanizmalarına ışık tutabilir, yeni moleküler hedeflerin belirlenmesinde ve bu sayede BYL-719 direncine karşı yeni tedavi opsiyonlarının geliştirilmesinde yardımcı olabilir.

Anahtar Kelimeler: Meme kanseri, PIK3CA, alpelisib, BYL-719, ilaç direnci

ACKNOWLEDGEMENTS

I would like to extend my gratitude to Dr. Özgür Şahin and Dr. Onur Çizmecioğlu for their kind and continuous support and valuable supervision during my studies. I am incredibly grateful for the opportunities they provided and experience they shared with me which helped a lot to improve myself as a scientist.

I am also very thankful to my lab mates and friends Ünal Metin Tokat, Pelin Ersan, Özge Akbulut and Özge Saatci for their endless support and valuable companionship. They certainly made my time during my master's studies a lot easier and more bearable. I would also like to thank Umar Raza and Nevin Belder for their valuable friendship and experience they shared with me when I first started my master's studies. I would also like to extend my gratitude to Erol Eyüpoğlu, Havva Kılgöz, Barış Küçükkaraduman and Ridho Assidicky for their friendship and support during my studies.

I am also very thankful to my friends İrem Evcili, Ege Dedeoğlu, Naz Bozbeyoğlu, Hazal Beril Çatalak, Erta Xhafa and Gökberk Kaya whom I started my master's journey with for their valuable friendship and support. I would also like to thank my friends Tuğçe Bildik, Aslı Bartan and Berfu Saraydar whom I met towards end of my studies and blessed with their warm and valuable friendship.

Finally, I am very thankful to my family for their tireless efforts throughout the years. Their endless support and patience are very much appreciated and very precious to me.

TEŞEKKÜRLER

İlk olarak Dr. Özgür Şahin'e ve Dr. Onur Çizmecioğlu'na sonsuz destekleri ve değerli yönlendirmeleri için çok teşekkür ederim. Sağladıkları olanaklar ve paylaştıkları tecrübeleri kendimi bir bilim insanı olarak geliştirmemde oldukça faydalı olmuştur.

Bunun yanı sıra lab arkadaşlarım Ünal Metin Tokat, Pelin Ersan, Özge Akbulut ve Özge Saatci sonsuz destekleri ve değerli dostlukları için de oldukça müteşekkirim. Yüksek lisans çalışmalarımı daha kolay ve katlanılabilir kıldılar. Ayrıca Umar Raza ve Nevin Belder'e de değerli arkadaşlıkları ve paylaştıkları deneyimler için teşekkür ederim. İlk yıllarımda bana sıkılmadan her konuda yol gösterdiler. Benzer şekilde Erol Eyüpoğlu, Havva Kılgöz, Barış Küçükkaraduman ve Ridho Assidicky'e de değerli dostlukları ve destekleri için çok teşekkür ederim.

Aynı dönem yüksek lisans çalışmalarına başladığım İrem Evcili, Ege Dedeoğlu, Naz Bozbeyoğlu, Hazal Beril Çatalak, Erta Xhafa ve Gökberk Kaya'ya ve sonradan tanışma şansına eriştiğim Tuğçe Bildik, Aslı Bartan ve Berfu Saraydar'a değerli dostlukları ve desteklerinden ötürü çok teşekkür ederim.

Son olarak, aileme yıllardır gösterdikleri sonsuz özveri için minnettarım. Hiçbir zaman eksik etmedikleri destekleri ve bitmek tükenmek bilmeyen sabırlarından dolayı kendilerine çok teşekkür ederim.

TABLE OF CONTENTS

ABSTRACT ii
ÖZET iv
ACKNOWLEDGEMENTS vi
TEŞEKKÜRLER vii
TABLE OF CONTENTS viii
LIST OF FIGURES xi
LIST OF TABLES xiii
ABBREVIATIONS xiv
CHAPTER 1 1
INTRODUCTION 1
1.1 Breast Cancer 1
1.1.1 Molecular Characterization of Breast Cancer Subtypes 2
1.2 Role of PI3K/AKT Pathway in Breast Cancer and Current Therapeutic Options 3
1.2.1 An Overview of the PI3K/AKT Pathway 3
1.2.2 Common Aberrations in the PI3K/AKT Pathway in Breast Cancer 5
1.2.2.1 Oncogenic Mutations in the PIK3CA Gene 6
1.2.3 Targeting PI3K Pathway 6
1.2.3.1 Pan-PI3K Inhibitors 7
1.2.3.2 Isotype-specific PI3K Inhibitors 7
1.2.3.2.1 Alpelisib (BYL-719) 8
1.3 Mechanisms of Resistance to PI3Kα Inhibition by BYL-719 9
1.3.1 AKT-Independent Mechanisms of Resistance to PI3Kα Inhibition 12
1.4 STK10 Kinase 13
1.4.1 ERM Family Proteins 15
1.5 Rationale and Aims of the Study 16
CHAPTER 2 17

MATERIALS AND METHODS 17
2.1 Materials 17
2.1.1 Buffers 17
2.1.2 Chemicals and Reagents 17
2.1.3 Media and Supplements 19
2.1.4 Kits 19
2.1.5 Equipment 20
2.1.6 Consumables 21
2.2 Methods 22
2.2.1 Cell Culturing 22
2.2.1.1 Culturing Cell Lines 22
2.2.1.2 Developing Drug Resistant Cell Line Models 23
2.2.1.3 siRNA and Vector Transfections 24
2.2.1.3.1 siRNA Transfections 24
2.2.1.3.2 Vector Transfections 25
2.2.2 Cell-based Assays 25
2.2.2.1 *In-vitro* Sensitization Assay 25
2.2.2.2 Soft Agar Colony Formation Assay 26
2.2.2.3 2-D Growth Assay 27
2.2.2.4 Scratch Assay 27
2.2.3 Molecular Biology 28
2.2.3.1 Construction of pBABE-Hygro-STK10 Plasmid 28
2.2.3.1.1 Polymerase Chain Reaction (PCR) 28
2.2.3.1.2 Restriction Enzyme Digestion and Ligation 29
2.2.4 Protein Biochemistry 31
2.2.4.1 Protein Isolation 31
2.2.4.2 Protein Quantification 32
2.2.4.3 Sodium Dodecyl Sulfate Polyacrylamide Gel Electrophoresis (SDS-PAGE) 32
2.2.4.4 Western Blotting 34

2.2.4.5 CCD Imaging of Membranes 36
2.2.5 Developing Stable Cells Using Retroviral Transduction 36
2.2.6 Bioinformatics and Statistical Analyses 37
CHAPTER 3 38
RESULTS 38
3.1 Identification of STK10 as a Potential Sensitizer for PI3K Pathway Inhibitor Resistance 38
3.2 Selecting the Most Suitable Cell Lines for Further Studies with STK10 42
3.3 Investigation of Potential Roles of STK10 in Untransformed Cells 50
3.3.1 Functional Validation of Retroviral pBABE-Hygro-STK10 Vector Product 50
3.3.2 Investigation of Possible Involvement of STK10 within the PI3K Pathway 51
3.3.3 Investigation of STK10 as a Potential Oncogene 56
3.4 Development and Characterization of BYL-719 Resistant Breast Cancer Cell Line Models 60
3.4.1 Developing BYL-719 Resistant Cell Line Models 60
3.4.2 Characterization of BYL-719 Resistant Cell Line Models 63
CHAPTER 4 69
DISCUSSION 69
4.1 Potential Involvement of STK10 in PI3K Pathway 69
4.2 STK10 as a Potential Agent for Tumorigenesis 73
4.3 BYL-719 Resistant Cell Models to Identify Novel Mechanisms of BYL-719 Resistance 76
BIBLIOGRAPHY 80
APPENDIX 87

LIST OF FIGURES

Figure 1.1. An illustration showing estimated new cancer cases and deaths by sex in the United States for the year 2020 1

Figure 1.2. An overview of PI3K/AKT Pathway 5

Figure 1.3. Common hotspot mutations in PI3K p110α subunit. 6

Figure 3.1. Identification of STK10 as a potential target for PI3K pathway inhibitor resistance, independent of AKT. 39

Figure 3.2. STK10-exclusive review of the bioinformatical data 40

Figure 3.3. STK10 levels are reduced upon BYL-719 treatment. 41

Figure 3.4. Western blot analysis of lysates obtained from a panel of breast cancer cell lines. 43

Figure 3.5. STK10 mRNA expression levels in a panel of breast cancer cell lines. . 44

Figure 3.6. STK10 knockdown sensitizes MDA-MB-436 cells to BYL-719. 45

Figure 3.7. Western blot analysis of MDA-MB-436 cells showing expression levels of various PI3K/AKT pathway markers upon combination of BYL-719 with (A) STK10 siRNA and (B) STK10 overexpression vector. 46

Figure 3.8. STK10 knockdown sensitizes BT20 cells to BYL-719. 47

Figure 3.9. Western blot analysis of BT20 cells showing expression levels of various PI3K/AKT pathway markers upon combination of BYL-719 with (A) STK10 siRNA and (B) stable STK10 over-expression. 48

Figure 3.10. SRB cell viability analysis of BT20.Control and BT20.STK10 cells upon BYL-719 treatment. 49

Figure 3.11. Western blot analysis of HMEC and MEF cells stably overexpressing STK10. 51

Figure 3.12. Western blot analysis of PI3K pathway components in starved (A) MEF and (B) HMEC cells stably overexpressing STK10 stimulated with 4% FBS for 10 minutes. 53

Figure 3.13. Western blot analysis of PI3K pathway components in starved (A) MEF and (B) HMEC cells stably overexpressing STK10 stimulated with 2 µg/mL insulin for 10 minutes. 54

Figure 3.14. Western blot analysis of PI3K pathway components in starved (A) MEF and (B) HMEC cells stably overexpressing STK10 stimulated with 20 ng/mL EGF for 10 minutes. 55

Figure 3.15. SRB cell viability assay performed on (A) HMEC and (B) MEF cells stably overexpressing STK10. 56

Figure 3.16. Colony formation assay showing colony formation capabilities of (A) HMEC and (B) MEF cells stably overexpressing STK10. 57

Figure 3.17. 2D growth assay performed on (A) HMEC and (B) MEF cells stably overexpressing STK10. 58

Figure 3.18. Scratch assay comparing migratory capabilities of MEF.Control and MEF.STK10 cells. 59

Figure 3.19. SRB cell viability assay showing respective IC25 and IC50 values of low passage MCF7 and T47D cells against BYL-719. 61

Figure 3.20. Illustration depicting BYL-719 resistant MCF and T47D cell line development process. 62

Figure 3.21. Viability curves comparing dose response of (A) MCF7 WT, BYLR and (B) T47D WT, BYLR towards BYL-719. 63

Figure 3.22. Western blot analysis of MCF7, T47D WT and BYLR cells probed with various cell surface markers. 64

Figure 3.23. Western blot analysis showing PI3K/AKT pathway elements upon treatment with increasing doses of BYL-719 in (A) MCF7 and (B) T47D WT versus BYLR cells lines. 66

Figure 3.24. STK10 silencing sensitizes T47D BYLR cells to BYL-719 inhibition. 67

LIST OF TABLES

Table 1.1. Breast cancer subtype definitions 3
Table 2.1. List of siRNAs used 25
Table 2.2. Primer sequences for cloning STK10 ORF 28
Table 2.3. PCR components for STK10 ORF amplification 28
Table 2.4. PCR program for STK10 ORF amplification 29
Table 2.5. Digestion protocol 29
Table 2.6. Ligation reaction protocol 30
Table 2.7. Contents of RIPA lysis buffer 31
Table 2.8. Contents of 4X protein loading dye 33
Table 2.9. Contents of stacking and resolving gels. 33
Table 2.10. List of primary and secondary antibodies used 35

ABBREVIATIONS

AKT	Serine/threonine-specific protein kinase (protein kinase B)
APS	Ammonium persulfate
BC	Breast cancer
BCA	Bicinchoninic acid
BSA	Bovine serum albumin
DMEM	Dulbecco's modified eagle medium
ECL	Enhanced chemiluminescence
EGF	Epidermal growth factor
EGFR	Epidermal growth factor receptor
ER	Estrogen receptor
FBS	Fetal bovine serum
FDA	U.S. Food and Drug Administration
GEO	Gene expression omnibus
GPCR	G protein-coupled receptors
HER2	Human epidermal growth factor receptor 2 (ERBB2)
INPP4B	Inositol Polyphosphate-4-Phosphatase
mRNA	Messenger RNA
mTOR	Mammalian target of rapamycin, serine/threonine kinase
NEAA	Non-essential amino acid
ORF	Open reading frame
P/S	Penicillin/streptomycin
PBS	Phosphate buffered saline
PCR	Polymerase chain reaction

PFS	Progression free survival
PIP_2	Phosphatidylinositol-4,5-bisphosphate
PIP_3	Phosphatidylinositol-3,4,5-trisphosphate
PI3K	Phosphatidylinositol 3-kinase
PR	Progesterone receptor
PTEN	Phosphate and tensin homolog
PVDF	Polyvinylidene difluoride
RB	Retinoblastoma
RIPA	Radio-Immunoprecipitation Assay
RNA	Ribonucleic acid
siRNA	Small-interfering RNA
SRB	Sulforhodamine B Dye
TBST	Tris buffer saline Tween20
TCA	Trichloroacetic acid
TEMED	Tetramethylethylenediamine
TNBC	Triple negative breast cancer
v/v	Volume/volume
w/v	Weight/volume

CHAPTER 1

INTRODUCTION

1.1 Breast Cancer

Breast cancer (BC) is the most frequently diagnosed cancer type in women worldwide, accounting for roughly 25% of total cancer cases. It is also the leading cause of death among women in most regions of Europe, Middle East, Asia, South America, and North Africa [1]. In 2020, breast cancer is estimated to account for 30% of all new cancer diagnoses among women in the United States. Mortality-wise, unlike worldwide trend, breast cancer is estimated to be ranked second in the US, accounting for 15% of all cancer related deaths following lung cancer (**Figure 1.1**) [2].

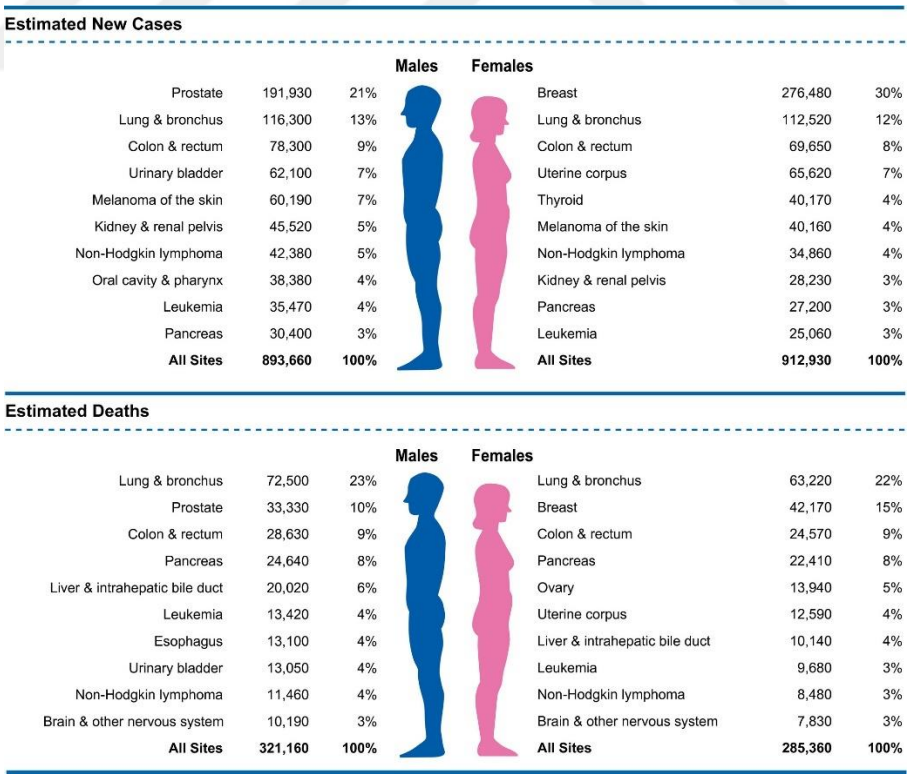

Estimated New Cases

Males			Females		
Prostate	191,930	21%	Breast	276,480	30%
Lung & bronchus	116,300	13%	Lung & bronchus	112,520	12%
Colon & rectum	78,300	9%	Colon & rectum	69,650	8%
Urinary bladder	62,100	7%	Uterine corpus	65,620	7%
Melanoma of the skin	60,190	7%	Thyroid	40,170	4%
Kidney & renal pelvis	45,520	5%	Melanoma of the skin	40,160	4%
Non-Hodgkin lymphoma	42,380	5%	Non-Hodgkin lymphoma	34,860	4%
Oral cavity & pharynx	38,380	4%	Kidney & renal pelvis	28,230	3%
Leukemia	35,470	4%	Pancreas	27,200	3%
Pancreas	30,400	3%	Leukemia	25,060	3%
All Sites	**893,660**	**100%**	**All Sites**	**912,930**	**100%**

Estimated Deaths

Males			Females		
Lung & bronchus	72,500	23%	Lung & bronchus	63,220	22%
Prostate	33,330	10%	Breast	42,170	15%
Colon & rectum	28,630	9%	Colon & rectum	24,570	9%
Pancreas	24,640	8%	Pancreas	22,410	8%
Liver & intrahepatic bile duct	20,020	6%	Ovary	13,940	5%
Leukemia	13,420	4%	Uterine corpus	12,590	4%
Esophagus	13,100	4%	Liver & intrahepatic bile duct	10,140	4%
Urinary bladder	13,050	4%	Leukemia	9,680	3%
Non-Hodgkin lymphoma	11,460	4%	Non-Hodgkin lymphoma	8,480	3%
Brain & other nervous system	10,190	3%	Brain & other nervous system	7,830	3%
All Sites	**321,160**	**100%**	**All Sites**	**285,360**	**100%**

Figure 1.1. An illustration showing estimated new cancer cases and deaths by sex in the United States for the year 2020 [2]. (See Appendix for copyright permission.)

1.1.1 Molecular Characterization of Breast Cancer Subtypes

Early work established by Sørlie and colleagues [3,4] utilized cDNA microarrays to classify breast carcinomas into at least four different subsets. In addition to subtype characterization based on cDNA microarrays, pathologists have been using several molecular markers such as estrogen receptor (ER), progesterone receptor (PR), human epidermal growth factor receptor 2 (HER2) and Ki67 proliferative marker staining to identify molecular subtypes. Molecular marker based characterization is more accessible therefore used frequently in the clinic, however both methods show good concordance with each other [5–7]. Accordingly, following table (**Table 1.1**) shows breast cancer subtype definitions based on molecular pathology markers [5,7].

Luminal A and Luminal B subtype breast cancers are both hormone receptor positive. Luminal A breast cancer subtype lacks any detectable levels of HER2, whereas Luminal B subtype breast cancers have amplified/over-expressed HER2 levels. Main systemic therapy strategy for hormone receptor positive breast cancer is to target estrogen and estrogen receptor function in these tumors. Therefore, selective estrogen receptor modulators (SERMs) such as tamoxifen, aromatase inhibitors (AI) such as anastrozole and letrozole and selective estrogen receptor down regulators (SERDs) such as fulvestrant are used [8]. In the last decade, CDK4/6 inhibitors and PI3K inhibitors have also been used in endocrine resistant ER+ patients [9]. HER2-positive breast cancer is characterized as being hormone receptor negative and HER2 overexpressed or amplified. Main strategy for treatment is to target HER2 receptor using inhibitors such as trastuzumab, lapatinib, pertuzumab, and antibody-drug conjugate (ADC), trastuzumab emtansine (T-DM1). Combination of HER2 inhibitors and chemotherapy has shown to be efficacious in HER2+ breast cancer patients [10].

Triple negative (basal-like) subtype breast cancer lacks any targetable receptors, therefore mainstay therapy for treatment of TNBC is chemotherapy. Given lack of DNA damage repair in triple negative tumors, DNA-crosslinking agents provide a critical platform for possible future drugs [8,11,12]. Importantly, the first immunotherapy (anti PD-L1) and an ADC (Sacituzumab Govitecan) have been FDA-approved for the treatment of aggressive TNBCs recently [13].

Table 1.1. Breast cancer subtype definitions [5,7].

Intrinsic Subtype	Pathologic definition
Luminal A	ER and/or PR positive HER2 negative Ki-67 low (<14%)
Luminal B	ER and/or PR positive HER2 over-expressed or amplified Any Ki67
HER2-positive	HER2 over-expressed or amplified ER and PR negative
Basal-like	ER and PR negative HER2 negative

1.2 Role of PI3K/AKT Pathway in Breast Cancer and Current Therapeutic Options

1.2.1 An Overview of the PI3K/AKT Pathway

Phosphoinositide 3-kinase (PI3K) pathway is one of the most frequently activated oncogenic pathway in cancer. Class I_A PI3Ks, which are the most studied class of PI3

kinases, consist of a heterodimer, a regulatory subunit named p85 and a catalytic subunit named p110 and receive signals through adaptor proteins from several cell surface receptors and oncoproteins such as ERBB receptors, FGFR and IGF-1R, G protein-coupled receptors (GPCRs) and Ras. Class I_B PI3K's receive signals exclusively from GPCRs [14–16]. *PIK3CA*, *PIK3CB* and *PIK3CD* genes encode p110 catalytic isoforms p110α, p110β and p110δ, respectively. These isoforms are highly homologous and possess 5 mutual domains: An N-terminal p85-binding domain, a RAS-binding domain, a membrane-binding domain called C2 followed by the helical domain, and finally the C-terminal catalytic domain. p85 regulatory subunit consists of 5 different isoforms, namely p85α, its splice variants p55α and p50α, p85β and p55γ. These isoforms share 3 main domains: inter-Src homology 2 (iSH2) domain that binds to p110 which is flanked by two SH2 domains [16,17].

During inactive state, p85 inhibits p110 catalytic activity by binding to the N-terminus of the p110 subunit *via* its iSH2 domain [16]. Adaptor proteins activated by cell surface RTK receptors bind and relieve p85 inhibition on p110 subunit. As a result, activated p85-p110 heterodimer binds lipid phosphatidylinositol-4,5-bisphosphate (PIP_2) at the plasma membrane and converts it to phosphatidylinositol-3,4,5-trisphosphate (PIP_3) *via* phosphorylation. PIP_3 recruits PDK1 and AKT through pleckstrin homology (PH) domain to plasma membrane where PDK1 phosphorylates AKT at Threonine 308 residue. AKT is fully activated when mTOR/Rictor (TORC2) complex phosphorylates AKT at Serine 473 residue. Activated AKT then phosphorylates its substrates, such as PRAS40 and Tuberin (TSC2). Phosphorylated TSC2 can no longer sustain its inhibitory effects on mTOR/Raptor (TORC1) complex. Active mTORC1 phosphorylates its targets such as S6K and 4EBP1. Overall

mTORC1 activity results in protein synthesis, RNA translation and cell growth. In addition, other AKT substrates include GSK3α, GSK3β, FoxO transcription factors, MDM2, BAD, and p27 KIP1 which leads to survival and cell cycle entry [14,15,18,19].

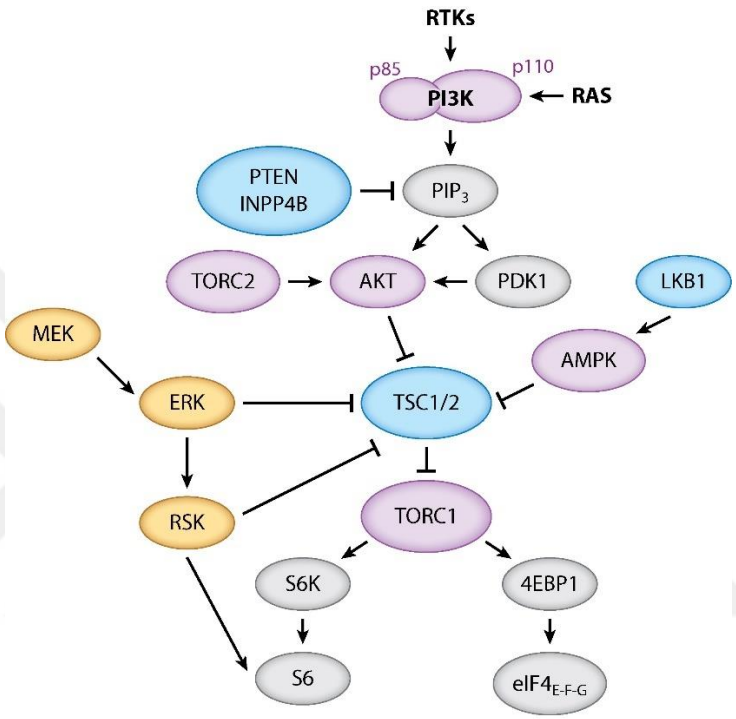

Figure 1.2. An overview of PI3K/AKT Pathway [14]. (See Appendix for copyright permission)

1.2.2 Common Aberrations in the PI3K/AKT Pathway in Breast Cancer

Over 70% of all breast cancer patients show mutations in genes involved in the PI3K/AKT pathway. Approximately 20-40% of patients show activating mutations in the *PIK3CA* gene, coding for PI3K catalytic subunit p110α, which is observed more frequently in Luminal subtype [20–22]. PTEN and INPP4B loss is also another frequent aberration resulting in hyperactivation of PI3K signaling, often observed in basal subtype patients [23,24]. PDK1 amplification or overexpression is also observed

frequently in luminal and HER2+ patients (22% each) and basal subtype patients (38%) [25]. Receptor activation/amplification of insulin-like growth factor receptor 1 (IGF-1R) and insulin receptor (IR) is observed in as much as 40-50% of luminal and basal subtype patients [24,26,27].

1.2.2.1 Oncogenic Mutations in the *PIK3CA* Gene

Exons 1, 9 and 20 of the *PIK3CA* gene harbors more than 91% of all the somatic mutations, which encode for p85 binding, helical and kinase domains, respectively. While most common activating mutations in the helical domain are E545K and E542K, most frequent mutation in the kinase domain is H1047R [12,13]. Miled and colleagues reported that a region of regulatory subunit p85 (termed p85ni), which inhibits activity of wild-type p110α, was unable impose such inhibitory effects when p110α harbored E542K, E545K, or Q546K mutations *in vitro* [29].

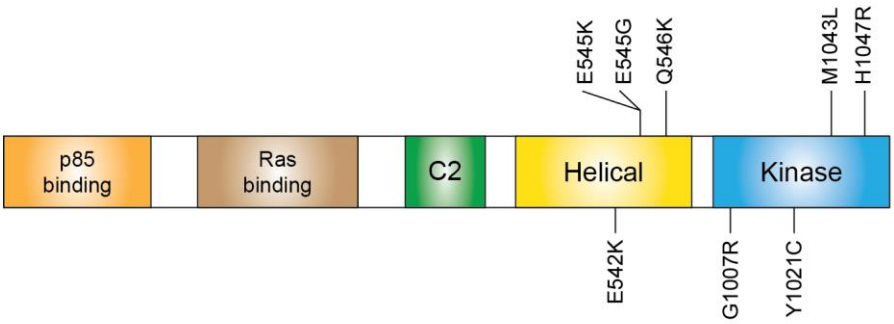

Figure 1.3. Common hotspot mutations in PI3K p110α subunit. Adapted from [30].

1.2.3 Targeting PI3K Pathway

PI3K pathway is frequently deregulated in breast cancer, making its constituent kinases critical targets for drug treatment. Although there are many inhibitors

developed against several key components in the PI3K pathway, such as PI3K, AKT, and mTOR, due to the scope of this thesis, only PI3K inhibitors will be covered here.

1.2.3.1 Pan-PI3K Inhibitors

Pan-PI3K inhibitors target all Class I p110 isoforms. Buparlisib (BKM120) is one of the most studied pan-PI3K inhibitor. Clinical trials revealed that although BKM120 is able to extend median progression free survival (PFS) of breast cancer patients, the drug was associated with severe adverse effects (grade ≥3), high levels of anxiety and depression, even leading to suicide attempts, in several patients. Such mood alterations are thought to be caused due to universal PI3K inhibition in brain since BKM120 is expected to cross the blood brain barrier [31–35]. Pictilisib is another pan-PI3K inhibitor that has been evaluated in two randomized clinical trials. In both of the studies Pictilisib failed to extend median PFS of the patients significantly [35–37].

Pan-PI3K inhibitors broadly target all PI3K isoforms that may provide better efficacy. However, targeting all isoforms narrows their therapeutic window due to severe adverse effects [15].

1.2.3.2 Isotype-specific PI3K Inhibitors

Severe adverse effects caused by pan-PI3K inhibitors were mostly rooted from inhibition of all PI3K isoforms that were also required to carry out regular cellular activities. Isotype-specific PI3K inhibitors were developed to minimize such adverse effects, therefore maximizing their therapeutic window, meanwhile still maintaining inhibition of major PI3K isoforms frequently mutated in cancer [15,35]. Currently, two isotype-specific PI3K inhibitors are being evaluated in multitude of clinical trials,

namely α-specific PI3K inhibitor Alpelisib (BYL-719) and α-specific and β-sparing PI3K inhibitor Taselisib (GDC-0032), former one is already approved for hormone receptor positive breast cancer [38].

1.2.3.2.1 Alpelisib (BYL-719)

The *PIK3CA* gene is frequently mutated in breast cancer, therefore it is a critical node for targeting the PI3K pathway [24]. Alpelisib is a small molecule, α-specific PI3K inhibitor that shows 50-fold specificity towards p110α subunit compared to other isoforms of PI3K [39].

SOLAR-1 clinical trial (NCT02437318) conducted with 572 patients who had HR-positive and HER2-negative breast cancer and had received/receiving aromatase inhibitor treatment (341 of which harbored *PIK3CA* mutations) revealed that in the cohort of patients with *PIK3CA* mutations, progression free survival (PFS) of patients who received fulvestrant in combination with Alpelisib was 11.0 months compared to placebo-fulvestrant group where the PFS was 5.7 months. However, survival benefit criteria were not met for *PIK3CA*-wild type patients. Serious adverse effects were observed in 34.9% of the patients receiving alpelisib in combination with fulvestrant, compared to 16.7% in the placebo–fulvestrant cohort [38].

Therefore, Alpelisib has been approved by the Food and Drug Administration (FDA) to be used in combination with fulvestrant for postmenopausal women and men, with HR+/HER2-, *PIK3CA*-mutated, advanced or metastatic breast cancer following the SOLAR-1 clinical trial [38,39].

1.3 Mechanisms of Resistance to PI3Kα Inhibition by BYL-719

PI3K pathway is a complex network of interactions with intricate feedback loops, and numerous crosstalk points, branching with parallel pathways. This can essentially serve as contingency plans to bypass pathway inhibition. Identifying such nodes of escape is vital to overcome PI3K pathway resistance. Here I summarize the recent findings with respect to the mechanisms of resistance to α-specific PI3K inhibition.

Persistent mTORC1 activity was correlated with resistance to PI3Kα inhibition by BYL-719. In their study, Elkabets and colleagues reported that in xenografts of JIMT-1 and MCF7 cells, BYL-719 treatment reduced p-AKT levels in both cell lines, but p-S6(S240/244) and p-S6(S235/236) levels were retained most prominently in *de novo* resistant JIMT-1 model. Furthermore, in patients who did not respond well to BYL-719 treatment, p-S6(S240/244) levels were found to be higher in tumor biopsies compared to that of responding patients. Moreover, patients who initially responded well to treatment but later on showed tumor progression again had p-S6(S240/244) levels comparable to that of initially non-responding patients [40]. All these studies show that PI3K/mTOR downstream pS6 could be a key inducer of resistance to BYL-719.

In another study, Juric and colleagues present a case of a patient with metastatic breast cancer bearing *PIK3CA* mutations that initially responded partially to BYL-719 treatment, yet soon after discontinued treatment due to disease progression in her lungs. In order to identify the genetic determinants that drive acquired resistance to

BYL-719 treatment, they performed whole genome sequencing comparing primary tumor biopsy with biopsies taken from multiple metastatic sites shortly after her demise. Metastatic sites showed copy loss of PTEN compared to pre-treatment biopsy. Immunohistochemistry (IHC) analysis also confirmed their findings where PTEN expression was lost in lung metastasis compared to primary tumor (prior to BYL-719 treatment) and periaortic lesion (stable disease phase during BYL-719 treatment) [41]. Similarly, Razavi and colleagues reported that 25% of *PIK3CA* mutant, hormone receptor positive metastatic breast cancer patients that were resistant to alpelisib plus aromatase inhibitor treatment had PTEN mutations. The authors also state that selective enrichment of mutant alleles can also be associated with therapy resistance. Their analyses revealed that frequency of activating *ESR1* mutations were also significantly increased in patients receiving alpelisib plus aromatase inhibitor. To test this, they utilized knock-in mice expressing either wild-type or mutant *ESR1* and observed that when alpelisib and estrogen deprivation was combined, disease progressed more rapidly in *ESR1*-mutant mice compared to wild type. Cumulatively, almost half of the patients in the clinical trial had PTEN loss or activating ESR1 mutations which was associated with poorer response to the combination therapy [42].

Insulin feedback regulation is also shown to keep PI3K pathway active even under inhibitory pressure of BKM120 and BYL-719. Hopkins and colleagues propose that certain dietary approaches such as ketogenic diet can be utilized to improve the efficacy of PI3K inhibitors. They demonstrated that combination of PI3K inhibition with either BKM120 or BYL-719 and ketogenic diet reduced p-S6(S235) levels in mice and prolonged survival compared to PI3K inhibition alone [43].

Vora and colleagues demonstrate that breast cancer cells that are chronically exposed to PI3K inhibition have retained RB phosphorylation compared to their wild type counterparts. Utilizing their PI3K inhibitor resistant cell lines, they performed a 42-compound drug screen where they compare single agent PI3K inhibition in combination with various drugs. As a result, they identified CDK4/6 inhibitor LEE011 as the most potent sensitizer to PI3K inhibition. When combined with PI3K inhibition, LEE011 was able to reduce retained p-RB signal in resistant cell lines. They show that active mTOR signaling under PI3K inhibition was the main reason for the maintenance of RB phosphorylation in the resistant cell lines. They also observed a similar phenomenon in patients enrolled to clinical trials of BYL-719. Patients that failed to respond to PI3K inhibition by BYL-719 had higher levels of RB phosphorylation compared to responding patients. They also show that combination of PI3K inhibition with CDK4/6 inhibitor LEE011 significantly reduced tumor growth in xenografts with *PIK3CA* mutant cells [44]. At the time of writing, LEE011, BYL-719 and aromatase inhibitor Letrozole are being evaluated in a clinical trial (NCT01872260) with 256 ER+/HER2- locally advanced or metastatic breast cancer patients in double (i.e., LEE011 and Letrozole, or BYL-719 and Letrozole) and triple combinations.

In one study, Leroy and colleagues identified a compensatory mechanism where under inhibitory pressure of BYL-719, p110β steps in as the signal transducer from IGF1R. Like previous findings described above, their resistant cell line models have sustained mTOR activity which results in BYL-719 resistance. Phosphoproteomics analyses revealed that in BYL-719 resistant cell lines, phosphorylation on tyrosine phosphosites of IGF1R, IRS1, IRS2, and p85 PI3K were increased compared to

parental cell lines. Immunoprecipitation experiments demonstrated that phosphorylated IRS and p85 proteins recruit p110β, thereby promoting resistance in the cells [45].

1.3.1 AKT-Independent Mechanisms of Resistance to PI3Kα Inhibition

AKT is the most thoroughly studied PI3K downstream effector and since been viewed as the primary path that relays upstream signals from PI3 kinase. Recent studies have shown that PI3K-dependent but AKT-independent pathways also play a pivotal role in transducing PI3K signal downstream and contributing to tumorigenesis and PI3K inhibitor resistance [46–49]. Here we summarize recent findings in AKT-independent but PI3K-dependent mechanisms of resistance to α-specific PI3K inhibition.

Castel and colleagues reveal that PDK1-SGK1 axis drives resistance to PI3Kα inhibition *via* residual mTORC1 downstream activity and blockade of either PDK1 or SGK1 sensitizes cancer cells to PI3Kα inhibition [46]. Previous work from the same group also indicate that BYL-719 sensitivity was associated with full inhibition of signaling through mTORC1 pathway [40]. Combining shRNA targeted to SGK1 with BYL-719 decreases phosphorylation levels of S6 and 4EBP1. Similarly, in cells overexpressing SGK1, BYL-719 fails to inhibit phosphorylation of S6 and 4EBP1. SGK1 is shown to interact with and phosphorylate TSC2 thereby promoting mTORC1 activity [46]. In another study, Orlacchio and colleagues also demonstrated that PDK1-SGK1 axis is vital for PI3K driven tumorigenesis. Their work in thyroid cancer reveals that AKT alone is not sufficient, and the activity of SGK1 is also required for tumor growth *in vitro* and *in vivo* [47]. Another member of the SGK family of AGC

kinases, SGK3 was also associated with AKT-independent signaling downstream of mutant PIK3CA [48].

In another study, PIM kinase is shown to confer resistance to BYL-719 by activating PI3K downstream in an AKT-independent manner. The authors utilized a gain-of-function approach to identify genes that can result in acquired resistance when upregulated. To achieve this, they transfected T47D cells with 15,970 different human open reading frames and treated cells with BYL-719. PIM1 resulted in increased growth under BYL-719 inhibition. T47D cells overexpressing PIM1 had higher phosphorylation levels of p70S6K1 and 4EBP1 compared to GFP control. Combination of PIM inhibitor (LGH447) and BYL-719 sensitized cell lines with high endogenous levels of PIM to BYL-719. Elevation of PIM was also observed in several patient biopsies who were receiving BYL-719, but had poor response to the drug [49].

1.4 STK10 Kinase

STK10 is a member of Ste20 family of serine/threonine kinases and is the human homolog of murine LOK. Unlike its murine homolog, which is predominantly expressed in lymphocytes, STK10 is expressed in wide range of tissues, although mostly in hematopoietic cells [50].

Human STK10 and murine LOK are highly conserved and show 88% amino acid similarity [51]. Mouse homolog LOK is a 130-kDa protein composed of 966-amino acids, with N-terminal kinase domain and C-terminal coiled coil domain [52]. Human

STK10 has an open reading frame of 968 amino acids and shows 98% and 93% similarity in kinase and coiled-coil domains to that of murine LOK, respectively [51].

One study reveals that STK10 is capable of autophosphorylation and shows highly similar domain structures to two polo-like kinase kinases human Slk and *Xenopus laevis* xPlkk1, 76% and 84% similarity within kinase domain and 61% and 70% similarity within coiled-coil domain with hSlk1 and xPlkk1, respectively. STK10 is shown to be immunoprecipitated together with Plk1 in nocodazole-treated samples and able to phosphorylate Plk1 *in vitro*. Researchers also expressed kinase-dead, dominant-negative version of STK10 in NIH3T3 cells and observed that mutant STK10 expressing cells grew more slowly compared to wild type STK10 expressing cells and showed DNA content abnormalities [50]. In another study, researchers identified a somatic mutation in *STK10* where an arginine residue is changed to a histidine (R634H), to cause carcinogenesis in Peripheral T-cell lymphoma (PTCL). It was shown that wild-type STK10 act as a tumor suppressor by suppressing NF-κB and potentiating dexamethasone-induced apoptosis. STK10(R634H) somatic mutation results in anti-apoptotic effects through activation of NF-κB, leading to carcinogenesis [53]. So far, STK10 has not been studied extensively in context of breast cancer. Despite evidence indicating potential tumor suppressor roles for wild type STK10, mutations in STK10 is shown to have tumorigenic potential in PTCL and with prospect of many more to be characterized. Furthermore, its association with Plk1 might present a critical node in terms of its oncogenic role in cancer.

1.4.1 ERM Family Proteins

Apart from participating in several cellular functions, such as cell proliferation and regulation of apoptosis as mentioned above, murine LOK has also been associated with rearrangement of cytoskeleton and cell motility by phosphorylating ERM family proteins. Studies in mice by Belkina and colleagues revealed that LOK is mainly localized near plasma membrane, mostly enriched in close proximity to ERM and is an ERM kinase both *in vitro* and *in vivo* [54].

ERM family proteins consist of three structurally similar proteins called ezrin, radixin, moesin and are responsible for linking actin filaments to the plasma membrane thereby controlling cell shape and consequently regulating cell adhesion, migration and division. ERM proteins consist of three major domains. N-terminal membrane binding domain (FERM) is the most conserved domain between the ERM proteins. C-terminal domain (CTD) is responsible for F-actin binding. These two domains are joined together by an α-helical domain [55]. A study by Pelaseyed and colleagues shed light on the intricate mechanism of ezrin activation by LOK. Upon PIP_2 binding, ezrin goes under a conformational change allowing LOK C-terminal domain to gain access and wedge apart the membrane and F-actin-binding domains of ezrin. LOK kinase domain can then phosphorylate the exposed threonine residue (T567 in ezrin) leading to activation of ezrin [56,57]. In this study, we used p-ERM antibody as an STK10 activity marker.

1.5 Rationale and Aims of the Study

Recent approval of Alpelisib (BYL-719) by FDA brought the drug under the spotlight. Even though the initial trial that led to the approval was a success, several patients had to discontinue treatment due to progression of their disease. Inevitably, as a result of the selective pressure drug imposes on the tumor, specific tumor population within the collective will prevail and be naturally selected, resulting in development of acquired resistance. Recent studies have revealed several key mechanisms where tumors escape inhibitory pressure of the drug. Resonating theme is that resistance is mainly driven by residual mTOR signaling downstream of PI3K.

PI3K pathway is a complex network of interactions. For years, AKT has been thought to be the main effector of PI3K-mediated tumorigenesis. Several studies have already identified PI3K-dependent, yet AKT-independent mechanisms where tumor cells take advantage in order to escape PI3K inhibition. Scientists question the reliability of AKT phosphorylation as a PI3K activity marker. AKT-independent signaling downstream of PI3K is a lesser explored realm to be dwelled on. In this line, we aimed the following:

- Identify and validate a <u>novel</u>, <u>AKT-independent</u>, <u>druggable</u> target downstream of PI3K that can potentially confer resistance to PI3K/AKT pathway inhibition.
- To generate BYL-719 resistant cell line models and discover molecular mechanisms of PI3K inhibitor resistance.

CHAPTER 2

MATERIALS AND METHODS

2.1 Materials

2.1.1 Buffers

1X Anode Buffer I	300 mM Tris, 20% (v/v) methanol
1X Anode Buffer II	25 mM Tris, 20% (v/v) methanol
1X Cathode Buffer	40 mM 6-aminocaparoic acid, 20% (v/v) methanol
1X PBS	137 mM NaCl, 2.7 mM KCl, 10 mM Na_2HPO_4, 2 mM KH_2PO_4 (pH: 7.4)
1X SDS-PAGE Running Buffer	25 mM Tris, 14.41 g/L glycine, 1% (v/v) SDS
1X TAE	40 mM Tris, 20 mM acetic acid, 1 mM EDTA
1X TBST	20 mM Tris, 8 g/L NaCl 0.2% (v/v) Tween20
RIPA Lysis Buffer	150 mM NaCl, 1% (v/v) NP-40, 0.5% (v/v) Sodium DOC, 50 mM Tris-HCl (pH 8.0), 50 mM NAF, 1 mM Na_3VO_4, 4% (v/v) Protease inhibitor, 4% (v/v) Phosphatase inhibitor

2.1.2 Chemicals and Reagents

4X protein loading dye	250 mM Tris HCl (pH:6.8), 10% (w/v) SDS, 0.1% (w/v) Bromophenol blue, 50% Glycerol (v/v), 25% (v/v) β-mercaptoethanol

6-aminocaparoic acid	Sigma Aldrich, St Louis, MO, USA
Acetic acid (glacial)	Isolab, Wertheim, Germany
Acrylamide/bisacrylamide	Applichem, Darmstadt, Germany
Agar	Sigma Aldrich, St Louis, MO, USA
Ammonium persulfate	Carlo Erba, Cornaredu, Italy
Bovine serum albumin	Santa Cruz, Dallas, TX, USA
Protease inhibitor cocktail	Roche Applied Science, Mannheim, Germany
ECL	Amersham Pharmacia Biotech, Amersham, UK
	Thermo Fisher Scientific, Waltham, MA, USA
Ethanol	Sigma Aldrich, St Louis, MO, USA
Ethidium bromide	Thermo Fisher Scientific, Waltham, MA, USA
Isopropanol	Sigma Aldrich, St Louis, MO, USA
Lipofectamine™ 2000	Invitrogen, Carlsbad, CA, USA
Methanol	Sigma Aldrich, St Louis, MO, USA
Nuclease free water	ChemCruz, Dallas, TX, USA
Page Ruler protein ladder	Thermo Fisher Scientific, Waltham, MA, USA
Phosstop	Roche Applied Science, Mannheim, Germany
Ponceu S	Sigma Aldrich, St Louis, MO, USA
Sodium chloride	Merck, Darmstandt, Germany
Sodium dodecyl sulfate	Merck, Darmstandt, Germany
Sulforhodamine B sodium salt	Sigma Aldrich, St Louis, MO, USA
TEMED	Serva, Heidelberg, Germany
Trichloroacetic acid	Sigma Aldrich, St Louis, MO, USA
Trizma base	Sigma Aldrich, St Louis, MO, USA

Tryptone	Sigma Aldrich, St Louis, MO, USA
Tween-20	VWR, Radnor,PA, USA
Yeast extract	Merck, Darmstandt, Germany

2.1.3 Media and Supplements

DMEM (low glucose)	Biowest, Nuaille, France
DMEM (wo/ phenol red)	Thermo Fisher Scientific, Waltham, MA, USA
DMEM (F12)	Sigma Aldrich, St Louis, MO, USA
Epidermal growth factor (EGF)	Peprotech, London, UK
Fetal bovine serum	Biowest, Nuaille, France
Hydrocortizone	Peprotech, London, UK
Insulin	Sigma Aldrich, St Louis, MO, USA
Non-essential aminoacids	Lonza, Basel, Switzerland
optiMEM	Invitrogen, Carlsbad, CA, USA
Penicillin/Streptomycin	Lonza, Basel, Switzerland
Trypsin (10X)	Biowest, Nuaille, France

2.1.4 Kits

LookOut® Mycoplasma Detection Kit	Sigma Aldrich, St Louis, MO, USA
E.Z.N.A.® Gel Extraction Kit	Omega Biotek, Norcross, GA, USA
E.Z.N.A.® Plasmid Mini Kit	Omega Biotek, Norcross, GA, USA

Pierce™ Protein Assay Kit	Pierce, Rockford, IL, USA
Phusion® High-Fidelity PCR Kit	NEB, Ipswich, MA, USA
Restriction enzymes (SalI-HF, HindIII-HF, EcoRI-HF)	NEB, Ipswich, MA, USA
Shrimp Alkaline Phosphatase	NEB, Ipswich, MA, USA
T4 DNA Ligase	NEB, Ipswich, MA, USA

2.1.5 Equipment

Amersham™ Imager 600	GE Healthcare, Chicago, Illinois, USA
Cell counting chamber	Marienfeld, Könighofen, Germany
Centrifuges	Thermo Fisher Scientific, Waltham, MA, USA
	Beckman, Pasadena, CA, USA
Freezer (-20°C)	Bosch, Stuttgart, Germany
Freezer (-80°C)	Hettich, Geldermansen, Germany
	Thermo Fisher Scientific, Waltham, MA, USA
Fridge (+4°C)	Bosch, Stuttgart, Germany
Horizontal shakers	FinePCR, Seoul, South Korea
	Bellco, Vineland, NJ, USA
Incubator	NuAire, Plymouth, MN, USA
Laminar flow hood	Nüve, Ankara, Turkey
Leica DMi8 Inverted Microscope	Leica Microsystems, Wetzlar, Germany
Mini-PROTEAN® gel casting module	Bio-Rad, Hercules, CA, USA

Mini-PROTEAN® Tetra Cell	Bio-Rad, Hercules, CA, USA
Multichannel pipette	Thermo Fisher Scientific, Waltham, MA, USA
NanoDrop 1000	Thermo Fisher Scientific, Waltham, MA, USA
Nikon TS300 Inverted Microscope	Nikon, Tokyo, Japan
Power supplies	Bio-Rad, Hercules, CA, USA
Synergy HT™ Multi-Mode Microplate Reader	Biotek, Winooski, VT, USA
Trans-Blot® Turbo™ Transfer System	Bio-Rad, Hercules, CA, USA
Thermal cycler	Applied Biosciences, Foster City, CA, USA
Vortex	Isolab, Wertheim, Germany
Water bath	Nüve, Ankara, Turkey

2.1.6 Consumables

100 mm cell culture dishes	TPP, Trasadingen, Switzerland
145 mm cell culture dishes	TPP, Trasadingen, Switzerland
6-well plates	Greiner bio-one, Frickenhausen, Germany
96-well plates	Greiner bio-one, Frickenhausen, Germany
Filtered pipette tips (10, 20, 200, 1000 µL)	Greiner bio-one, Frickenhausen, Germany
Cell scrapers	Greiner bio-one, Frickenhausen, Germany
Coverslips	Marienfeld, Königshofen, Germany

Cryovials	Greiner bio-one, Frickenhausen, Germany
Micropipettes (Pipetman)	Gilson, Middleton, WI, USA
Parafilms	VWR, Radnor, PA, USA
PCR tubes	Greiner bio-one, Frickenhausen, Germany
Plastic pipettes (5 mL)	Isolab, Wertheim, Germany
Plastic pipettes (10, 25 mL)	Greiner bio-one, Frickenhausen, Germany
PVDF membrane	Bio-Rad, Hercules, CA, USA
Reaction tubes (0.5, 1.5, 2 mL)	Greiner bio-one, Frickenhausen, Germany
Storage bottles	Corning Incorporated, Corning, NY, USA
Unfiltered tips (1000 µL)	LP Italiana, Milano, Italy
Unfiltered tips (10, 200 µL)	Corning Incorporated, Corning, NY, USA
Whatman paper	GE Healthcare, Little Chalfont, UK

2.2 Methods

2.2.1 Cell Culturing

2.2.1.1 Culturing Cell Lines

All cells were grown on 10cm petri dishes and maintained at 37°C and 5% CO_2. Cells were passaged every 3-4 days. Non-confluent cells after indicated period were only subjected to medium change. MDA-MB-436 and BT20 cells were split in 1:3 ratio, HEK293FT, MCF7 and T47D cells were split in 1:5 ratio and HMEC and MEF cells were split in 1:7 ratio. MDA-MB-436, BT20, HEK293FT and MEF cells were maintained in low glucose Dulbecco Modified Eagle Medium (DMEM) supplemented

with 10% heat inactivated fetal bovine serum (FBS), 1% penicillin/streptomycin (P/S), 1% non-essential amino acids (NEAA) and 1% L-glutamine. MCF-7 and T47D cells and their resistant counterparts were maintained in phenol red free DMEM supplemented with 10% heat inactivated FBS, 1% P/S, 1% NEAA and 0.01 mg/mL insulin. HMEC cells were maintained in DMEM/F12 supplemented with 4% heat inactivated FBS, 0.01 ng/mL EGF, 25 ng/mL hydrocortisone, 1% P/S, 1% L-glutamine and 0.025 mg/mL insulin. For cell splitting, growth media was aspirated, and cells were washed twice with 5 mL PBS. Subsequently, 1-2 mL trypsin was added and incubated at 37°C for 5 minutes. Following incubation, trypsin was inactivated by diluting with cell culture media at a ratio of 1:3. All cell lines were tested for mycoplasma contamination periodically.

2.2.1.2 Developing Drug Resistant Cell Line Models

MCF7 and T47D cells were initially tested for mycoplasma and Alpelisib (BYL719) response. BYL719 resistant cell lines, hereinafter referred to as BYLR, were developed under continuous BYL719 exposure for over a period of 9-10 months, at increasing doses starting from parental IC25. BYL719 was added to culture media one day after cell splitting and kept for 3 days. Cell splitting or medium change was performed based on cell confluency. All cell lines were tested for mycoplasma contamination and BYL719 response periodically.

2.2.1.3 siRNA and Vector Transfections

2.2.1.3.1 siRNA Transfections

siRNA transfections were performed using Lipofectamine 2000™ and OptiMEM reduced serum media. For 6 well plates, cells were seeded at a density of 100.000 cells/well, 120.000 cells/well and 200.000 cells/well for HMEC/MEF, BT20/MCF7/T47D and MDA-MB-436 cells, respectively. For 96 well plates, cells were seeded at a density of 4000 cells/well and 5000 cells/well for BT20/MCF7/T47D and MDA-MB-436 cells, respectively.

siRNAs (see **TABLE 2.1**) were transfected at a concentration of 20 nM diluted in 250 µL and 20 µL OptiMEM for 6 and 96 well plates, respectively. 2-4 µL lipofectamine was diluted in 250 µL OptiMEM and 0.2-0.4 µL lipofectamine was diluted in 20 µL OptiMEM for 6 and 96 well plates, respectively. Each mixture was vortexed at high intensity for 10 seconds and left to incubate at room temperature for 10 minutes. After that, both vials were mixed in 1:1 (v/v) ratio totaling up to 500 µL and 40 µL transfection mixture per well for 6 and 96 well plates, respectively. Transfection mixtures were vortexed at low intensity for 30 seconds followed by 30 minutes of incubation at room temperature. Transfection mixture was added on top of 1000 µL and 80 µL P/S-free media for 6 and 96 well plates, respectively. The plates were then left to incubate at 37°C and 5% CO_2. Further treatments were performed the next day. Drugs were added in 200 µL and 30 µL for 6 and 96 well plates, respectively.

Table 2.1. List of siRNAs used

siRNA	Catalog Number	Company
siAllStars	1027280	Qiagen
siSTK10 #1	D-004168-05-0002	GE Dharmacon
siSTK10 #2	D-004168-06-0002	GE Dharmacon
siSTK10 #3	D-004168-07-0002	GE Dharmacon

2.2.1.3.2 Vector Transfections

Vector transfections were performed using Lipofectamine 2000™ and OptiMEM reduced serum media. For 6 well plates, cells were seeded at a density of 250.000 cells/well and 500.000 cells/well for BT20/MCF7/T47D and MDA-MB-436/HEK293FT cells, respectively. For vector and drug combinations cells were seeded initially at 6 well plates, transfected and trypsinized the following day where they were seeded onto 96 well plates.

500-1000 ng vector was diluted in 250 µL OptiMEM. 2-4 µL lipofectamine was diluted in 250 µL OptiMEM. Rest of the protocol is identical to that of siRNA described previously in **Section 2.2.1.3.1**. Cells were incubated in vector transfection mix for 24-48 hours and then treated with drug in 200 µL.

2.2.2 Cell-based Assays

2.2.2.1 *In-vitro* Sensitization Assay

Sulforhodamine B (SRB) assay was used to measure cell viability in 96 well plate format. Briefly, 25% trichloroacetic acid (TCA) was added into wells containing

media at 1:2.5 ratio for fixation. After incubation at +4ºC for an hour, wells were washed five times with dH_2O and dried via tapping. Subsequently, 50 µL of 0.4% SRB sodium salt in 1% acetic acid was added to each well and incubated at room temperature while shaking at low intensity for 30 minutes. After that, excess dye was removed by washing five times with 1% acetic acid. Plates were left to dry overnight at room temperature, protected from direct light. Next day, 150 µL of 10 mM Tris base was added to dissolve the dye and incubated at room temperature while shaking at high intensity for 15 minutes. Luminescence at 564 nm was recorded using Synergy HT™ microplate reader.

2.2.2.2 Soft Agar Colony Formation Assay

For 6 well plates, 2.5 mL of bottom agar mixture (Bottom agar mix for a total of 45 mL consists of 25 mL 2X DMEM, 5 mL ddH_2O and 15 mL 2.25% agarose) was added per well and left to solidify 30 minutes at room temperature. Meanwhile 2-parts of 2X DMEM was mixed with 1-part ddH_2O to be used later with top agar mixture. Cells were trypsinized and then counted. For MEF and HMEC, accounting for triplicates, 200.000 and 300.000 cells/well were counted and pelleted, respectively. Cells were mixed with 9 mL of 2X DMEM/ddH_2O mix and 2.7 mL 2.25% agarose. 2 mL from the mixture was added per well on top of solidified bottom agar. Top agar was let to solidify at room temperature for 50 minutes. Subsequently, the wells were fed with 2-3 mL of cell-type specific media. Media was changed every 3-4 days during an experimental span of 3 weeks. After 3 weeks, media was aspirated, and colonies were stained with 0.005% crystal violet solution and representative pictures were obtained using 4X magnification of Leica DMi8 inverted microscope.

2.2.2.3 2-D Growth Assay

HMEC and MEF cells were seeded at a density of 40.000 cells/well onto 12 well plates. Cells were fixed with 10% (v/v) acetic acid, 10% (v/v) ethanol fixing solution overnight at room temperature (2 mL added per well of a 12 well plate). After fixation wells were washed once with 1X PBS solution. Fixed cells were then stained with 0.4% (w/v) crystal violet and 20% (v/v) ethanol solution for 1 hour at room temperature. (1 mL crystal violet solution added per well of a 12 well plate). After staining crystal violet solution was discarded and the wells were washed three times with dH_2O. Plates were left to dry overnight. Wells were then de-stained with 10% (v/v) acetic acid solution (1 mL de-staining solution added per well of a 12 well plate). 200 µL solution from each well were transferred to a 96 well plate and absorbance at 595 nm was measured using BioTek Microplate Reader.

2.2.2.4 Scratch Assay

For scratch assay, MEF cells were seeded to 90% confluency. Then cell monolayer was scratched using a fine tip 200 µL micropipette tip. Subsequently, cells were washed twice with PBS and supplemented with 1% FBS containing DMEM. Depending on the condition, drug was added to the media. Images were taken at 0-6-12-24 hour time points using 4X magnification of Leica DMi8 inverted microscope. Images were then analyzed automatically using TScratch software [58].

2.2.3 Molecular Biology

2.2.3.1 Construction of pBABE-Hygro-STK10 Plasmid

2.2.3.1.1 Polymerase Chain Reaction (PCR)

STK10 open reading frame (ORF) was amplified from pCMV-XL4-STK10 vector obtained from Origene using primers listed in **TABLE 2.2**. PCR components and program used to amplify STK10 ORF is given in **TABLE 2.3** and **TABLE 2.4**, respectively.

Table 2.2. Primer sequences for cloning STK10 ORF

Direction	Primer Sequence
Forward	5'-GGCGCCACCGTCGACGCGCCCCCGGCCATGG-3'
Reverse	5'-CCAGCCACAGCCCCGGGTCGACGCGGTTGTTAAGAAGCA-3'

Table 2.3. PCR components for STK10 ORF amplification

Component	10 µL reaction
5X Phusion GC Buffer	2 µL
10 mM dNTPs	0.2 µL
Forward primer	0.5 µL
Reverse primer	0.5 µL
pCMV-XL4-STK10	0.5 µL
DMSO	1 µL
Phusion polymerase	0.1 µL
DEPC	5.2 µL

Table 2.4. PCR program for STK10 ORF amplification

Step	Temperature	Duration
Initial denaturation	98ºC	30 secs
	98ºC	10 secs
25 cycles	68.9ºC	20 secs
	72ºC	2 mins
Final extension	72ºC	10 secs
Final hold	4ºC	Ind.

2.2.3.1.2 Restriction Enzyme Digestion and Ligation

STK10 ORF was run on gel following PCR and band of interest was excised from the gel using E.Z.N.A.® Gel Extraction Kit according to manufacturer's instructions. pBABE-Hygro empty plasmid and STK10 ORF amplicons were both digested with *SalI-HF* for 2 hours at 37ºC using the protocol described in **TABLE 2.5**.

Table 2.5. Digestion protocol

Component	Vector Digestion	Amplicon digestion
DNA	5 µg (x µL)	Total gel extraction product (y µL)
SalI-HF	5 µL	5 µL
10X CutSmart buffer	5 µL	5 µL
DEPC water	(40-x) µL	(40-y) µL

SalI-HF digested pBABE-Hygro vector was run on gel and vector backbone was excised from the gel using E.Z.N.A.® Gel Extraction Kit according to manufacturer's instructions. Subsequently, gel extraction product was subjected to dephosphorylation

using Shrimp Alkaline Phosphatase (rSAP) according to manufacturer's instructions. PCR cleanup was performed on digested amplicon and dephosphorylated vector. Ligation of digested pBABE-Hygro and STK10 ORF was performed at room temperature for 2 hours using the protocol shown in **TABLE 2.6**. Vector and insert concentrations were calculated as follows:

$$Insert\ (ng) = Vector\ (50\ ng) * \frac{Insert}{Vector}\ molar\ ratio * \frac{Insert\ length}{Vector\ length}$$

Table 2.6. Ligation reaction protocol

Component	**Control**	**1:3**	**1:5**
T4 DNA Ligase	1.5 µL	1.5 µL	1.5 µL
10X T4 DNA Ligase Buffer	3 µL	3 µL	3 µL
SalI digested and dephosphorylated pBABE-Hygro vector	50 ng	50 ng	50 ng
SalI digested STK10 ORF amplicon	-	87 ng	145 ng
DEPC water	Up to 30 µL		

5 µL of ligation product from each group was transformed into E. coli *C3040I* strain bacteria using heat shock at 42ºC for 30 seconds. 800 µL LB media was added to transformed bacteria and left to incubate at 37ºC shaker at 200 RPM for 30 minutes. Following incubation, bacteria were spread onto LB agar plates containing 500 µg/mL ampicillin and incubated at 37°C overnight. Following day, 4 colonies from amplicon introduced groups (1:3 and 1:5) were picked and left to incubate in 5 mL LB-ampicillin media at 37ºC shaker at 200 RPM overnight. Plasmid was isolated from bacteria using E.Z.N.A.® Plasmid Mini Kit. Isolated plasmids were then digested with *HindIII-HF* to verify correct insert orientation. Vectors harboring ligands in correct orientation were selected and subsequently transfected into HEK293FT cells to

confirm functional STK10 expression referring to STK10 and p-ERM (STK10 substrate) levels.

2.2.4 Protein Biochemistry

2.2.4.1 Protein Isolation

Cell seeding and treatments were performed as previously described (*see Section 2.2.1.3*). Following incubation for either 24, 48 or 72 hours, medium was collected into 1.5 mL reaction tubes and centrifuged at 5.000 RPM for 5 minutes to collect apoptotic bodies. Meanwhile, wells were washed with 1 mL PBS and aspirated. Then, 40 µL RIPA was added per well. Cells were scraped while in RIPA buffer (see **TABLE 2.7** for buffer contents) for 1-2 minutes on ice. Next, scraped cells were transferred onto their respective reaction tubes and incubated on ice while being vortexed for 10 seconds every 5 minutes for a total of 15 minutes. After that, mixture was centrifuged at 14.000 RPM for 20 minutes. Supernatants containing protein were transferred into fresh 1.5 mL reaction tubes and stored at -80ºC for future experiments.

Table 2.7. Contents of RIPA lysis buffer

Ingredient	Stock Concentration	Final Concentration	For 1 mL
NaCl	2 M	150 mM	75 µL
NP-40	10%	1%	100 µL
Sodium DOC	10%	0.5%	50 µL
SDS	10%	0.1%	10 µL
Tris HCl (pH 8.0)	2 M	50 mM	25 µL
NAF	1 M	50 mM	50 µL

Na_3VO_4	100 mM	1 mM	10 µL
Protease inh.	25X	4%	40 µL
Phosphatase inh.	20X	4%	40 µL
ddH_2O			600 µL

2.2.4.2 Protein Quantification

Protein quantification was performed using Pierce™ BCA Protein Assay Kit. Nine standard solutions containing bovine serum albumin (BSA) between concentrations of 0-2 µg/µL were prepared. Standards and protein samples were added in duplicates in 96 well plate at a ratio of 7:1 (21 µL standard and 3 µL protein sample). 200 µL of Solution A and B mixture (50-parts Solution A and 1-part Solution B) was added onto the wells with protein and incubated at 37°C for 30 minutes. Absorbance at 562 nm was measured using SynergyHT microplate reader. Protein sample concentrations were determined by plotting a standard curve based on BSA standard readings.

2.2.4.3 Sodium Dodecyl Sulfate Polyacrylamide Gel Electrophoresis (SDS-PAGE)

Protein concentration between different samples were equalized by mixing calculated amounts of protein (15-20 µg per well), dH_2O and 4X protein loading dye (see **TABLE 2.8** for contents). Subsequently, the mixture was boiled at 95°C for 3 minutes to facilitate further linearization of protein domains. Stacking and resolving gels were prepared based on **TABLE 2.9**.

Table 2.8. Contents of 4X protein loading dye

Ingredient	Stock Concentration	Final Concentration	For 10 mL
Glycerol	100%	40%	4 mL
Tris HCl (pH 6.8)	1M	240 mM	2.4 mL
SDS	-	8%	0.8 g
Bromophenol blue	-	0.04%	0.004 g
β-mercaptoethanol	100%	5%	0.5 mL
ddH_2O			Up to 10 mL

Table 2.9. Contents of stacking and resolving gels.

Ingredient	8% resolving gel	10% resolving gel	5% stacking gel
dH_2O	2.3 mL	1.9 mL	1.36 mL
30% acrylamide mix	1.3 mL	1.7 mL	0.34 mL
1M Tris	1.3 mL (pH 8.8)	1.3 mL (pH 8.8)	260 µL (pH 6.8)
10% SDS	50 µL	50 µL	20 µL
10% APS	50 µL	50 µL	20 µL
TEMED	5 µL	5 µL	2 µL
Total volume	**5 mL**	**5 mL**	**2 mL**

For gel preparation, initially resolving gel was poured into Mini-Protean gel casting module and topped off with isopropanol to eliminate bubbles and level the gel. After polymerization, stacking gel was poured and either 10 well or 15 well comb was placed. 15-20 µg protein was loaded in 20 µL and 15 µL for 10 and 15 well combs, respectively. 1 and 1.5 µL protein ladder (Thermo Scientific PageRuler™ Plus Prestained Protein Ladder Product# 26619) was loaded in 10 and 15 well combs,

respectively. Electrophoresis was performed at 80V for 20 minutes and bumped up to 120V until tracking dye reached bottom of the gel.

2.2.4.4 Western Blotting

Proteins were transferred to PVDF membranes using semi-dry transfer method performed with Bio-Rad Trans-Blot® Turbo™ Transfer System. Whatman papers, 3 mm in thickness, were cut in 7 cm x 9 cm dimensions and 4X, 2x and 5x Whatman papers were dipped in Anode I, Anode II and Cathode buffers, respectively. PVDF membrane was activated in methanol for 3 minutes and then dipped in Anode Buffer II for a minute. Layers were stacked in transfer system cassette from bottom to top as follows: 4X Anode I buffer dipped Whatman papers, 2x Anode II buffer dipped Whatman papers, activated PVDF membrane (cut in 6.5 cm x 8 cm dimensions), the gel and 5x Cathode buffer dipped Whatman papers. Transfer was performed at 25V for 30 minutes.

After transfer was completed, the membrane was dipped in Ponceau S solution to assess transfer quality and left to incubate for 3 minutes with fast agitation. Membrane was then washed with dH_2O until Ponceau S stain is removed. Membrane was cut at appropriate molecular weights harboring protein of interest. Membrane fragments were blocked with either 5% (w/v) milk: TBST or 5% (w/v) BSA: TBST for an hour at room temperature with slow agitation. After blocking, membrane fragments were probed with appropriate primary antibodies overnight at +4°C with slow agitation. Following overnight incubation membranes were washed three times with TBST for 10 minutes each totaling to 30 minutes with fast agitation. Membrane fragments were

then incubated with appropriate secondary antibodies overnight at +4°C with slow agitation. Membranes were washed three times with TBST for 10 minutes each totaling to 30 minutes with fast agitation and then put in TBS buffer for CCD imaging. List of primary and secondary antibodies are given in **TABLE 2.10**.

Table 2.10. List of primary and secondary antibodies used

Antibody	Company	Catalog Number	Dilution
p-4EBP1	Cell Signaling Technology	CST 9451	1:2000
β-actin	Sigma-Aldrich	A5441	1:10.000
AKT	Cell Signaling Technology	CST 9272	1:1000
p-AKT (T308)	Cell Signaling Technology	CST 4056	1:1000
p-AKT (S473)	Cell Signaling Technology	CST 9018	1:1000
EGFR	Cell Signaling Technology	CST 2646	1:1000
ERα-F10	Santa Cruz Biotechnology	sc-8002	1:1000
p-ERM	Cell Signaling Technology	CST 3726	1:2000
HER2	Thermo Fisher Scientific	MA5-13105	1:1000
LOK (STK10)	Abcam	ab70484	1:2000
p-mTOR	Cell Signaling Technology	CST 5536	1:1000
PR	Santa Cruz Biotechnology	sc-7208	1:1000
S6	Cell Signaling Technology	CST 2217	1:4000
p-S6 (S235/236)	Cell Signaling Technology	CST 2211	1:4000
p-S6 (S240/244)	Cell Signaling Technology	CST 5364	1:4000
HRP-coupled anti-rabbit IgG	Cell Signaling Technology	CST 7074	1:10.000
HRP-coupled anti-mouse IgG	Cell Signaling Technology	CST 7076	1:10.000

2.2.4.5 CCD Imaging of Membranes

Membrane images were captured using Amersham™ Imager 600. Membrane fragments were placed in white bottom tray and ECL reagents were mixed in 1:1 ratio and applied onto the membranes. Tray was then placed in the upper position. Membranes were exposed in "Auto" capture mode. Captured TIFF images were then imported to Bio-Rad Image Lab software version 6.0.1 and automatically background-corrected for improved clarity.

2.2.5 Developing Stable Cells Using Retroviral Transduction

For viral production, HEK293-FT cells were seeded to 70% confluency. Two mixtures were prepared. First one contained DNA mixture of 1 µg pCMV-VSV-G (envelope protein), 1 µg gag/pol packaging plasmid and 2 µg of pBABE-Hygro-STK10 vector in 250 µL DMEM. Second one contained 5 µL lipofectamine in 250 µL DMEM. DNA content tube was mixed with lipofectamine tube and incubated at room temperature for 15 minutes. Following incubation, wells containing HEK293-FT cells were aspirated and 1.5 mL DMEM containing 8% (v/v) FBS was added. 500 µL from the final mixture was added dropwise to the corresponding wells. Next day, cell media was replenished, and first viral particles were harvested 24 hours following media replenishment. Meanwhile wild-type MEF and HMEC cells were seeded onto 6 well plates at a density of 70% confluency. Second harvest was collected 24 hours later and pooled together with the initial harvest in a 15 mL reaction tube. Viral harvest was then filtered with 0.45 µm filter and subsequently mixed with polybrene (1:1000). Media of MEF and HMEC cells were aspirated and 1 mL of viral mixture was added onto their corresponding wells. Next day, viral media was aspirated, and suitable

media was added for MEF and HMEC cells. Cells transduced with the virus were selected using hygromycin for over a period of 2 weeks. Following selection, stable overexpression of STK10 was validated using western blot.

2.2.6 Bioinformatics and Statistical Analyses

Data from METABRIC and GEO datasets GSE17785, GSE48216 were utilized in this work. Mantel-Cox test was used to calculate significance in survival analyses of patients. Two experimental groups were compared using 2-tailed Student's t-test. Multiple t-test was used for grouped analyses. Graphs were prepared using GraphPad software (GraphPad software Inc., La Jolla, CA, USA). Significance thresholds were denoted as * $p<0.05$, ** $p<0.01$, *** $p< 0.001$, where significant and applicable.

CHAPTER 3

RESULTS

3.1 Identification of STK10 as a Potential Sensitizer for PI3K Pathway Inhibitor Resistance

Recent work by Castel et. al and Le et. al [46,49] have associated known kinases with resistance to PI3Kα inhibition *via* AKT-independent mechanisms. Roles of such kinases in cancer have since been overlooked, as AKT has been viewed as the main branch where PI3K pathway mediates tumorigenesis. Identification of new molecular targets provide novel therapeutic approaches to combat PI3Kα resistance in breast cancer. With this line of thinking our study aimed to identify genes that can confer resistance to PI3Kα inhibition in an AKT-independent manner.

In order to identify genes potentially involved in PI3K pathway resistance in an AKT-independent manner, we initially utilized a dataset that has mRNA expression data from a collection of 84 breast cancer cell lines, out of which 70 of them has been tested for response to 138 compounds (**Figure 3.1)** [59]. After filtering differentially expressed mRNA in PI3K mutant breast cancer cell lines based on sensitivity to PI3K/AKT/mTOR inhibition, we ended up with 196 genes upregulated in resistant *PIK3CA* mutated cell lines. Subsequently, to filter out genes related to AKT signaling, we used patient phospho-proteomics data coupled to mRNA expression data [60] and eliminated genes positively correlated with AKT phosphorylation (Pearson correlation coefficient > 0.15). This further reduced our gene count to 150. To further narrow our gene list, we performed survival analyses using METABRIC dataset and

identified 12 genes predicting survival in *PIK3CA* mutated patients. Finally, we utilized data from a paper by Wallin and colleagues [61] which includes mRNA expression data (GSE17785) from MCF10A cells that were over-expressing mutant PI3K (H1047R). We identified STK10, whose expression levels were significantly upregulated upon expression of ectopic mutant PI3K compared to control cells (**Figure 3.1**).

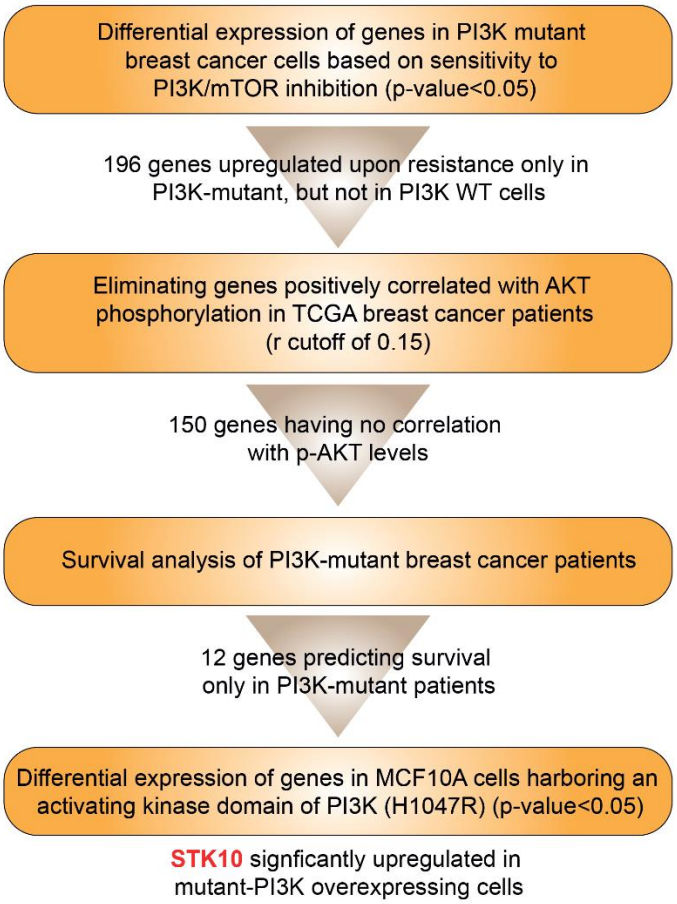

Figure 3.1. Identification of STK10 as a potential target for PI3K pathway inhibitor resistance, independent of AKT. Workflow of bioinformatical analyses for identification of STK10 with potential involvement in PI3K/AKT pathway inhibitor resistance in an AKT-independent manner.

When reviewed in an STK10-exclusive manner, cell line data shows STK10 significantly elevated in cell lines resistant to Sigma AKT1-2 inhibitor (**Figure 3.2A left panel**) and GSK1059615, PI3K-mTOR inhibitor (**Figure 3.2A right panel**) [59]. Furthermore, METABRIC data suggests that STK10 expression predicts overall survival in both *PIK3CA* mutant and wild type patients, albeit to a lesser extent in the latter. Patients with elevated STK10 levels show poorer survival (**Figure 3.2B**). STK10 mRNA levels were also found to be elevated in MCF10A cells transfected with kinase domain mutant *PIK3CA* (H1047R) expressing vector compared to un-transfected cells. Vector and PIK3CA inhibitor (GDC-0941) combination resulted in a decrease in STK10 mRNA levels [61].

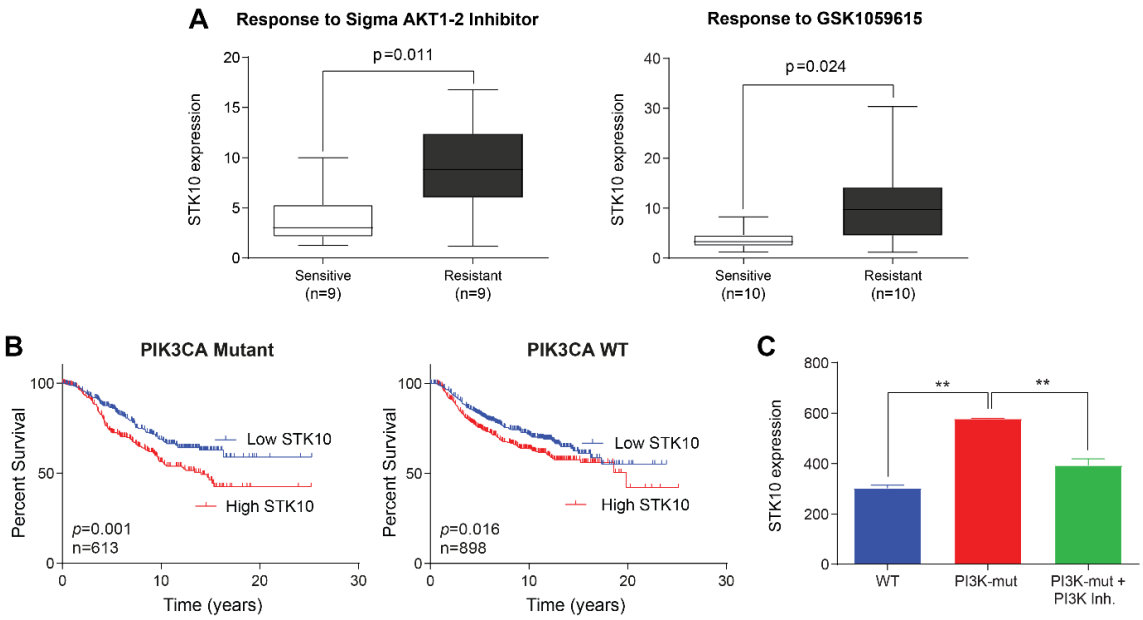

Figure 3.2. STK10-exclusive review of the bioinformatical data (A) STK10 expression in cell lines either resistant or sensitive towards Sigma AKT1-2 inhibitor (left panel) and GSK1059615 (PI3K-mTOR inhibitor) (right panel) [59]. **(B)** Kaplan-Meier plot showing the effects of STK10 expression levels on patient survival in

breast cancer patients with either mutated or wild-type *PIK3CA*. **(C)** STK10 mRNA levels upon expression of mutant PIK3CA (H1047R) in MCF10A cells (GSE17785) [61].

Lack of α-specific inhibitor resistance expression dataset forced us to use mRNA data from cells treated with PI3K-mTOR dual inhibitor GSK1059615 and AKT1-2 inhibitor. However, given p110α is the isoform transducing majority of PI3K signaling, we reasoned that this data might also be applicable to α-specific PI3K inhibition [62].

To confirm data from **Figure 3.2C**, we treated MCF7 (*PIK3CA*-mutant: E542K and E545K) and T47D cells (*PIK3CA*-mutant: H1047R) [63] with BYL-719 for 72 hours. STK10 levels were reduced markedly as a result of BYL-719 inhibition.

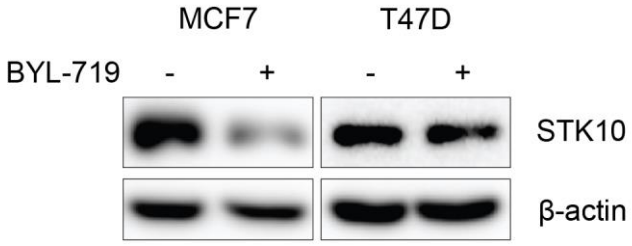

Figure 3.3. STK10 levels are reduced upon BYL-719 treatment. MCF7 and T47D cells were treated with BYL-719 for 72 hours. Beta-actin is used as loading control.

To summarize, our bioinformatical analyses revealed STK10 kinase to be potentially involved in PI3K pathway in an AKT-independent manner. We also demonstrated that

STK10 levels are decreased upon PI3Kα inhibition, further supporting our bioinformatical data.

3.2 Selecting the Most Suitable Cell Lines for Further Studies with STK10

To identify the most suitable breast cancer cell model to study cellular functions of STK10, we collected lysates from a multitude of breast cancer cells and performed Western blot (**Figure 3.4**). At first glance, we observed that STK10 is expressed mostly in MDA-MB-436 cells, which is a *PIK3CA* WT cell line. Even though it contradicts with our initial bioinformatical analyses, we reasoned that being a PTEN-null model [64] it will have an overactive PI3K pathway. Moreover, MDA-MB-436 cells are shown to be highly resistant to α-specific PI3K inhibition by BYL-719 [65] and having such high levels of STK10 make MDA-MB-436 cells a perfect model to assess roles of STK10 in *de novo* PI3Kα resistance.

To identify another TNBC cell line that can complement studies with MDA-MB-436 cell line, we selected BT20 cell line, which has moderate amount of STK10 expression within our breast cancer cell line panel. Having relatively lower levels of STK10 made BT20 cell line a preferred model to study STK10 overexpression. Moreover, BT20 cells are also shown to be mildly resistant to α-specific PI3K inhibition by BYL-719 [65]. In addition, BT20 cells harbor two different *PIK3CA* mutations, C1616G in exon 9 which corresponds to kinase domain and A3140G in exon 20 which is located within the helical domain. The protein product therefore has P539R and H1047R mutations, making BT20 cell line a suitable model considering the starting point of our bioinformatical analyses [66].

Luminal A cell lines such as MCF7 and T47D also display moderate levels of STK10. Both cells have *PIK3CA* mutations, MCF7 cells harbor kinase domain E542K and E545K mutations and T47D cells harbor helical H1047R mutation [63]. These cell models are of another importance since FDA has recently approved α-specific PI3K inhibitor Alpelisib (BYL-719) to be used on PI3K mutant, hormone receptor positive patients in combination with fulvestrant. Developing BYL-719 resistant counterparts of these cells, being both *PIK3CA* mutant and hormone receptor positive, can potentially shed light on novel resistance mechanisms that can be beneficial for the patient subset that does not respond well to the drug. Inhibitors developed for the molecular targets to be identified from these cells can be used in combination with BYL-719 to improve drug response, thus aiding tumor recession. Therefore, we started developing BYL-resistant cells from MCF7 and T47D cells v*ia* chronic BYL-719 treatment, which will be reviewed in second part of this thesis.

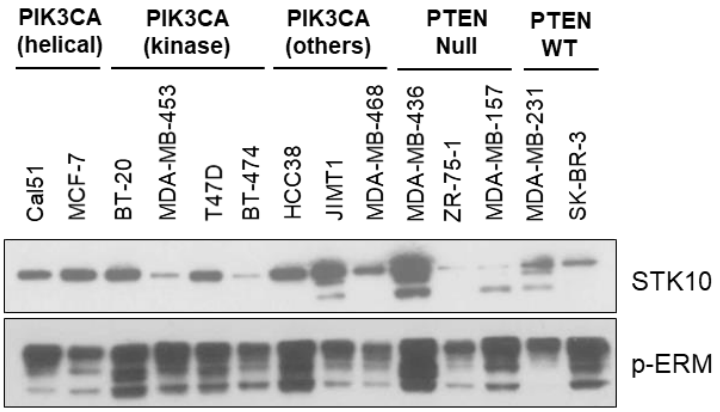

Figure 3.4. Western blot analysis of lysates obtained from a panel of breast cancer cell lines. p-ERM is used as an activity marker for STK10.

Next, we wanted to validate our Western blot results (**Figure 3.4**) referring to some datasets with cell line mRNA expression data. We utilized data from The Cancer Cell Line Encyclopedia (CCLE) [67]. Grouping breast cancer cell lines based on their subtype revealed that *STK10* mRNA is mostly expressed in TNBC cell lines followed by Luminal A cell lines (**Figure 3.5**). We can again see that MDA-MB-436 cells have the highest STK10 mRNA expression. BT20 expression data is not available.

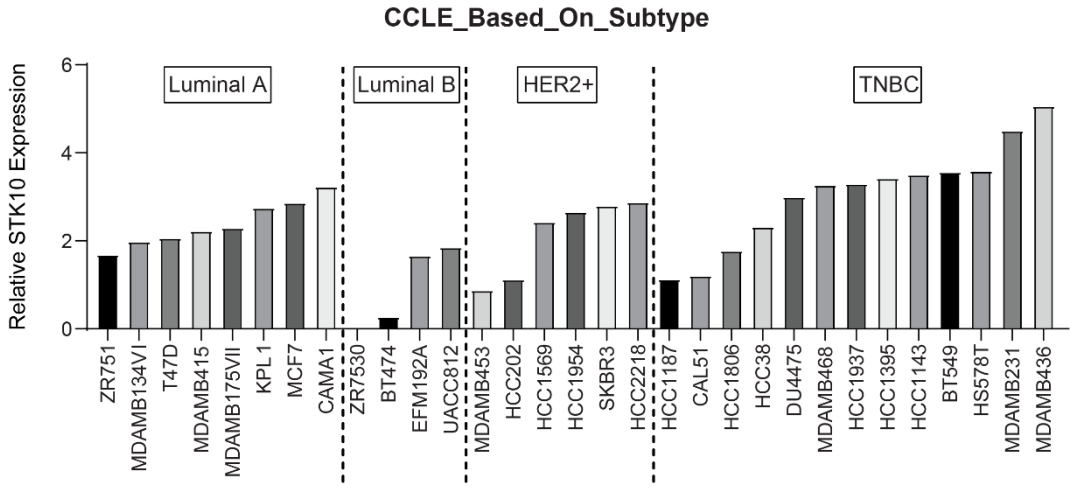

Figure 3.5. STK10 mRNA expression levels in a panel of breast cancer cell lines. Cell line data was separated based on subtype. mRNA expression data was obtained from The Cancer Cell Line Encyclopedia (CCLE).

After deciding which cell models to conduct our study on, we first wanted to validate whether STK10 knockdown sensitizes TNBC cell line MDA-MB-436 to α-specific PI3K inhibition by BYL-719, we transfected cells with siRNA specific to STK10 and then combined it with BYL-719 inhibition. **Figure 3.6** shows the results of cell viability assay. Combination of STK10 siRNA with BYL-719 inhibition showed better growth inhibition compared to single agent inhibition at both 7.5 and 10 μM of

BYL-719. STK10 siRNA sensitized MDA-MB-436, which is a *de novo* resistant cell line to BYL-719, towards BYL-719.

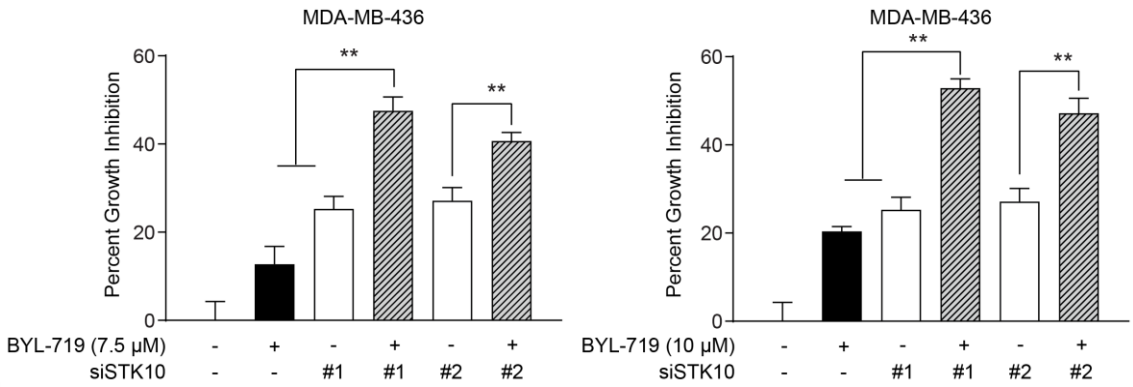

Figure 3.6. STK10 knockdown sensitizes MDA-MB-436 cells to BYL-719. MDA-MB-436 cells were treated with either 7.5 µM (left panel) or 10 µM (right panel) BYL-719, 24 hours following transfection with STK10 siRNA. Viability readings were measured 72 hours following drug treatment in triplicates.

Next, we wanted to determine whether this sensitization effect is driven through the PI3K pathway. Indeed, combination of especially siSTK10 #1 and BYL-719 resulted in marked reduction of S6 phosphorylation, an mTOR activity marker downstream, at both Serine 235/236 and Serine 240/244 (**Figure 3.7A**). Similarly, 4EBP1 phosphorylation, another mTOR downstream marker, was also reduced upon combination. Interestingly though one can see that combination also affected AKT phosphorylation at Threonine 308 residue, which rather contradicts with our initial hypothesis where STK10 was thought to act within the PI3K pathway, but independent of AKT.

Even though MDA-MB-436 cells have already high endogenous STK10 expression, we wanted to see whether overexpression of STK10 with a vector can affect mTOR downstream targets such as S6 and 4EBP1. Therefore, we overexpressed STK10 and combined it with BYL-719 inhibition (**Figure 3.7B)**. The aim was to test whether STK10 overexpression can rescue mTOR downstream targets from inhibitory effects of BYL-719. However, we failed to observe any change in phosphorylation levels of S6 and 4EBP1 upon exogenous STK10 expression.

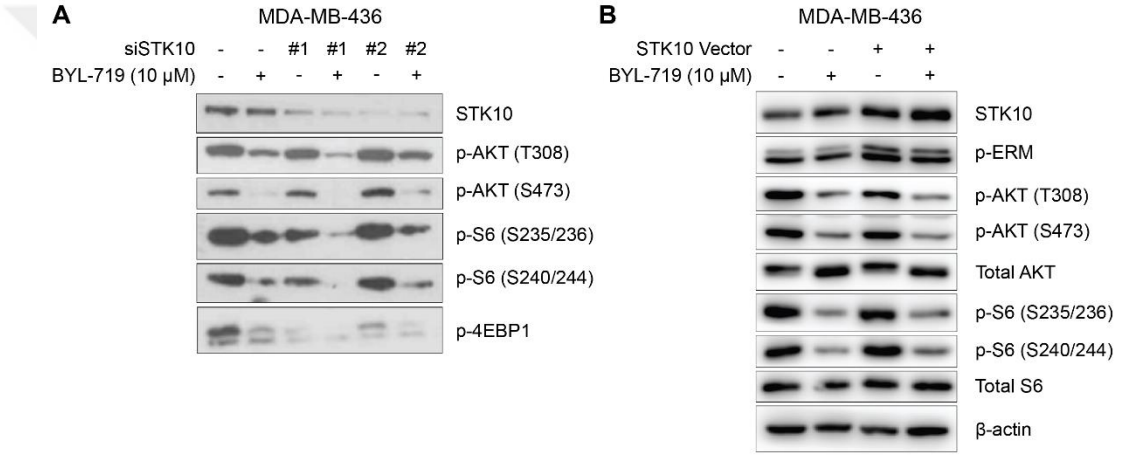

Figure 3.7. Western blot analysis of MDA-MB-436 cells showing expression levels of various PI3K/AKT pathway markers upon combination of BYL-719 with (A) STK10 siRNA and (B) STK10 overexpression vector. BYL-719 treatment was performed for 4 hours.

We then moved on to our next TNBC cell line model BT20. We again performed cell viability assay with STK10 siRNA transfection in combination with BYL-719 inhibition (**Figure 3.8**). Similar to the results obtained with MDA-MB-436 cells, the

combination of siSTK10 #1 and BYL-719 showed better growth inhibition and sensitized BT20 cells to BYL-719 inhibition.

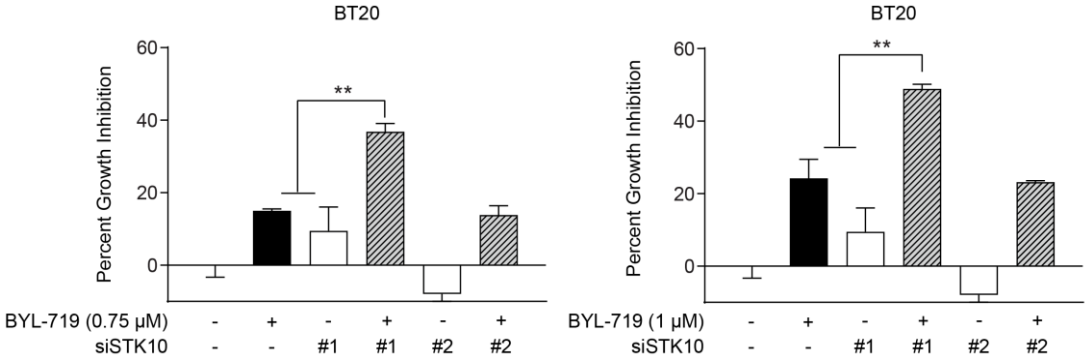

Figure 3.8. STK10 knockdown sensitizes BT20 cells to BYL-719. BT20 cells were treated with either 0.75 µM (left panel) or 1 µM (right panel) BYL-719, 24 hours following transfection with STK10 siRNA. Viability readings were measured 72 hours following drug treatment in triplicates.

We then wanted to check changes in PI3K pathway upon combination of STK10 siRNA with BYL-719 treatment. According to our hypothesis, we expected to observe further decrease in phosphorylation levels of mTOR downstream targets (**Figure 3.9A**). Unfortunately, this time downstream markers of mTOR activity such as S6 and 4EBP1 phosphorylation were not altered upon combination of siRNA and BYL-719. This led us to think that initial effects observed with MDA-MB-436 cell might be cell line-specific. We then used our stably STK10 overexpressing BT20 cells to check whether STK10 can rescue mTOR downstream signaling from inhibitory effects of BYL-719. Similar to the effects observed with the siRNA experiment, stably STK10 overexpressing BT20 cells also showed no alteration to signaling when coupled with BYL-719 treatment. In other words, STK10 overexpression failed to rescue inhibition

of mTOR downstream targets, such as S6 and 4EBP1 (**Figure 3.9B**). Interestingly, mTOR phosphorylation was rescued in STK10 overexpressing cells compared to controls; however, the same effect was not relayed to downstream targets. Even though STK10 siRNA was able to sensitize BT20 cells to BYL-719, this effect seems to rather be propagated *via* another pathway, possibly parallel to PI3K specific to this cell line.

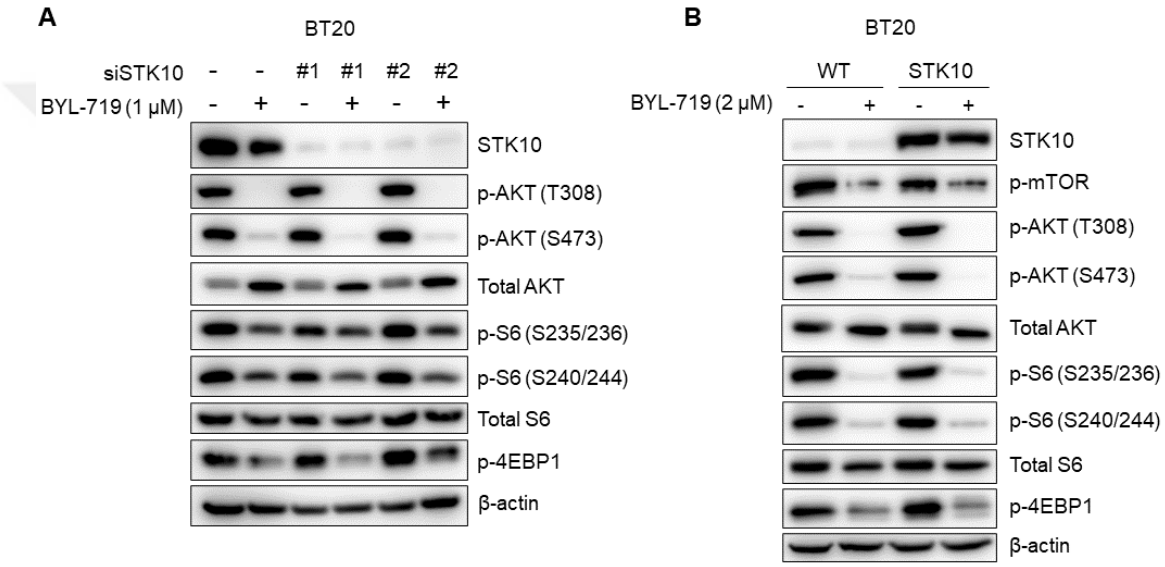

Figure 3.9. Western blot analysis of BT20 cells showing expression levels of various PI3K/AKT pathway markers upon combination of BYL-719 with (A) STK10 siRNA and (B) stable STK10 over-expression. BYL-719 treatment was performed for 4 hours.

We also utilized our stably STK10 overexpressing BT20 cells to test whether STK10 overexpression could lessen the inhibitory effects imposed by BYL-719. Control and BT20.STK10 cells (STK10-overexpressing counterpart) were seeded onto 96 well plates and treated them with various doses of BYL-719 (**Figure 3.10**). We then

performed SRB cell viability assay. We showed that STK10 overexpression did not provide any survival benefit to BT20 cells in the presence of BYL-719.

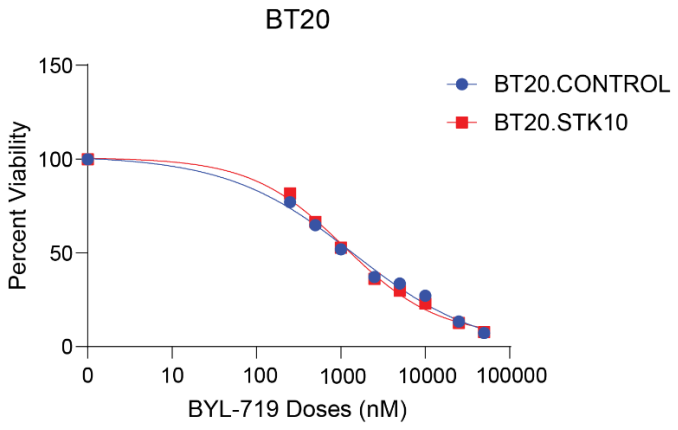

Figure 3.10. SRB cell viability analysis of BT20.Control and BT20.STK10 cells upon BYL-719 treatment. Cells were treated with varying doses of BYL-719 (0.25, 0.5, 1, 2.5, 5, 10, 25 and 50 µM) for 72 hours. Cell viability was measured in triplicates.

SUMMARY

To summarize, we observed significant increase in growth inhibition upon combination of siSTK10 and BYL-719 in both MDA-MB-436 and BT20 cells. These effects seem to arise from reduction of residual mTOR downstream signaling in combination for MDA-MB-436 cells. However, we failed to reproduce the same pathway inhibition in BT20 cells suggesting possible involvement of cell type specific effects. In addition, overexpression of STK10 in both cell lines did not rescue mTOR downstream inhibition when coupled with BYL-719 treatment. We reasoned that inherent genomic alterations accumulated by these cell lines might be resulting in phenotypes, such as having over-active PI3K pathway, and consequently masking

possible effects of STK10 within the cellular environment. Therefore, we decided to continue our study with untransformed cells.

3.3 Investigation of Potential Roles of STK10 in Untransformed Cells

For our study in untransformed cells, we selected human mammary epithelial cell line, HMEC and mouse embryonic fibroblast cell line, MEF. These cells have relatively unaltered (quasi-normal) signaling pathways, therefore provide better cellular environment to study roles of STK10. Moreover, HMEC cell line is of epithelial lineage and MEF cells are of mesenchymal lineage which will us to decipher physiological functions of STK10 in different tissue types.

3.3.1 Functional Validation of Retroviral pBABE-Hygro-STK10 Vector Product

To assess role of STK10 within the cells, we transduced HMEC and MEF cells with retroviral particles and performed selection for two weeks. At the end of selection, lysates were collected, and Western blot analysis was performed. We were able to observe significant increase in STK10 levels in both cell lines (**Figure 3.11**). This was also accompanied with an elevation of p-ERM levels, an STK10 substrate, indicating presence of functional protein product.

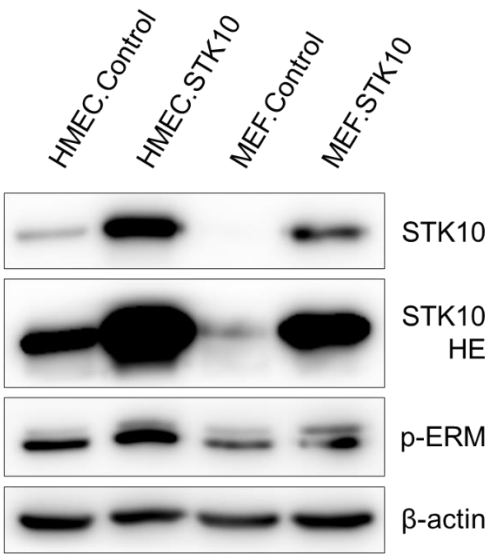

Figure 3.11. Western blot analysis of HMEC and MEF cells stably overexpressing STK10. p-ERM was used as STK10 activity marker and beta-actin was used as loading control (HE: High exposure).

3.3.2 Investigation of Possible Involvement of STK10 within the PI3K Pathway

To understand role of STK10 within the PI3K pathway, we starved MEF and HMEC cells stably overexpressing STK10 and performed BYL-719 pre-treatment 30 minutes prior to stimulation (**Figure 3.12**). We hypothesized that we would observe rescue in phosphorylation levels of PI3K pathway components, especially mTOR downstream targets in presence of STK10.

In STK10 overexpressing MEF cells, we observed rescue of p-AKT, p-S6 and p-4EBP1 levels (**Figure 3.12A**). Residual AKT activation was present in starved condition of STK10 overexpressing MEF cells, compared to no signal in control MEF

cells (lane 4 versus lane 1). p-S6 (S240/244) levels were also rescued in STK10 overexpressing MEF cells when BYL-719 inhibited cells were stimulated with 4% FBS (lane 3 versus lane 6). However, the most notable difference was observed in p-4EBP1 levels. Even during starved condition, STK10 overexpressing cells were able to maintain residual levels of 4EBP1 phosphorylation, which was also protected from inhibitory effects of BYL-719.

HMEC cells, on the other hand, displayed a much different phenotype. Even though we observed increase in phosphorylation levels of PI3K pathway components, having STK10 present in the system did not affect downstream signaling under BYL-719 inhibition (**Figure 3.12B**). Even a further decrease in p-S6 levels were observed compared to control cells. STK10 was only able to rescue the decrease in p-ERM levels during starvation, where STK10 overexpressing cells had undisturbed p-ERM levels comparing lanes 1 and 4, and during drug-stimulation combination treatment, where p-ERM levels are higher in lane 6 compared to lane 3.

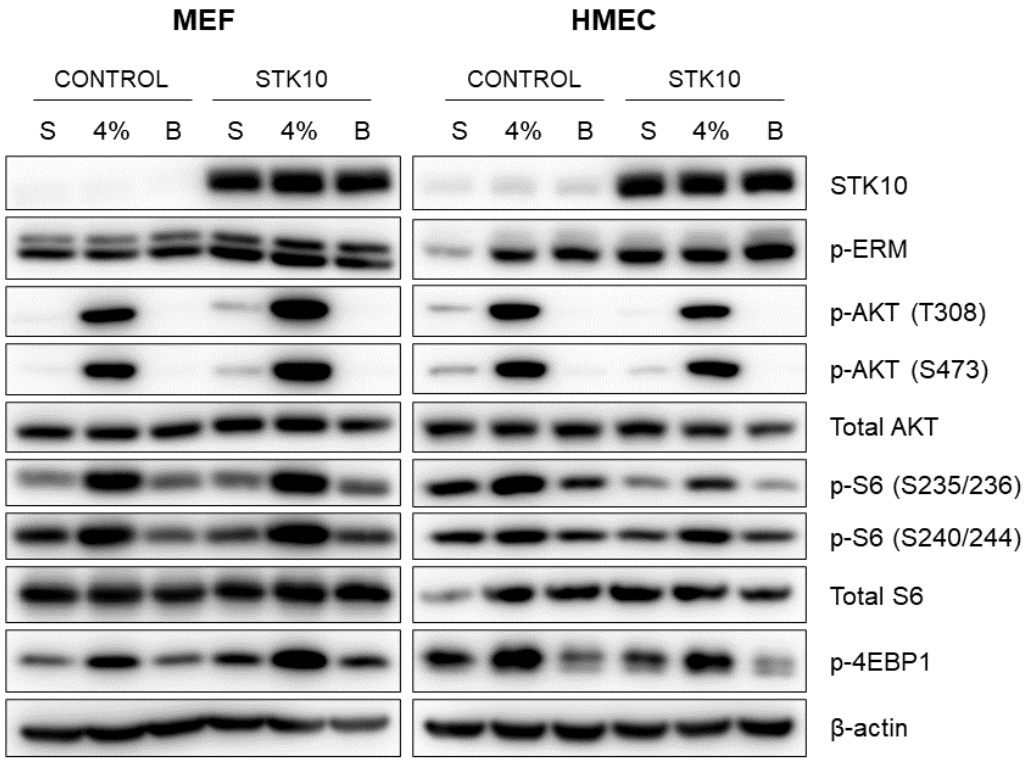

Figure 3.12. Western blot analysis of PI3K pathway components in starved (A) MEF and (B) HMEC cells stably overexpressing STK10 stimulated with 4% FBS for 10 minutes. BYL-719 pre-treatment was performed 30 minutes prior to FBS induction. (S: Starved, 4%: 4% FBS induction, B: BYL719 pre-treatment). Beta-actin was used as loading control.

FBS contains multitude of different growth factors, thus results in activation of different pathways at once. To add further specificity to those activated pathways, we used the same setup from **Figure 3.12**, but this time we used insulin which specifically activates PI3K and MAPK signaling downstream of insulin receptor A (IR-A), insulin receptor B (IR-B) and insulin-like growth factor receptor 1 (IGF-1R) through Shc and IRS1/2 adaptor proteins [68] (**Figure 3.13**). When stimulated with insulin, in both cell lines, STK10 overexpression failed to rescue BYL-719 mediated inhibition of PI3K

pathway components, suggesting STK10 is not involved with signaling downstream of IR-A, IR-B or IGF-1R.

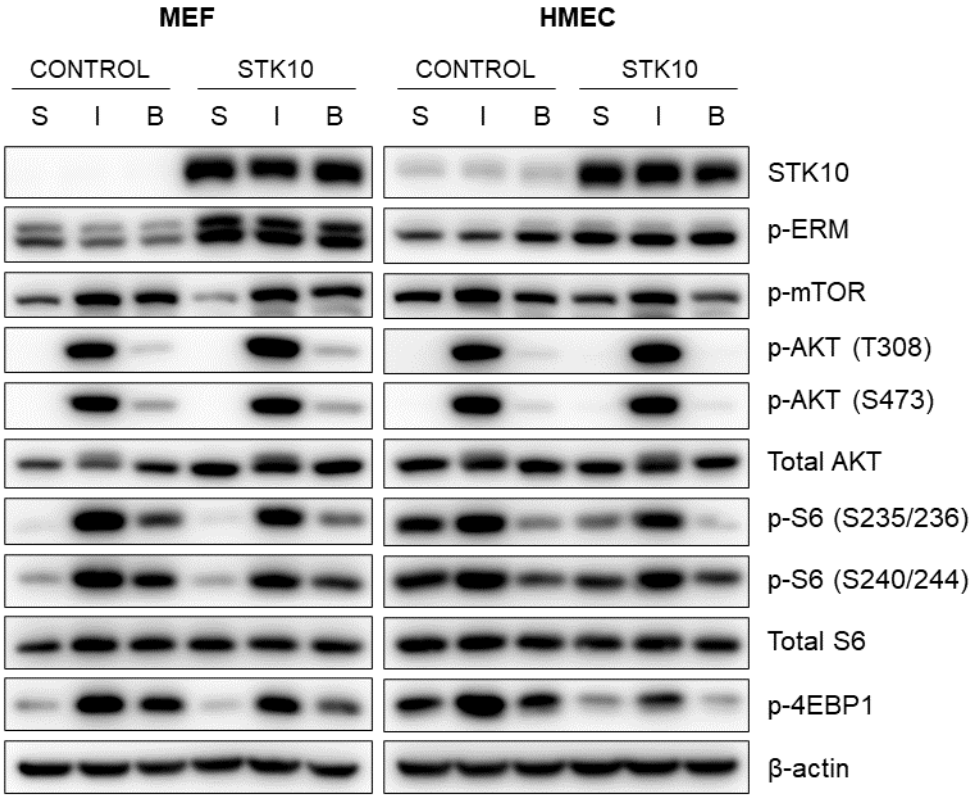

Figure 3.13. Western blot analysis of PI3K pathway components in starved (A) MEF and (B) HMEC cells stably overexpressing STK10 stimulated with 2 µg/mL insulin for 10 minutes. BYL-719 pre-treatment was performed 30 minutes prior to FBS induction. (S: Starved, I: 2 µg/mL insulin stimulation, B: BYL719 pre-treatment). Beta-actin was used as loading control.

We also stimulated cells with epidermal growth factor (EGF) in a similar setting (**Figure 3.14**). Stimulation of EGFR leads to activation of PI3K pathway and as well as RAS/RAF/MEK/ERK pathway [69]. Similarly, we failed to observe any rescue in

phosphorylation levels of AKT, S6 or 4EBP1. One can say that STK10 is not located downstream of EGF receptor family.

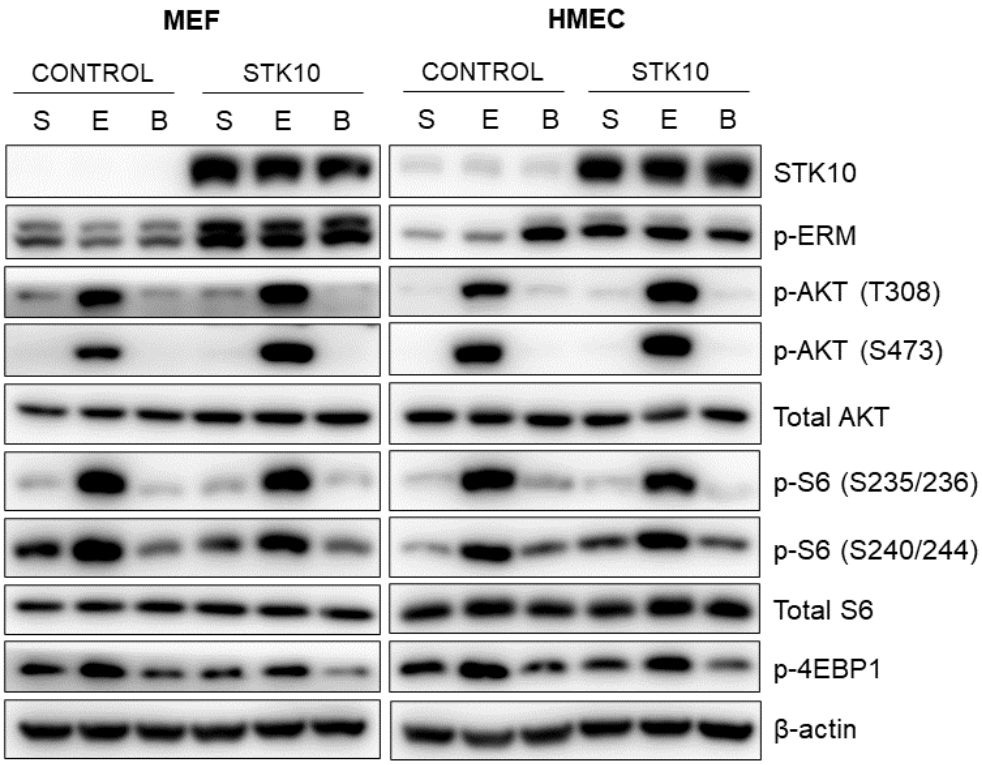

Figure 3.14. Western blot analysis of PI3K pathway components in starved (A) MEF and (B) HMEC cells stably overexpressing STK10 stimulated with 20 ng/mL EGF for 10 minutes. BYL-719 pre-treatment was performed 30 minutes prior to FBS induction. (S: Starved, E: 20 ng/mL EGF stimulation, B: BYL719 pre-treatment). Beta-actin was used as loading control.

We then wanted to test whether STK10 overexpression confers any resistance to BYL-719. We treated control and STK10 overexpressing cells with various doses of BYL-719 and observed that similar to the results with TNBC cell lines, STK10

overexpression did not provide any survival benefit to HMEC and MEF cells as well (**Figure 3.15A and B**).

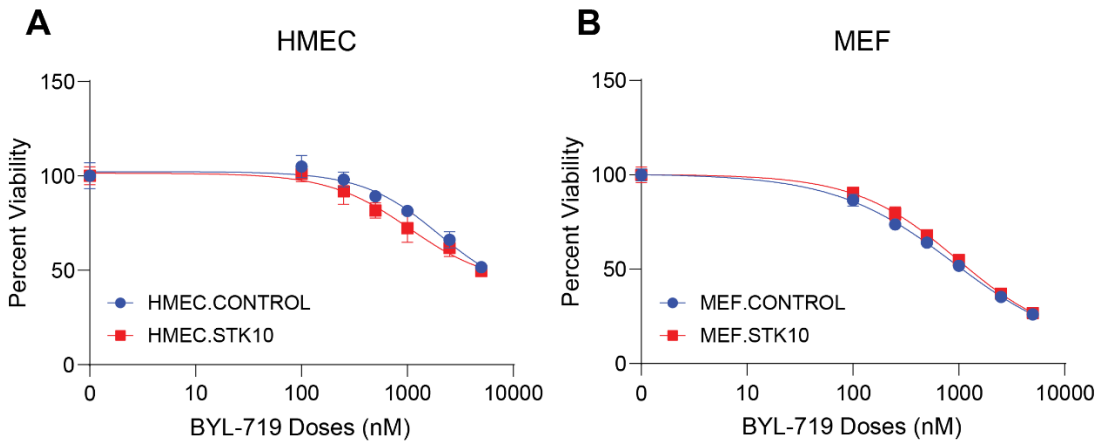

Figure 3.15. SRB cell viability assay performed on (A) HMEC and (B) MEF cells stably overexpressing STK10. Cells were treated with varying doses of BYL-719 (0.1, 0.25, 0.5, 1, 2.5 and 5 µM) for 72 hours. Cell viability was measured in quadruplets.

3.3.3 Investigation of STK10 as a Potential Oncogene

We then directed our focus to potential roles STK10 might have as an oncogenic factor. Initially, we wanted to study whether STK10 can promote anchorage-independent growth of these cell lines. So, in order to assess whether STK10 can promote anchorage-independent growth and induce transformation in HMEC and MEF cells, we performed soft agar growth assay utilizing our stable STK10 overexpressing cells. Our expectation was to observe an increase in colony forming capabilities of these cell lines; however, no difference in colony number was observed in stable STK10 overexpressing cells and controls (**Figure 3.16**).

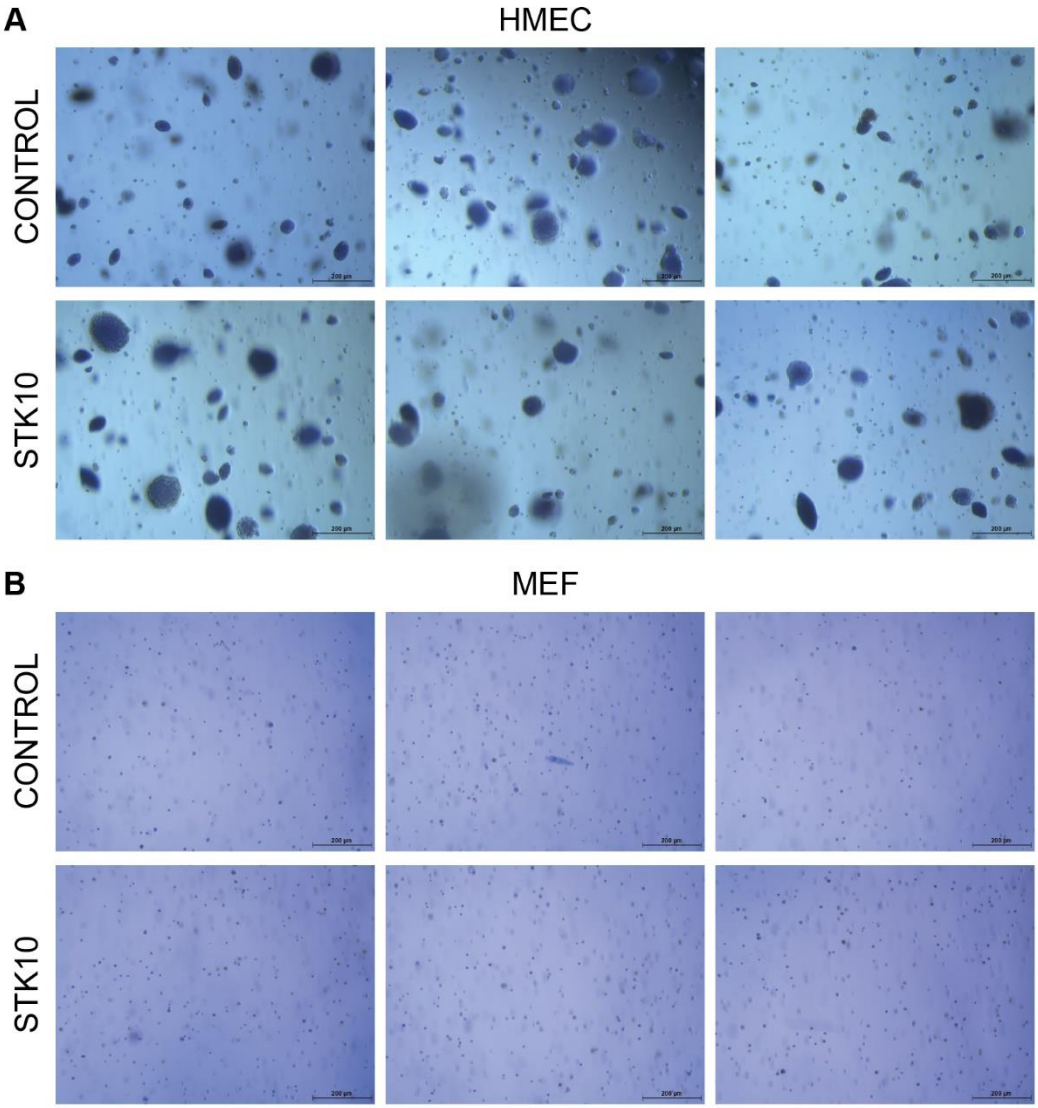

Figure 3.16. Colony formation assay showing colony formation capabilities of (A) HMEC and (B) MEF cells stably overexpressing STK10. Cells were seeded in triplicates and grown in soft agar for three weeks.

We then wanted to test whether STK10 had any effect on growth rate of our stable cells. Therefore, we performed 2D growth assay and plotted cellular growth over a period of 48 hours and determined cell growth using crystal violet stain (**Figure 3.17**). We observed that in both cell lines STK10 overexpression led to an increased growth

rate compared to control cells. The effect on growth rate was most notable with HMEC cells (**Figure 3.17A**).

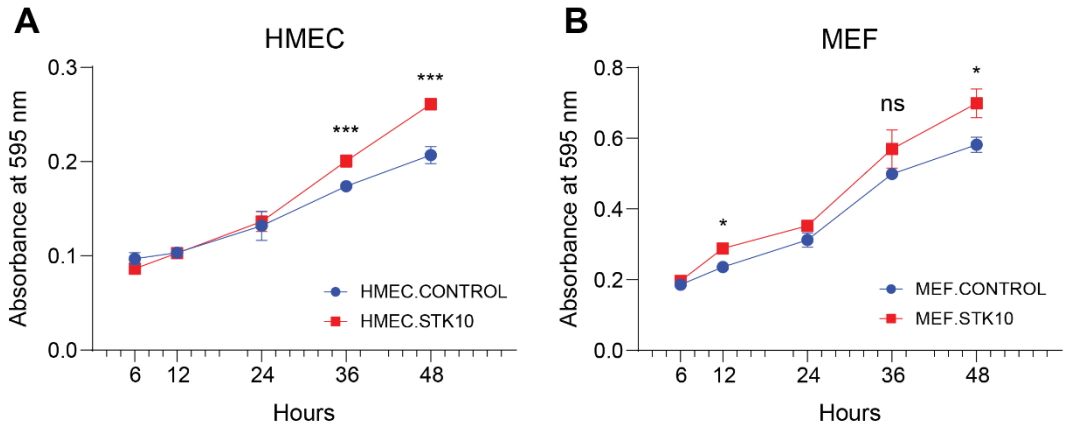

Figure 3.17. 2D growth assay performed on (A) HMEC and (B) MEF cells stably overexpressing STK10. Absorbance at 554 nm was measured in triplicates. Significance denoted as: *** $p<0.001$, ** $p<0.01$ and * $p<0.05$.

To test whether STK10 can modulate migratory capabilities of cells, we performed scratch assay with MEF cells. STK10 overexpressing cells did not show any enhancement of migratory capabilities compared to controls (**Figure 3.18**). Small difference observed in the graph can possibly be attributed to increased growth rate of stable STK10 overexpression (refer to **Figure 3.17B**). Furthermore, when BYL-719 was present in the culture medium, STK10 overexpression did not provide any migratory benefit over control cells.

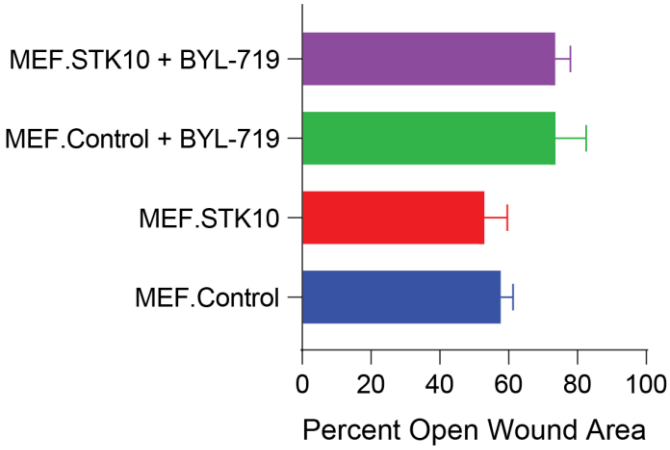

Figure 3.18. Scratch assay comparing migratory capabilities of MEF.Control and MEF.STK10 cells. Cells were seeded in triplicates and mean percent open wound area was calculated automatically by TScratch software comparing open wound area at wound introduction and 12 hours following wound introduction [58].

SUMMARY

Overall, our studies with untransformed HMEC and MEF cells revealed that STK10 might be involved with the PI3K pathway through a receptor currently unknown to us, exclusively in MEF cells, again underlining cell type-specific nature of the kinase. STK10 overexpression alone was not enough to transform these cell lines. Consistently, both cell lines had their growth rates increased when STK10 is overexpressed, albeit this did not confer any resistance to PI3Kα inhibition by BYL-719 nor did it provide any migratory benefits.

3.4 Development and Characterization of BYL-719 Resistant Breast Cancer Cell Line Models

3.4.1 Developing BYL-719 Resistant Cell Line Models

Luminal breast cancer is the most common subtype among all breast cancer incidents, comprising about 75% of all patients [70]. Endocrine therapy has been the standard of care treatment for hormone receptor positive breast cancer patients with main goal of estrogen deprivation. There are multiple options to be used as first-line therapy for HR+ breast cancer patients; these can be divided into 3 main subgroups: selective estrogen receptor modulators (SERMs), aromatase inhibitors (AIs) and selective estrogen receptor down regulators (SERDs). Briefly, SERMs are estrogen receptor agonist or antagonist molecules depending on the tissue. Binding of a SERM to ER dictates whether ER will be coupled with a coactivator or corepressor. Known SERMs for metastatic breast cancer are tamoxifen and toremifene [71]. Unlike SERMs, AIs reduce estrogen levels in the plasma by targeting aromatases, which are responsible for converting androgenic substrates to estrogens. Some known AIs are letrozole and anastrozole [72]. SERDs such as fulvestrant are developed to eliminate risks associated with agonist and antagonistic effects of SERMs. SERDs competitively bind to ER and impair receptor dimerization, consequently blocking localization of ER to nucleus [73]. Nevertheless, all the drugs mentioned above are still prone to drug resistance. One of the most frequent mechanisms of resistance to endocrine therapy is overactivated PI3K pathway [74]. As such many clinical trials combine endocrine therapy with PI3K pathway inhibitors.

Alpelisib (BYL-719) has been approved by the FDA to be used in combination with fulvestrant following the successful clinical trial on 572 patients who had HR-positive and HER2-negative breast cancer and had received/receiving aromatase inhibitor treatment. The drug combination proved to increase survival of those patients that had PIK3CA mutations [38]. However, like all drugs BYL-719 is also prone to *de novo* or acquired mechanisms of resistance. We investigated *de novo* mechanisms of resistance towards BYL-719 in the first part of this thesis. Now, in order to study possible mechanisms of acquired BYL-719 resistance, we utilized MCF7 and T47D cell lines, which harbor helical E545K and catalytic H1047R PIK3CA mutations, respectively [63]. This renders them a perfect model to study acquired BYL-719 resistance in a clinically relevant manner.

MCF7 and T47D wild type cells at low passage were tested for BYL-719 response, IC25 for these cell lines were found to be around 3.0 µM and 0.2 µM, respectively (**Figure 3.19**).

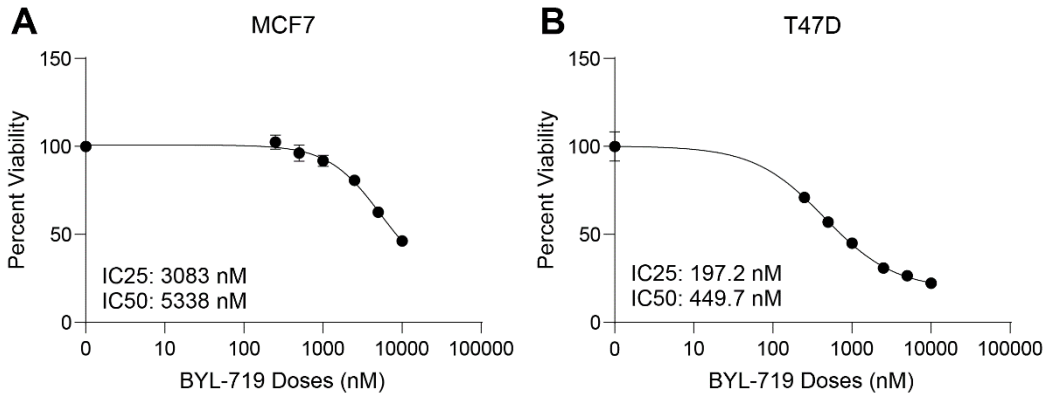

Figure 3.19. SRB cell viability assay showing respective IC25 and IC50 values of low passage MCF7 and T47D cells against BYL-719. Cells were treated with

various doses of BYL-719 (0.25, 0.5, 1, 2.5, 5 and 10 µM) for 72 hours. Cell viability was measured in quadruplets.

To develop acquired BYL-719 resistance, MCF7 and T47D cells were separated into two cohorts. Wild type labeled cells only received DMSO (vehicle), meanwhile MCF7 and T47D BYLR (BYL-719 resistant) cohort were initially treated with 2.5 and 0.2 µM BYL-719, respectively. These doses were selected referring to their respective IC25 values (**Figure 3.19**) and BYL-719 doses were increased gradually throughout a period of 10 months and capped off at 9 µM and 6 µM, respectively (**Figure 3.20**).

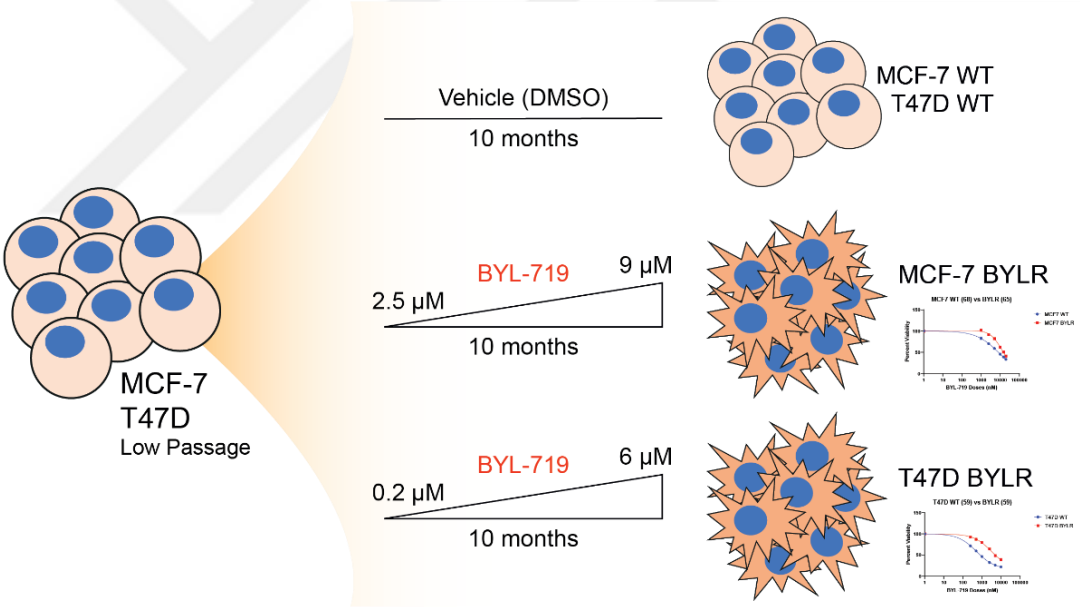

Figure 3.20. Illustration depicting BYL-719 resistant MCF and T47D cell line development process. Low passage MCF7 and T47D cells were subjected to BYL-719 treatment with increasing doses over a period of 10 months. Initial drug dose was determined based on IC25 of MC7 and T47D cells at 2.5 and 0.2 µM and capped off at 9 and 6 µM, respectively. Drug resistance was validated using SRB cell viability assay.

3.4.2 Characterization of BYL-719 Resistant Cell Line Models

After 10 months of chronic BYL-719 exposure, drug response of MCF7 and T47D BYLR cells were assessed by treating them with various doses of BYL-719 and comparing their response to their wild type counterparts using SRB cell viability assay (**Figure 3.21**). MCF7 cells more resistant to BYL-719(WT IC50: 7.3 µM). After 10 months of drug exposure, MCF BYLR cells had doubled their IC50 to around 13.8 µM (**Figure 3.21A**). T47D cell line was more sensitive to BYL-719 (WT IC50: 0.6 µM). After 10 months of drug exposure, T47D BYLR cells increased their IC50 by 5 fold to around 3 µM (**Figure 3.21B**).

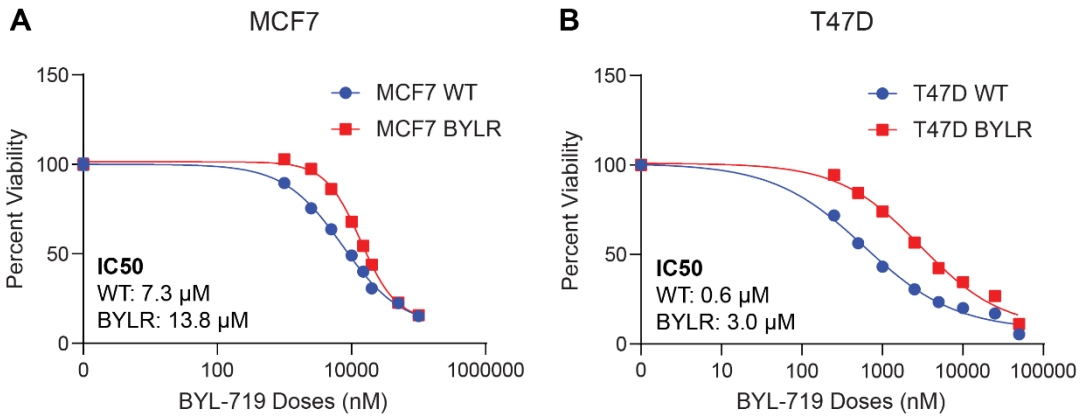

Figure 3.21. Viability curves comparing dose response of (A) MCF7 WT, BYLR and (B) T47D WT, BYLR towards BYL-719. SRB viability assay results for MCF7, T47D WT and BYLR cell lines treated with various doses of BYL-719 for 72 hours. Data points/doses used for MCF7: 1, 2.5, 5, 10, 15, 20, 50, and 100 µM. Data points/doses used for T47D: 0.25, 0.5, 1, 2.5, 5, 10, 25 and 50 µM. Cell viability was measured in triplicates.

After confirming acquired resistance these cell lines have developed with cell viability assay, we wanted to see altered signaling process between WT and BYLR cohorts. In order to identify how receptor signaling landscape have changed in our resistant cell line models, we compared expression of major receptors between wild type and resistant cells using Western blot (**Figure 3.22**). In both cell lines, EGFR expression is diminished in resistant counterparts. Moreover, we observed an increase in ER levels in resistant counterparts of both cell lines. However, rest of the receptors we examined show varying expression pattern. In MCF7 BYLR cells, EGFR and PR expression decrease, meanwhile we see a slight increase in HER2 levels. In T47D BYLR cells, HER2 and EGFR expression is decreased, meanwhile PR expression is increased.

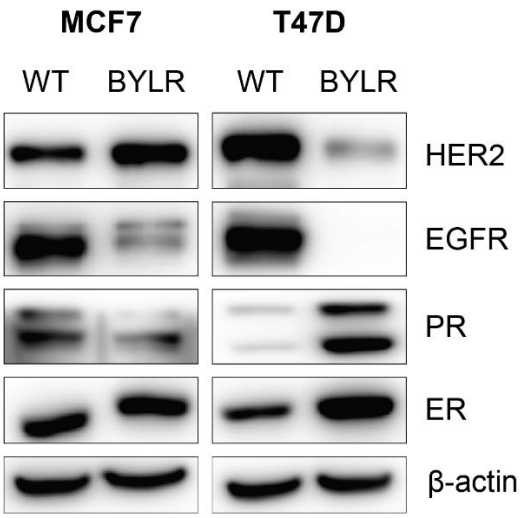

Figure 3.22. Western blot analysis of MCF7, T47D WT and BYLR cells probed with various cell surface markers. Beta-actin was used as loading control.

We were then intrigued to find how resistant cells were able to keep up with the continuous inhibitory pressure from BYL-719, so we treated MCF7 and T47D WT and BYLR cells with increasing doses of BYL-719 for 24 hours. Our Western blot analysis revealed that PI3K signaling landscape differs between WT and BYLR cells. In both resistant cell lines, AKT phosphorylations are retained even more so than their wild type counterparts as BYL-719 dose increases, more prominent in T47D BYLR cell line. AKT phosphorylation being more protected in resistant cell lines imply that resistance mechanism most likely involves AKT as well. Consequently, mTOR downstream markers like S6 and 4EBP1 also maintain active state more distinctly in BYLR cells, again most prominently in T47D BYLR cells. Out of all the markers probed, most striking effect has been observed in phosphorylation levels of 4EBP1. Overall, these results suggest that resistance to BYL-719 inhibition is also mediated through downstream components of PI3K pathway as well.

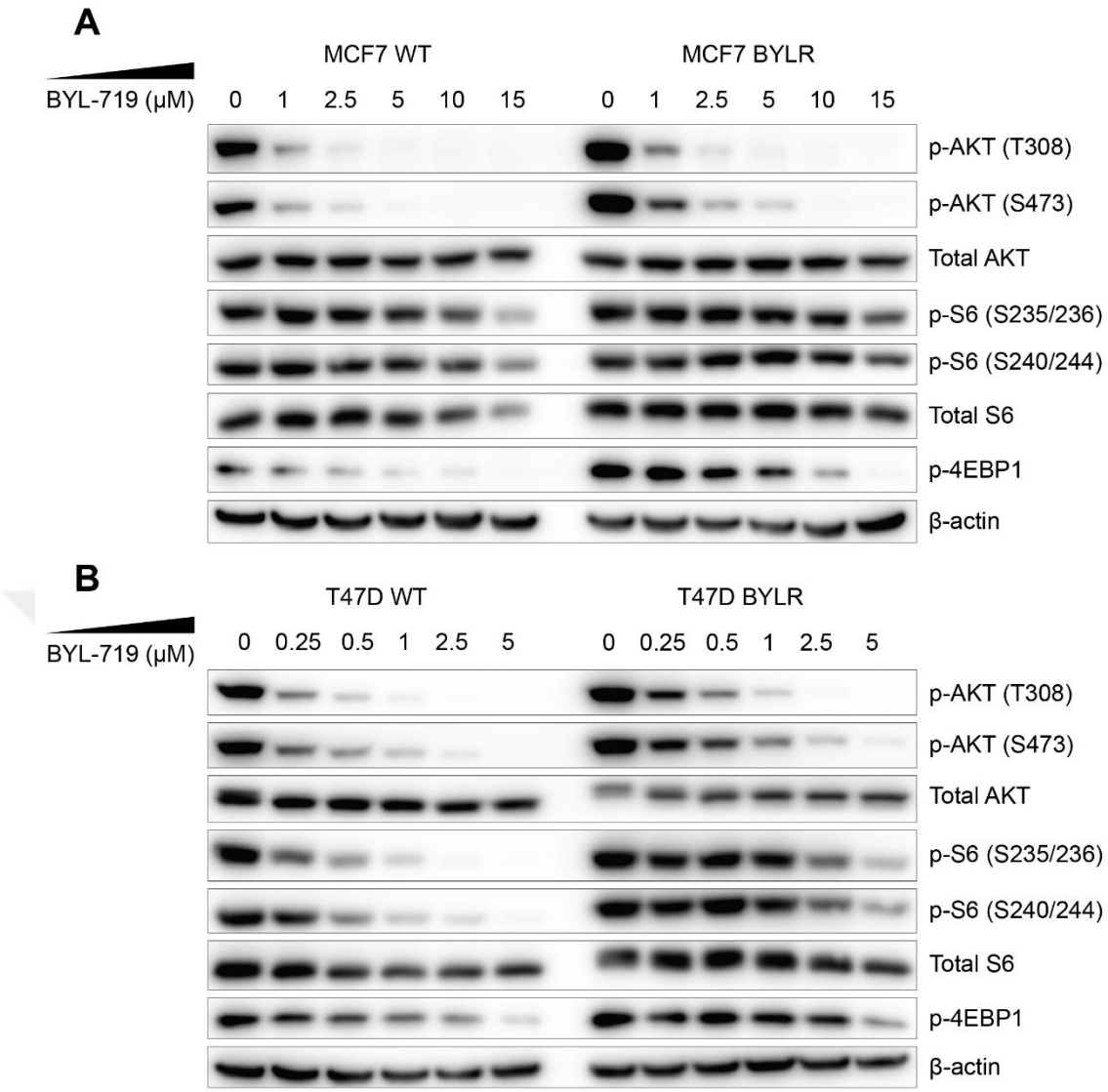

Figure 3.23. Western blot analysis showing PI3K/AKT pathway elements upon treatment with increasing doses of BYL-719 in (A) MCF7 and (B) T47D WT versus BYLR cells lines. Cells were treated with BYL-719 for 24 hours. Beta-actin was used as loading control.

We also discovered in lysates collected from cells, STK10 expression was elevated in T47D BYLR cells compared to WT counterparts (**Figure 3.24A**). Based on this finding, we questioned whether siSTK10 treatment can sensitize resistant cells to BYL-719. Indeed, combination of siSTK10 and BYL-719 led to significant increase

in percent inhibition compared to single treatment (**Figure 3.24B**). Similar with previous findings (**Figure 3.6** and **Figure 3.8**), STK10 silencing acted as a sensitizer for BYL-719 treatment. We also tested PI3K pathway markers upon combination of siSTK10 and BYL-719; however, there was no alteration in combination group compared to single treatment, again indicating possible activity of parallel pathways (data not shown). STK10 might be triggering other pathways currently unclear to us, thereby modulating response to BYL-719 inhibition.

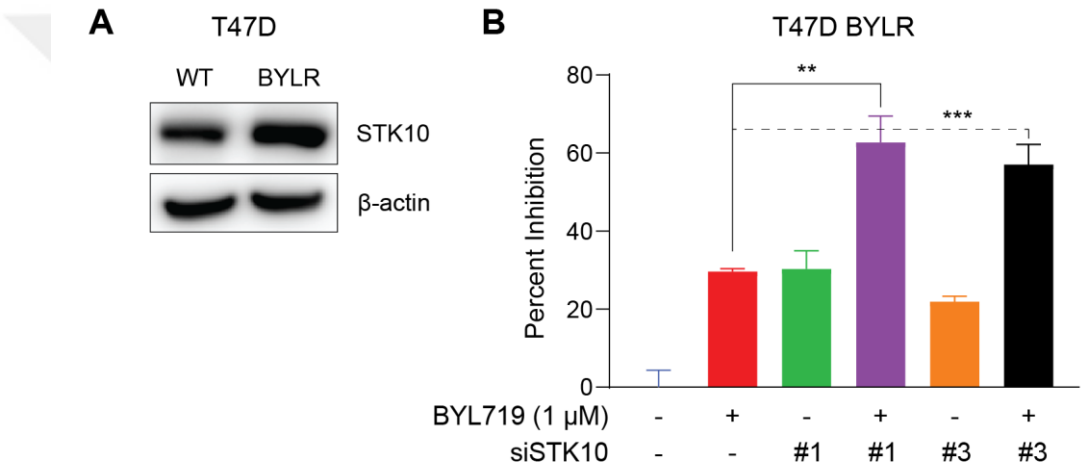

Figure 3.24. STK10 silencing sensitizes T47D BYLR cells to BYL-719 inhibition. (A) Western blot analysis of STK10 levels in T47D WT and BYLR cells. (B) SRB cell viability analysis showing percent inhibition upon either single or combination treatment of siSTK10 and BYL-719. Cell viability was measured in triplicates. Significance denoted as: *** $p<0.001$, ** $p<0.01$ and * $p<0.05$.

SUMMARY

To summarize, in our acquired BYL-719 resistance studies, we were able to develop BYL-719 resistant cell lines, as confirmed by SRB viability assays. Both MCF7 and

T47D BYLR cell lines have decreased expression of EGFR. Moreover, they can sustain AKT and mTOR downstream signaling even under inhibitory pressure of BYL-719 compared to their wild type counterparts. We also proposed two ways of sensitizing these cells to BYL-719 treatment. First, STK10 was found to be elevated in T47D BYLR cells. siRNA-mediated silencing of STK10 synergized with BYL-719 treatment and resulted in further decrease of cell viability. Secondly, we used tamoxifen, an ER antagonist, to target elevated ER expression in these cell lines,. In both cell lines we observed synergism between tamoxifen and BYL-719. Further characterization of these cell lines using RNA-seq analyses will help propel these sensitization studies even further.

CHAPTER 4

DISCUSSION

PI3K receives signals from a wide range of tyrosine kinase receptors, GPCRs, Ras and involved in wide range cellular functions, such as proliferation, survival, differentiation, chemotaxis and homeostasis [75,76]. PI3K pathway is implicated to be involved in many cancers [77]. Therefore, there has been a great effort to develop inhibitors targeting several key nodes at PI3K pathway. First generation of drugs targeting PI3K, such as Wortmannin and LY294002 never made it into clinical trials due to specificity issues and heavy side effects [78]. Over the years, more potent inhibitors have been developed. Recent development of isoform specific PI3K inhibitors helped alleviate heavy side effects observed with pan-PI3K inhibitors. However, drug resistance remains to be a major problem.

4.1 Potential Involvement of STK10 in PI3K Pathway

In our study, we initially aimed at identifying molecular targets that can modulate PIK3CA inhibition resistance in a PI3K-dependent, but AKT-independent manner. AKT has been studied extensively; therefore, identifying AKT-independent molecular targets can create novel therapeutic approaches to combat PIK3CA inhibition resistance. Recent studies also demonstrate the importance of AKT-independent mechanisms involved in PIK3CA resistance. In clinical trials, patients who do not respond well to PIK3CA inhibition, or develop resistance show increased phosphorylation of mTOR downstream targets yet having suppressed AKT phosphorylations compared to responding patients [40]. Lately, SGK1 and PIM

kinases were also identified as alternative paths that can drive PI3Kα resistance by maintaining an active mTOR downstream signal without AKT phosphorylation [46,49]. This also raises the question whether probing AKT phosphorylation can be a faithful marker of PI3K activity in patients. Clearly, an active PI3K pathway without displaying AKT phosphorylation can still propagate the signal further downstream of mTOR *via* alternative paths. Therefore, assessing phosphorylation levels of S6 as surrogate marker can be more effective in determining PI3K pathway activity than AKT [79]. Our approach to identify AKT-independent molecular targets is therefore relevant with recent findings in cell-based models and clinics.

Our bioinformatical analyses identified STK10 to be significantly upregulated in cells displaying PI3K and AKT inhibitor resistance (**Figure 3.2**). We identified STK10 to be upregulated at mRNA levels in cells resistant to PI3K and AKT inhibition. Furthermore, STK10 is a good indicator of patient survival based on METABRIC dataset. All patients, irrespective of their PIK3CA status showed poorer survival when STK10 levels were high, although biggest separation was observed in *PIK3CA* mutant patients (**Figure 3.2**).

Our wet lab experiments, on the other hand, displayed cell line-specific effects. In TNBC cell lines, MDA-MB-436 and BT20, STK10 was able to sensitize these cells to BYL-719 consistently, although mechanism of such sensitization was rather cell line-specific. In MDA-MB-436 cells we observed further decrease in phosphorylation levels of both AKT, S6 and 4EBP1 upon STK10 knockdown, indicating presence of an <u>AKT-dependent</u> mechanism of sensitization (**Figure 3.7A**). BT20 cells displayed no change in PI3K/AKT pathway components (**Figure 3.9**). This might be attributed

to baseline PIP_2 levels in these cell lines, given p-ERM activation is shown to be PIP_2-dependent [56]. One can assume that low levels of baseline PIP2 levels would lead to less efficient activation of ERM proteins. In both cell lines overexpression of STK10 failed to rescue PI3Kα specific inhibition. Even though we saw a significant increase in p-ERM levels, STK10 substrate which indicates functional STK10 overexpression, PI3K pathway was untouched. This led us to think that STK10 might not be located within the PI3K pathway at all, and the sensitization to BYL-719 inhibition might be mediated through some parallel pathways such as MAPK. We addressed this partially by stimulating HMEC and MEF cells stably expressing STK10 by insulin and EGF, which also alternatively activates MAPK on top of PI3K pathway (**Figure 3.14**) [69].

STK10 overexpression did not rescue phosphorylation levels of AKT, S6 or 4EBP1. This result is also in line with the literature. Kuramochi and colleagues identified that STK10 catalytic domain showed high homology with STE20 family proteins which are known to be involved with many MAPK cascades. When tested, STK10 failed to activate ERK2, JNK/SAPK and p38 MAPK [52]. With our stimulation experiments with insulin and EGF, we were able to cross out the possible involvement of STK10 with IR, IGF1-R and EGFR induced PI3K and MAPK cascade activation. This leaves out GPCR mediated activation of PI3K pathway. However, inducing GPCRs is a daunting task. Human genome is estimated to encode around 800-1000 different GPCR subtypes with over 200 different ligands identified to activate these receptors [80,81]. When stimulated with 4% FBS, we were able to observe a rescue of downstream targets in STK10 overexpressing MEF cells (**Figure 3.12**); however, FBS contains amino acids and multiple growth factors, activating many pathways at once,

making it impossible to pinpoint exact pathway STK10 is involved in and exerts its effect from.

The standing issue is, we are still not sure how STK10 can potentially be involved with PI3Kα resistance while displaying cell type specific effects on PI3K downstream markers. To uncover possible mechanisms of resistance STK10 might be involved in, a more direct approach must be adopted. Identifying interaction partners of STK10 using mass spectrometry will be the most robust way to unravel such mechanism of resistance and possible involvement of STK10 within the PI3K pathway. Our group is currently working on methods to identify interaction partners of STK10 by utilizing proximity labeling methods, such as APEX2 or BioID coupled to mass spectrometry. Compared to conventional affinity purification methods, biotin-based proximity labeling approaches are superior in identification of weak and transient interactions between proteins. Moreover, use of biotin ligases (BioID) or peroxidases (APEX) allow for high resolution labeling of proximal targets within a radius as small as 10 nm, thereby reducing background contaminants and increasing specificity [82–84].

Another point to consider while interpreting the data is the exact location of STK10 within the PI3K cascade. Is it directly involved in signaling, or just a transcriptional end-product of PI3K activity? **Figure 3.3** might give a clue whether STK10 is just a transcriptional product. When MCF7 and T47D cells are treated with BYL-719, STK10 levels were also found to be decreased. Similarly, **Figure 3.2C** might be hinting in the same direction. Expression of helical domain mutant *PIK3CA* (H1047R) which yields an overactive PI3 kinase, results in elevation of *STK10* mRNA levels. And consistent with **Figure 3.3**, PI3K inhibition results in a decrease of mRNA

product. Moreover, if we were to assume that PI3K pathway is more active in cells resistant to PI3K and/or AKT inhibition, we can use a similar reasoning to interpret the data in **Figure 3.2A**. Hypothetically, an active PI3K pathway in "resistant" cells can also result in more active transcription of end targets like STK10 (if we were to assume so), which is unsurprisingly elevated in "resistant" cells. To uncover this, the next step should be to thoroughly investigate STK10 promoter for binding site of familiar transcription factors, such as forkhead box proteins (FOXO), nuclear factor kappa B (NFκB) and cAMP Response Element Binding (CREB) protein [85].

Protein localization also plays an important role in proper functioning of the protein, since it dictates access to interaction partners [86]. Therefore, it is also important to ascertain whether STK10 directly localizes to plasma membrane when overexpressed. Although ERM phosphorylation upon STK10 overexpression is a confirmation of that, N-myristoylation can be utilized to target STK10 to the plasma membrane, where the kinase can unleash its full potential [87]. It will be interesting to perform similar experiments with myr-STK10 and check for any involvement with the PI3K pathway. Nevertheless, all our STK10 overexpression experiments failed to induce resistance to BYL-719 inhibition, even though we had success sensitizing cells to BYL-719 with siRNA mediated knockdown of STK10.

4.2 STK10 as a Potential Agent for Tumorigenesis

Soft agar colony formation assays measure ability of cells to grow and divide without needed to attach to extracellular matrix, also known as anchorage-independent growth. Normal cells lack such ability and undergo anoikis, a form of cell death.

Transformed cells, on the other hand, do not need extracellular matrix to divide and grow. Therefore, this assay is an easy method to evaluate cellular transformation *in vitro* [88,89]. In our experiments with HMEC and MEF cells, we observed that stable STK10 overexpression affects number of colonies compared to controls. In other words, STK10 did not increase the ability of anchorage-independent growth (**Figure 3.16**). Given soft agar colony formation assay is one of the most stringent method to test cellular transformation, we reasoned that depending on a single agent (STK10) to induce transformation might be too optimistic. Coupling STK10 overexpression with mutant *PIK3CA* expressing HMEC or MEF cells can help alleviate such issues. We, therefore, plan to perform same experiment with HMEC and MEF cells expressing mutant PIK3CA (H1047R) that are readily available in our lab and transduce them to overexpress STK10 and assess the effect of combination on cellular transformation.

We also observed that stably STK10 overexpressing HMEC and MEF cells grew more significantly than their control counterparts within a period as short as 48 hours (**Figure 3.17**). This observation is also in line with the literature. In one study, STK10 knockdown was shown to decrease cell growth in Ewing's sarcoma cell models. Off note, STK10 knockdown was also shown to induce apoptosis [90]. In addition, STK10 has been shown to interact with and phosphorylate PLK1 *in vitro* and cells expressing kinase dead version of STK10 were observed to grow more slowly [50]. Collectively, these results may suggest a role for STK10 in cell cycle progression and cell division *via* PLK1.

ERM family of proteins link actin cytoskeleton to the plasma membrane. ERM proteins when phosphorylated by many of its targeting kinases, such as protein kinase

Cα (PKCα, θ), NIK (NFκB-inducing kinase), LOK (Lymphocyte-Oriented Kinase) and MST4 [54,91–95] at conserved threonine residues near its F-actin binding site, the protein changes conformation to an open state with the help of PIP_2 [56]. At this open state, ERM proteins can also interact with cytoplasmic domains of several membrane proteins, such as CD44 and intracellular adhesion molecule (ICAM) [96], which is shown to have roles in migration and cell proliferation [97]. ERM was shown to be involved in migration at wound edges through association with PKCα. Phosphorylation of ezrin at T567 was critical in PKCα mediated migration and T567A mutation inhibited migration during wound closure [92]. To this end, we used p-ERM as an activity marker of STK10. In most cell lines, we observed consisted phosphorylation of ERM proteins upon STK10 overexpression (**Figure 3.7** and **Figure 3.11**). Based on literature, we wanted to know whether STK10 can have a role in migration through ERM proteins. To investigate this, we performed scratch assay with stably STK10 over-expressing MEF cells (**Figure 3.18**). However, we failed to observe any change in migratory capabilities of MEF cells. Moreover, STK10 overexpressing cells also did not show enhanced migration even under BYL-719 inhibition. There is also evidence in the literature confirming these results. In lymphocytes, ERM phosphorylation is associated with cellular rigidity. In cells transfected with LOK kinase domain (KD), increased ERM phosphorylation resulted in decreased lymphocyte mobility [54]. Overall, we can say that ERM mediated migration may not be propagated through STK10.

4.3 BYL-719 Resistant Cell Models to Identify Novel Mechanisms of BYL-719 Resistance

BYL-719 was approved by FDA to be used in combination with fulvestrant in hormone receptor positive, *PIK3CA* mutant patients [38]. In our study, we were able to successfully develop two BYL-719 resistant cell lines from wild-type MCF7 and T47D cells *via* chronic BYL-719 treatment (**Figure 3.20**). We validated resistance by SRB cell viability method and observed as much as 4-fold increase in IC50 in T47D cells (**Figure 3.21**). Given approval of BYL-719 in hormone receptor positive and *PIK3CA* mutant patients, these cell lines represent a perfect model to study α-specific inhibition by BYL-719 since both are Luminal A subtype and *PIK3CA* mutant.

Initial characterization experiments revealed mixed results when we look at expression levels of key receptors. Loss of EGFR can be observed in both resistant cell lines (**Figure 3.22**). This might be hinting for possible re-routing of signaling away from major receptors like EGFR and IGFR. EGFR loss has been observed in HCC827, non-small cell lung cancer cell line, which was associated with acquired resistance towards AZD9291, mutant selective EGFR inhibitor [98]. However, literature lacks possible explanations to such a case in the context of BYL-719 resistance. In addition, discrepancy between the trend observed in HER2 and PR levels might indicate different mechanisms of resistance adopted by MCF7 and T47D BYLR cells. This can partly be attributed to initiation of selection with different BYL-719 doses when generating acquired BYL-719 resistant counterparts. Given MCF7 parental cells had higher tolerance to BYL-719 inhibition (**Figure 3.19**), one might argue that use of higher BYL-719 doses to develop resistant MCF7 cells might have targeted other p110 isoforms (β, δ and γ) non-specifically due to elevated drug doses.

Whereas in T47D cells use of lower doses of BYL-719 might only be sufficient to primarily target p110α while developing resistant cells. Difference in BYL-719 doses used to generate resistant cells and therefore p110 isoforms targeted non-specifically as a result of high BYL-719 doses, as is the case with MCF7 cells, might explain adoption of different resistance mechanisms in these cell lines.

PI3K and ER pathways show high levels of crosstalk. Preclinical analyses revealed that PI3K inhibition led to upregulation of estrogen receptor [79]. In a study it was shown that inhibition of PI3Kα resulted in a compensatory mechanism where KMT2D, an epigenetic modulator often associated with open chromatin state, gets reactivated due to diminishing inhibitory AKT phosphorylations and consequently activate estrogen receptor dependent transcription [99]. In a follow up study, authors revealed that KMT2D mediated activation of ER transcriptional activity led to SGK1 transcription *via* direct promoter binding, which was also shown to substitute for AKT signaling under BYL-719 treatment and result in BYL-719 inhibitor resistance through mTOR downstream activity. Moreover, it was shown that SGK1 also phosphorylate and inactivate KMT2D, thereby inhibiting ER transcriptional activity [46,100]. Furthermore, our group have also revealed a reverse phenotype in tamoxifen resistant MCF7 and T47D cells, designated TamR. TamR cells displayed increased expression of EGFR, meanwhile showing decreased ERα expression [101]. Consistent with the literature we also observed increase in expression levels of ERα in our resistant cell lines compared to their wild type counterparts (**Figure 3.22**). One might argue about a possible shift from EGFR to ERα mediated PI3K signaling.

We also revisited a protein that we initially identified as a potential sensitizer to PI3Kα inhibition resistance. Interestingly, STK10 was found to be elevated exclusively in T47D BYLR cells compared to wild type counterparts (**Figure 3.24**). siRNA mediated knockdown of STK10 sensitized T47D BYLR cells to BYL-719. Even though our efforts failed to identify potential involvement of STK10 within the PI3K pathway, STK10 knockdown experiments we performed successfully sensitized subject cell lines to BYL-719. Therefore, it is critical to identify interaction partners of STK10 and consequently identify pathways it might mediate PI3Kα inhibitor resistance.

Further characterization experiments revealed that resistant cells are able to preserve phosphorylation of AKT, S6 and 4EBP1 under BYL-719 inhibition better compared to control cells (**Figure 3.23**). However, upstream elements implicated in such phenotype remains to be identified. Increased accessibility of RNA sequencing technology has been pivotal in identification of key transcripts involved in drug resistance [102]. Transcriptomic and proteomic analyses to be performed on these cell lines will provide new insights on BYL-719 resistance mechanisms and help identify novel molecular targets for new therapeutic approaches in combatting BYL-719 resistance in patients.

CONCLUSIONS

Overall, in our studies to identify potential molecular targets that can confer resistance to PI3Kα inhibition in a PI3K-dependent but AKT-independent manner, we identified STK10 as a potential target. Even though siRNA mediated knockdown of STK10 sensitized cells to BYL-719, we failed to prove its direct involvement in the PI3K pathway. Overexpression of STK10 also did not confer any resistance to BYL-719

inhibition nor did it induce any change in PI3K pathway components. We revealed that STK10 overexpression increased growth rate of untransformed HMEC and MEF cells. Furthermore, we developed BYL-719 resistant cell lines. STK10 was found to be elevated in one of our models, T47D BYLR. STK10 was able to sensitize these cells to BYL-719 as well.

To conclude, identification of interaction partners of STK10 *via* mass spectrometry and performing RNA-seq analyses on our resistant cell lines to identify potential transcripts that confer resistance to BYL-179 will be future studies that can develop these projects further.

BIBLIOGRAPHY

[1] Bray F, Ferlay J, Soerjomataram I, Siegel RL, Torre LA, Jemal A. Global cancer statistics 2018: GLOBOCAN estimates of incidence and mortality worldwide for 36 cancers in 185 countries. *CA Cancer J Clin*. 2018;68(6):394-424. doi:10.3322/caac.21492

[2] Siegel RL, Miller KD, Jemal A. Cancer statistics, 2020. *CA Cancer J Clin*. 2020;70(1):7-30. doi:10.3322/caac.21590

[3] Sørlie T, Perou CM, Tibshirani R, et al. Gene expression patterns of breast carcinomas distinguish tumor subclasses with clinical implications. *Proc Natl Acad Sci*. 2001;98(19):10869-10874. doi:10.1073/pnas.191367098

[4] Sørlie T, Tibshirani R, Parker J, et al. Repeated observation of breast tumor subtypes in independent gene expression data sets. *Proc Natl Acad Sci*. 2003;100(14):8418-8423. doi:10.1073/pnas.0932692100

[5] Goldhirsch A, Wood WC, Coates AS, Gelber RD, Thürlimann B, Senn H-J. Strategies for subtypes—dealing with the diversity of breast cancer: highlights of the St Gallen International Expert Consensus on the Primary Therapy of Early Breast Cancer 2011. *Ann Oncol*. 2011;22(8):1736-1747. doi:10.1093/annonc/mdr304

[6] Cheang MCU, Chia SK, Voduc D, et al. Ki67 Index, HER2 Status, and Prognosis of Patients With Luminal B Breast Cancer. *JNCI J Natl Cancer Inst*. 2009;101(10):736-750. doi:10.1093/jnci/djp082

[7] de Ronde JJ, Hannemann J, Halfwerk H, et al. Concordance of clinical and molecular breast cancer subtyping in the context of preoperative chemotherapy response. *Breast Cancer Res Treat*. 2010;119(1):119-126. doi:10.1007/s10549-009-0499-6

[8] Waks AG, Winer EP. Breast Cancer Treatment: A Review. *JAMA*. 2019;321(3):288-300. doi:10.1001/jama.2018.19323

[9] Ribnikar D, Volovat SR, Cardoso F. Targeting CDK4/6 pathways and beyond in breast cancer. *The Breast*. 2019;43:8-17. doi:10.1016/j.breast.2018.10.001

[10] Figueroa-Magalhães MC, Jelovac D, Connolly RM, Wolff AC. Treatment of HER2-positive breast cancer. *The Breast*. 2014;23(2):128-136. doi:10.1016/j.breast.2013.11.011

[11] Prat A, Pineda E, Adamo B, et al. Clinical implications of the intrinsic molecular subtypes of breast cancer. *The Breast*. 2015;24:S26-S35. doi:10.1016/j.breast.2015.07.008

[12] Denkert C, Liedtke C, Tutt A, von Minckwitz G. Molecular alterations in triple-negative breast cancer-the road to new treatment strategies. *Lancet Lond Engl*. 2017;389(10087):2430-2442. doi:10.1016/S0140-6736(16)32454-0

[13] Li Z, Qiu Y, Lu W, Jiang Y, Wang J. Immunotherapeutic interventions of Triple Negative Breast Cancer. *J Transl Med*. 2018;16. doi:10.1186/s12967-018-1514-7

[14] Mayer IA, Arteaga CL. The PI3K/AKT Pathway as a Target for Cancer Treatment. *Annu Rev Med*. 2016;67(1):11-28. doi:10.1146/annurev-med-062913-051343

[15] Guerrero-Zotano A, Mayer IA, Arteaga CL. PI3K/AKT/mTOR: role in breast cancer progression, drug resistance, and treatment. *Cancer Metastasis Rev*. 2016;35(4):515-524. doi:10.1007/s10555-016-9637-x
[16] Liu P, Cheng H, Roberts TM, Zhao JJ. Targeting the phosphoinositide 3-kinase pathway in cancer. *Nat Rev Drug Discov*. 2009;8(8):627-644. doi:10.1038/nrd2926
[17] Jia S, Roberts TM, Zhao JJ. Truncated Title: p110 isoforms in cancer. *Curr Opin Cell Biol*. 2009;21(2):199-208. doi:10.1016/j.ceb.2008.12.007
[18] Manning BD, Cantley LC. AKT/PKB Signaling: Navigating Downstream. *Cell*. 2007;129(7):1261-1274. doi:10.1016/j.cell.2007.06.009
[19] Guertin DA, Sabatini DM. Defining the role of mTOR in cancer. *Cancer Cell*. 2007;12(1):9-22. doi:10.1016/j.ccr.2007.05.008
[20] Bachman KE, Argani P, Samuels Y, et al. The PIK3CA gene is mutated with high frequency in human breast cancers. *Cancer Biol Ther*. 2004;3(8):772-775. doi:10.4161/cbt.3.8.994
[21] Stemke-Hale K, Gonzalez-Angulo AM, Lluch A, et al. An integrative genomic and proteomic analysis of PIK3CA, PTEN, and AKT mutations in breast cancer. *Cancer Res*. 2008;68(15):6084-6091. doi:10.1158/0008-5472.CAN-07-6854
[22] Campbell IG, Russell SE, Choong DYH, et al. Mutation of the PIK3CA gene in ovarian and breast cancer. *Cancer Res*. 2004;64(21):7678-7681. doi:10.1158/0008-5472.CAN-04-2933
[23] Fedele CG, Ooms LM, Ho M, et al. Inositol polyphosphate 4-phosphatase II regulates PI3K/Akt signaling and is lost in human basal-like breast cancers. *Proc Natl Acad Sci*. 2010;107(51):22231-22236. doi:10.1073/pnas.1015245107
[24] Miller TW, Rexer BN, Garrett JT, Arteaga CL. Mutations in the phosphatidylinositol 3-kinase pathway: role in tumor progression and therapeutic implications in breast cancer. *Breast Cancer Res BCR*. 2011;13(6):224. doi:10.1186/bcr3039
[25] Maurer M, Su T, Saal LH, et al. 3-Phosphoinositide-dependent kinase 1 potentiates upstream lesions on the phosphatidylinositol 3-kinase pathway in breast carcinoma. *Cancer Res*. 2009;69(15):6299-6306. doi:10.1158/0008-5472.CAN-09-0820
[26] Fu P, Ibusuki M, Yamamoto Y, et al. Insulin-like growth factor-1 receptor gene expression is associated with survival in breast cancer: a comprehensive analysis of gene copy number, mRNA and protein expression. *Breast Cancer Res Treat*. 2011;130(1):307-317. doi:10.1007/s10549-011-1605-0
[27] Law JH, Habibi G, Hu K, et al. Phosphorylated insulin-like growth factor-i/insulin receptor is present in all breast cancer subtypes and is related to poor survival. *Cancer Res*. 2008;68(24):10238-10246. doi:10.1158/0008-5472.CAN-08-2755
[28] Saal LH, Holm K, Maurer M, et al. PIK3CA mutations correlate with hormone receptors, node metastasis, and ERBB2, and are mutually exclusive with PTEN loss in human breast carcinoma. *Cancer Res*. 2005;65(7):2554-2559. doi:10.1158/0008-5472-CAN-04-3913
[29] Miled N, Yan Y, Hon W-C, et al. Mechanism of two classes of cancer mutations in the phosphoinositide 3-kinase catalytic subunit. *Science*. 2007;317(5835):239-242. doi:10.1126/science.1135394
[30] Wang L, Hu H, Pan Y, et al. PIK3CA mutations frequently coexist with EGFR/KRAS mutations in non-small cell lung cancer and suggest poor

prognosis in EGFR/KRAS wildtype subgroup. *PloS One*. 2014;9(2):e88291. doi:10.1371/journal.pone.0088291

[31] Martín M, Chan A, Dirix L, et al. A randomized adaptive phase II/III study of buparlisib, a pan-class I PI3K inhibitor, combined with paclitaxel for the treatment of HER2- advanced breast cancer (BELLE-4). *Ann Oncol Off J Eur Soc Med Oncol*. 2017;28(2):313-320. doi:10.1093/annonc/mdw562

[32] Di Leo A, Johnston S, Lee KS, et al. Buparlisib plus fulvestrant in postmenopausal women with hormone-receptor-positive, HER2-negative, advanced breast cancer progressing on or after mTOR inhibition (BELLE-3): a randomised, double-blind, placebo-controlled, phase 3 trial. *Lancet Oncol*. 2018;19(1):87-100. doi:10.1016/S1470-2045(17)30688-5

[33] Baselga J, Im S-A, Iwata H, et al. Buparlisib plus fulvestrant versus placebo plus fulvestrant in postmenopausal, hormone receptor-positive, HER2-negative, advanced breast cancer (BELLE-2): a randomised, double-blind, placebo-controlled, phase 3 trial. *Lancet Oncol*. 2017;18(7):904-916. doi:10.1016/S1470-2045(17)30376-5

[34] Bendell JC, Rodon J, Burris HA, et al. Phase I, dose-escalation study of BKM120, an oral pan-Class I PI3K inhibitor, in patients with advanced solid tumors. *J Clin Oncol Off J Am Soc Clin Oncol*. 2012;30(3):282-290. doi:10.1200/JCO.2011.36.1360

[35] Janku F, Yap TA, Meric-Bernstam F. Targeting the PI3K pathway in cancer: are we making headway? *Nat Rev Clin Oncol*. 2018;15(5):273-291. doi:10.1038/nrclinonc.2018.28

[36] Krop IE, Mayer IA, Ganju V, et al. Pictilisib for oestrogen receptor-positive, aromatase inhibitor-resistant, advanced or metastatic breast cancer (FERGI): a randomised, double-blind, placebo-controlled, phase 2 trial. *Lancet Oncol*. 2016;17(6):811-821. doi:10.1016/S1470-2045(16)00106-6

[37] Vuylsteke P, Huizing M, Petrakova K, et al. Pictilisib PI3Kinase inhibitor (a phosphatidylinositol 3-kinase [PI3K] inhibitor) plus paclitaxel for the treatment of hormone receptor-positive, HER2-negative, locally recurrent, or metastatic breast cancer: interim analysis of the multicentre, placebo-controlled, phase II randomised PEGGY study. *Ann Oncol Off J Eur Soc Med Oncol*. 2016;27(11):2059-2066. doi:10.1093/annonc/mdw320

[38] André F, Ciruelos E, Rubovszky G, et al. Alpelisib for PIK3CA-Mutated, Hormone Receptor–Positive Advanced Breast Cancer. *N Engl J Med*. Published online May 15, 2019. doi:10.1056/NEJMoa1813904

[39] Fritsch C, Huang A, Chatenay-Rivauday C, et al. Characterization of the novel and specific PI3Kα inhibitor NVP-BYL719 and development of the patient stratification strategy for clinical trials. *Mol Cancer Ther*. 2014;13(5):1117-1129. doi:10.1158/1535-7163.MCT-13-0865

[40] Elkabets M, Vora S, Juric D, et al. mTORC1 Inhibition Is Required for Sensitivity to PI3K p110α Inhibitors in PIK3CA-Mutant Breast Cancer. *Sci Transl Med*. 2013;5(196):196ra99-196ra99. doi:10.1126/scitranslmed.3005747

[41] Juric D, Castel P, Griffith M, et al. Convergent loss of PTEN leads to clinical resistance to a PI3Kα inhibitor. *Nature*. 2015;518(7538):240-244. doi:10.1038/nature13948

[42] Razavi P, Dickler MN, Shah PD, et al. Alterations in PTEN and ESR1 promote clinical resistance to alpelisib plus aromatase inhibitors. *Nat Cancer*. 2020;1(4):382-393. doi:10.1038/s43018-020-0047-1

[43] Hopkins BD, Pauli C, Du X, et al. Suppression of insulin feedback enhances the efficacy of PI3K inhibitors. *Nature*. 2018;560(7719):499-503. doi:10.1038/s41586-018-0343-4
[44] Vora SR, Juric D, Kim N, et al. CDK 4/6 Inhibitors Sensitize PIK3CA Mutant Breast Cancer to PI3K Inhibitors. *Cancer Cell*. 2014;26(1):136-149. doi:10.1016/j.ccr.2014.05.020
[45] Leroy C, Ramos P, Cornille K, et al. Activation of IGF1R/p110β/AKT/mTOR confers resistance to α-specific PI3K inhibition. *Breast Cancer Res*. 2016;18(1):41. doi:10.1186/s13058-016-0697-1
[46] Castel P, Ellis H, Bago R, et al. PDK1-SGK1 Signaling Sustains AKT-Independent mTORC1 Activation and Confers Resistance to PI3Kα Inhibition. *Cancer Cell*. 2016;30(2):229-242. doi:10.1016/j.ccell.2016.06.004
[47] Orlacchio A, Ranieri M, Brave M, et al. SGK1 Is a Critical Component of an AKT-Independent Pathway Essential for PI3K-Mediated Tumor Development and Maintenance. *Cancer Res*. 2017;77(24):6914-6926. doi:10.1158/0008-5472.CAN-17-2105
[48] Vasudevan KM, Barbie DA, Davies MA, et al. AKT-independent signaling downstream of oncogenic PIK3CA mutations in human cancer. *Cancer Cell*. 2009;16(1):21-32. doi:10.1016/j.ccr.2009.04.012
[49] Le X, Antony R, Razavi P, et al. Systematic functional characterization of resistance to PI3K inhibition in breast cancer. *Cancer Discov*. 2016;6(10):1134-1147. doi:10.1158/2159-8290.CD-16-0305
[50] Walter SA, Cutler RE, Martinez R, Gishizky M, Hill RJ. Stk10, a New Member of the Polo-like Kinase Kinase Family Highly Expressed in Hematopoietic Tissue. *J Biol Chem*. 2003;278(20):18221-18228. doi:10.1074/jbc.M212556200
[51] Kuramochi S, Matsuda Y, Okamoto M, Kitamura F, Yonekawa H, Karasuyama H. Molecular cloning of the human gene STK10 encoding lymphocyte-oriented kinase, and comparative chromosomal mapping of the human, mouse, and rat homologues. *Immunogenetics*. 1999;49(5):369-375. doi:10.1007/s002510050509
[52] Kuramochi S, Moriguchi T, Kuida K, et al. LOK Is a Novel Mouse STE20-like Protein Kinase That Is Expressed Predominantly in Lymphocytes. *J Biol Chem*. 1997;272(36):22679-22684. doi:10.1074/jbc.272.36.22679
[53] Fukumura K, Yamashita Y, Kawazu M, et al. STK10 missense mutations associated with anti-apoptotic function. *Oncol Rep*. 2013;30(4):1542-1548. doi:10.3892/or.2013.2605
[54] Belkina NV, Liu Y, Hao J-J, Karasuyama H, Shaw S. LOK is a major ERM kinase in resting lymphocytes and regulates cytoskeletal rearrangement through ERM phosphorylation. *Proc Natl Acad Sci U S A*. 2009;106(12):4707-4712. doi:10.1073/pnas.0805963106
[55] Niggli V, Rossy J. Ezrin/radixin/moesin: Versatile controllers of signaling molecules and of the cortical cytoskeleton. *Int J Biochem Cell Biol*. 2008;40(3):344-349. doi:10.1016/j.biocel.2007.02.012
[56] Pelaseyed T, Viswanatha R, Sauvanet C, Filter JJ, Goldberg ML, Bretscher A. Ezrin activation by LOK phosphorylation involves a PIP2-dependent wedge mechanism. Lappalainen P, ed. *eLife*. 2017;6:e22759. doi:10.7554/eLife.22759
[57] Pelaseyed T, Bretscher A. Regulation of actin-based apical structures on epithelial cells. *J Cell Sci*. 2018;131(20). doi:10.1242/jcs.221853

[58] Gebäck T, Schulz MMP, Koumoutsakos P, Detmar M. TScratch: a novel and simple software tool for automated analysis of monolayer wound healing assays. *BioTechniques*. 2009;46(4):265-274. doi:10.2144/000113083
[59] Daemen A, Griffith OL, Heiser LM, et al. Modeling precision treatment of breast cancer. *Genome Biol*. 2013;14(10):R110. doi:10.1186/gb-2013-14-10-r110
[60] Iorio F, Knijnenburg TA, Vis DJ, et al. A Landscape of Pharmacogenomic Interactions in Cancer. *Cell*. 2016;166(3):740-754. doi:10.1016/j.cell.2016.06.017
[61] Wallin JJ, Guan J, Edgar KA, et al. Active PI3K Pathway Causes an Invasive Phenotype Which Can Be Reversed or Promoted by Blocking the Pathway at Divergent Nodes. *PLoS ONE*. 2012;7(5). doi:10.1371/journal.pone.0036402
[62] Jia S, Roberts TM, Zhao JJ. Should individual PI3 kinase isoforms be targeted in cancer? *Curr Opin Cell Biol*. 2009;21(2):199-208. doi:10.1016/j.ceb.2008.12.007
[63] Schneck H, Blassl C, Meier-Stiegen F, et al. Analysing the mutational status of PIK3CA in circulating tumor cells from metastatic breast cancer patients. *Mol Oncol*. 2013;7(5):976-986. doi:10.1016/j.molonc.2013.07.007
[64] Saal LH, Gruvberger-Saal SK, Persson C, et al. Recurrent gross mutations of the PTEN tumor suppressor gene in breast cancers with deficient DSB repair. *Nat Genet*. 2008;40(1):102-107. doi:10.1038/ng.2007.39
[65] Yang W, Soares J, Greninger P, et al. Genomics of Drug Sensitivity in Cancer (GDSC): a resource for therapeutic biomarker discovery in cancer cells. *Nucleic Acids Res*. 2013;41(D1):D955-D961. doi:10.1093/nar/gks1111
[66] Wu G, Xing M, Mambo E, et al. Somatic mutation and gain of copy number of PIK3CA in human breast cancer. *Breast Cancer Res*. 2005;7(5):R609-R616. doi:10.1186/bcr1262
[67] Barretina J, Caponigro G, Stransky N, et al. The Cancer Cell Line Encyclopedia enables predictive modelling of anticancer drug sensitivity. *Nature*. 2012;483(7391):603-607. doi:10.1038/nature11003
[68] Singh P, Alex JM, Bast F. Insulin receptor (IR) and insulin-like growth factor receptor 1 (IGF-1R) signaling systems: novel treatment strategies for cancer. *Med Oncol*. 2013;31(1):805. doi:10.1007/s12032-013-0805-3
[69] Wee P, Wang Z. Epidermal Growth Factor Receptor Cell Proliferation Signaling Pathways. *Cancers*. 2017;9(5). doi:10.3390/cancers9050052
[70] Wang G-S, Zhu H, Bi S-J. Pathological features and prognosis of different molecular subtypes of breast cancer. *Mol Med Rep*. 2012;6(4):779-782. doi:10.3892/mmr.2012.981
[71] Pickar JH, MacNeil T, Ohleth K. SERMs: Progress and future perspectives. *Maturitas*. 2010;67(2):129-138. doi:10.1016/j.maturitas.2010.05.009
[72] Smith IE, Dowsett M. Aromatase Inhibitors in Breast Cancer. http://dx.doi.org/10.1056/NEJMra023246. doi:10.1056/NEJMra023246
[73] El Sayed R, El Jamal L, El Iskandarani S, Kort J, Abdel Salam M, Assi H. Endocrine and Targeted Therapy for Hormone-Receptor-Positive, HER2-Negative Advanced Breast Cancer: Insights to Sequencing Treatment and Overcoming Resistance Based on Clinical Trials. *Front Oncol*. 2019;9. doi:10.3389/fonc.2019.00510
[74] Ciruelos Gil EM. Targeting the PI3K/AKT/mTOR pathway in estrogen receptor-positive breast cancer. *Cancer Treat Rev*. 2014;40(7):862-871. doi:10.1016/j.ctrv.2014.03.004

[75] Katso R, Okkenhaug K, Ahmadi K, White S, Timms J, Waterfield MD. Cellular function of phosphoinositide 3-kinases: implications for development, homeostasis, and cancer. *Annu Rev Cell Dev Biol*. 2001;17:615-675. doi:10.1146/annurev.cellbio.17.1.615
[76] Martini M, Santis MCD, Braccini L, Gulluni F, Hirsch E. PI3K/AKT signaling pathway and cancer: an updated review. *Ann Med*. 2014;46(6):372-383. doi:10.3109/07853890.2014.912836
[77] Yang J, Nie J, Ma X, Wei Y, Peng Y, Wei X. Targeting PI3K in cancer: mechanisms and advances in clinical trials. *Mol Cancer*. 2019;18(1):26. doi:10.1186/s12943-019-0954-x
[78] Cleary JM, Shapiro GI. Development of Phosphoinositide-3 Kinase Pathway Inhibitors for Advanced Cancer. *Curr Oncol Rep*. 2010;12(2). doi:10.1007/s11912-010-0091-6
[79] Vasan N, Toska E, Scaltriti M. Overview of the relevance of PI3K pathway in HR-positive breast cancer. *Ann Oncol*. 2019;30:x3-x11. doi:10.1093/annonc/mdz281
[80] New DC, Wu K, Kwok AWS, Wong YH. G protein-coupled receptor-induced Akt activity in cellular proliferation and apoptosis. *FEBS J*. 2007;274(23):6025-6036. doi:https://doi.org/10.1111/j.1742-4658.2007.06116.x
[81] Pierce KL, Premont RT, Lefkowitz RJ. Seven-transmembrane receptors. *Nat Rev Mol Cell Biol*. 2002;3(9):639-650. doi:10.1038/nrm908
[82] Multidimensional Tracking of GPCR Signaling via Peroxidase-Catalyzed Proximity Labeling - ScienceDirect. Accessed November 9, 2020. https://www.sciencedirect.com/science/article/pii/S0092867417303471?via%3Dihub
[83] Firat-Karalar EN, Stearns T. Chapter 9 - Probing mammalian centrosome structure using BioID proximity-dependent biotinylation. In: Basto R, Oegema K, eds. *Methods in Cell Biology*. Vol 129. Centrosome & Centriole. Academic Press; 2015:153-170. doi:10.1016/bs.mcb.2015.03.016
[84] Trinkle-Mulcahy L. Recent advances in proximity-based labeling methods for interactome mapping. *F1000Research*. 2019;8:135. doi:10.12688/f1000research.16903.1
[85] Mantamadiotis T. Towards Targeting PI3K-Dependent Regulation of Gene Expression in Brain Cancer. *Cancers*. 2017;9(6). doi:10.3390/cancers9060060
[86] Scott MS, Calafell SJ, Thomas DY, Hallett MT. Refining Protein Subcellular Localization. *PLoS Comput Biol*. 2005;1(6). doi:10.1371/journal.pcbi.0010066
[87] Farazi TA, Waksman G, Gordon JI. The Biology and Enzymology of ProteinN-Myristoylation. *J Biol Chem*. 2001;276(43):39501-39504. doi:10.1074/jbc.R100042200
[88] Borowicz S, Van Scoyk M, Avasarala S, et al. The Soft Agar Colony Formation Assay. *J Vis Exp JoVE*. 2014;(92). doi:10.3791/51998
[89] Taddei ML, Giannoni E, Fiaschi T, Chiarugi P. Anoikis: an emerging hallmark in health and diseases. *J Pathol*. 2012;226(2):380-393. doi:10.1002/path.3000
[90] Arora S, Gonzales IM, Hagelstrom RT, et al. RNAi phenotype profiling of kinases identifies potential therapeutic targets in Ewing's sarcoma. *Mol Cancer*. 2010;9:218. doi:10.1186/1476-4598-9-218
[91] Pietromonaco SF, Simons PC, Altman A, Elias L. Protein kinase C-theta phosphorylation of moesin in the actin-binding sequence. *J Biol Chem*. 1998;273(13):7594-7603. doi:10.1074/jbc.273.13.7594

[92] Ng T, Parsons M, Hughes WE, et al. Ezrin is a downstream effector of trafficking PKC-integrin complexes involved in the control of cell motility. *EMBO J*. 2001;20(11):2723-2741. doi:10.1093/emboj/20.11.2723
[93] Baumgartner M, Sillman AL, Blackwood EM, et al. The Nck-interacting kinase phosphorylates ERM proteins for formation of lamellipodium by growth factors. *Proc Natl Acad Sci U S A*. 2006;103(36):13391-13396. doi:10.1073/pnas.0605950103
[94] ten Klooster JP, Jansen M, Yuan J, et al. Mst4 and Ezrin induce brush borders downstream of the Lkb1/Strad/Mo25 polarization complex. *Dev Cell*. 2009;16(4):551-562. doi:10.1016/j.devcel.2009.01.016
[95] Arpin M, Chirivino D, Naba A, Zwaenepoel I. Emerging role for ERM proteins in cell adhesion and migration. *Cell Adhes Migr*. 2011;5(2):199-206. doi:10.4161/cam.5.2.15081
[96] Yonemura S, Hirao M, Doi Y, et al. Ezrin/Radixin/Moesin (ERM) Proteins Bind to a Positively Charged Amino Acid Cluster in the Juxta-Membrane Cytoplasmic Domain of CD44, CD43, and ICAM-2. *J Cell Biol*. 1998;140(4):885-895. doi:10.1083/jcb.140.4.885
[97] Nam K, Oh S, Lee K, Yoo S, Shin I. CD44 regulates cell proliferation, migration, and invasion via modulation of c-Src transcription in human breast cancer cells. *Cell Signal*. 2015;27(9):1882-1894. doi:10.1016/j.cellsig.2015.05.002
[98] Xu J, Zhao X, He D, et al. Loss of EGFR confers acquired resistance to AZD9291 in an EGFR-mutant non-small cell lung cancer cell line with an epithelial-mesenchymal transition phenotype. *J Cancer Res Clin Oncol*. 2018;144(8):1413-1422. doi:10.1007/s00432-018-2668-7
[99] Toska E, Osmanbeyoglu HU, Castel P, et al. PI3K pathway regulates ER-dependent transcription in breast cancer through the epigenetic regulator KMT2D. *Science*. 2017;355(6331):1324-1330. doi:10.1126/science.aah6893
[100] Toska E, Castel P, Chhangawala S, et al. PI3K Inhibition Activates SGK1 via a Feedback Loop to Promote Chromatin-Based Regulation of ER-Dependent Gene Expression. *Cell Rep*. 2019;27(1):294-306.e5. doi:10.1016/j.celrep.2019.02.111
[101] Mishra RR, Belder N, Ansari SA, et al. Reactivation of cAMP Pathway by PDE4D Inhibition Represents a Novel Druggable Axis for Overcoming Tamoxifen Resistance in ER-positive Breast Cancer. *Clin Cancer Res Off J Am Assoc Cancer Res*. 2018;24(8):1987-2001. doi:10.1158/1078-0432.CCR-17-2776
[102] Stark R, Grzelak M, Hadfield J. RNA sequencing: the teenage years. *Nat Rev Genet*. 2019;20(11):631-656. doi:10.1038/s41576-019-0150-2

APPENDIX

COPYRIGHT PERMISSIONS

Copyright permission for Figure 1.1

JOHN WILEY AND SONS LICENSE
TERMS AND CONDITIONS

Nov 26, 2020

This Agreement between İhsan Doğramacı Bilkent Üniversitesi -- Oğuzhan Tarman ("You") and John Wiley and Sons ("John Wiley and Sons") consists of your license details and the terms and conditions provided by John Wiley and Sons and Copyright Clearance Center.

License Number	4956381469525
License date	Nov 26, 2020
Licensed Content Publisher	John Wiley and Sons
Licensed Content Publication	CA: Cancer Journal for Clinicians
Licensed Content Title	Cancer statistics, 2020
Licensed Content Author	Rebecca L. Siegel, Kimberly D. Miller, Ahmedin Jemal
Licensed Content Date	Jan 8, 2020
Licensed Content Volume	70
Licensed Content Issue	1
Licensed Content Pages	24

Type of use	Dissertation/Thesis
Requestor type	University/Academic
Format	Print and electronic
Portion	Figure/table
Number of figures/tables	1
Will you be translating?	No
Title	INVESTIGATION OF RESISTANCE MECHANISMS IN RESPONSE TO PIK3CA INHIBITION IN BREAST CANCER
Institution name	Bilkent University
Expected presentation date	Dec 2020
Portions	Figure 1
Requestor Location	İhsan Doğramacı Bilkent Üniversitesi Üniversiteler, 06800 Çankaya/Ankara Ankara, 06800 Turkey Attn: İhsan Doğramacı Bilkent Üniversitesi
Publisher Tax ID	EU826007151
Total	0.00 USD

Terms and Conditions

TERMS AND CONDITIONS

This copyrighted material is owned by or exclusively licensed to John Wiley & Sons, Inc. or one of its group companies (each a"Wiley Company") or handled on behalf of a society with which a Wiley Company has exclusive publishing rights in relation to a particular work (collectively "WILEY"). By clicking "accept" in connection with completing this licensing transaction, you agree that the following terms and conditions apply to this transaction (along with the billing and payment terms and conditions established by the Copyright Clearance Center Inc., ("CCC's Billing and Payment terms and conditions"), at the time that you opened your RightsLink account (these are available at any time at http://myaccount.copyright.com).

Terms and Conditions

- The materials you have requested permission to reproduce or reuse (the "Wiley Materials") are protected by copyright.

- You are hereby granted a personal, non-exclusive, non-sub licensable (on a stand-alone basis), non-transferable, worldwide, limited license to reproduce the Wiley Materials for the purpose specified in the licensing process. This license, **and any CONTENT (PDF or image file) purchased as part of your order,** is for a one-time use only and limited to any maximum distribution number specified in the license. The first instance of republication or reuse granted by this license must be completed within two years of the date of the grant of this license (although copies prepared before the end date may be distributed thereafter). The Wiley Materials shall not be used in any other manner or for any other purpose, beyond what is granted in the license. Permission is granted subject to an appropriate acknowledgement given to the author, title of the material/book/journal and the publisher. You shall also duplicate the copyright notice that appears in the Wiley publication in your use of the Wiley Material. Permission is also granted on the understanding that nowhere in the text is a previously published source acknowledged for all or part of this Wiley Material. Any third party content is expressly excluded from this permission.

- With respect to the Wiley Materials, all rights are reserved. Except as expressly granted by the terms of the license, no part of the Wiley Materials may be copied, modified, adapted (except for minor reformatting required by the new Publication), translated, reproduced, transferred or distributed, in any form or by any means, and no derivative works may be made based on the Wiley Materials without the prior permission of the respective copyright owner.**For STM Signatory Publishers clearing permission under the terms of the STM Permissions Guidelines only, the terms of the license are extended to include subsequent editions and for editions in other languages, provided such editions are for the work as a whole in situ and does not involve the separate exploitation of the permitted figures or extracts,** You may not alter, remove or suppress in any manner any copyright, trademark or other notices displayed by the Wiley Materials. You may not license, rent, sell, loan, lease, pledge, offer as security, transfer or assign the Wiley Materials on a stand-alone basis, or any of the rights granted to you hereunder to any other person.

- The Wiley Materials and all of the intellectual property rights therein shall at all times remain the exclusive property of John Wiley & Sons Inc, the Wiley Companies, or their respective licensors, and your interest therein is only that of having possession of and the right to reproduce the Wiley Materials pursuant to Section 2 herein during the continuance of this Agreement. You agree that you own no right, title or interest in or to the Wiley Materials or any of the intellectual property rights therein. You shall have no rights hereunder other than the license as provided for above in Section 2. No right,

license or interest to any trademark, trade name, service mark or other branding ("Marks") of WILEY or its licensors is granted hereunder, and you agree that you shall not assert any such right, license or interest with respect thereto

- NEITHER WILEY NOR ITS LICENSORS MAKES ANY WARRANTY OR REPRESENTATION OF ANY KIND TO YOU OR ANY THIRD PARTY, EXPRESS, IMPLIED OR STATUTORY, WITH RESPECT TO THE MATERIALS OR THE ACCURACY OF ANY INFORMATION CONTAINED IN THE MATERIALS, INCLUDING, WITHOUT LIMITATION, ANY IMPLIED WARRANTY OF MERCHANTABILITY, ACCURACY, SATISFACTORY QUALITY, FITNESS FOR A PARTICULAR PURPOSE, USABILITY, INTEGRATION OR NON-INFRINGEMENT AND ALL SUCH WARRANTIES ARE HEREBY EXCLUDED BY WILEY AND ITS LICENSORS AND WAIVED BY YOU.

- WILEY shall have the right to terminate this Agreement immediately upon breach of this Agreement by you.

- You shall indemnify, defend and hold harmless WILEY, its Licensors and their respective directors, officers, agents and employees, from and against any actual or threatened claims, demands, causes of action or proceedings arising from any breach of this Agreement by you.

- IN NO EVENT SHALL WILEY OR ITS LICENSORS BE LIABLE TO YOU OR ANY OTHER PARTY OR ANY OTHER PERSON OR ENTITY FOR ANY SPECIAL, CONSEQUENTIAL, INCIDENTAL, INDIRECT, EXEMPLARY OR PUNITIVE DAMAGES, HOWEVER CAUSED, ARISING OUT OF OR IN CONNECTION WITH THE DOWNLOADING, PROVISIONING, VIEWING OR USE OF THE MATERIALS REGARDLESS OF THE FORM OF ACTION, WHETHER FOR BREACH OF CONTRACT, BREACH OF WARRANTY, TORT, NEGLIGENCE, INFRINGEMENT OR OTHERWISE (INCLUDING, WITHOUT LIMITATION, DAMAGES BASED ON LOSS OF PROFITS, DATA, FILES, USE, BUSINESS OPPORTUNITY OR CLAIMS OF THIRD PARTIES), AND WHETHER OR NOT THE PARTY HAS BEEN ADVISED OF THE POSSIBILITY OF SUCH DAMAGES. THIS LIMITATION SHALL APPLY NOTWITHSTANDING ANY FAILURE OF ESSENTIAL PURPOSE OF ANY LIMITED REMEDY PROVIDED HEREIN.

- Should any provision of this Agreement be held by a court of competent jurisdiction to be illegal, invalid, or unenforceable, that provision shall be deemed amended to achieve as nearly as possible the same economic effect as the original provision, and the legality, validity and enforceability of the remaining provisions of this Agreement shall not be affected or impaired thereby.

- The failure of either party to enforce any term or condition of this Agreement shall not constitute a waiver of either party's right to enforce each and every term and condition of this Agreement. No breach under this agreement shall be deemed waived or excused by either party unless such waiver or consent is in writing signed by the party granting such waiver or consent. The waiver by or consent of a party to a breach of any provision of this Agreement shall not operate or be construed as a waiver of or consent to any other or subsequent breach by such other party.

- This Agreement may not be assigned (including by operation of law or otherwise) by you without WILEY's prior written consent.

- Any fee required for this permission shall be non-refundable after thirty (30) days from receipt by the CCC.
- These terms and conditions together with CCC's Billing and Payment terms and conditions (which are incorporated herein) form the entire agreement between you and WILEY concerning this licensing transaction and (in the absence of fraud) supersedes all prior agreements and representations of the parties, oral or written. This Agreement may not be amended except in writing signed by both parties. This Agreement shall be binding upon and inure to the benefit of the parties' successors, legal representatives, and authorized assigns.
- In the event of any conflict between your obligations established by these terms and conditions and those established by CCC's Billing and Payment terms and conditions, these terms and conditions shall prevail.
- WILEY expressly reserves all rights not specifically granted in the combination of (i) the license details provided by you and accepted in the course of this licensing transaction, (ii) these terms and conditions and (iii) CCC's Billing and Payment terms and conditions.
- This Agreement will be void if the Type of Use, Format, Circulation, or Requestor Type was misrepresented during the licensing process.
- This Agreement shall be governed by and construed in accordance with the laws of the State of New York, USA, without regards to such state's conflict of law rules. Any legal action, suit or proceeding arising out of or relating to these Terms and Conditions or the breach thereof shall be instituted in a court of competent jurisdiction in New York County in the State of New York in the United States of America and each party hereby consents and submits to the personal jurisdiction of such court, waives any objection to venue in such court and consents to service of process by registered or certified mail, return receipt requested, at the last known address of such party.

WILEY OPEN ACCESS TERMS AND CONDITIONS

Wiley Publishes Open Access Articles in fully Open Access Journals and in Subscription journals offering Online Open. Although most of the fully Open Access journals publish open access articles under the terms of the Creative Commons Attribution (CC BY) License only, the subscription journals and a few of the Open Access Journals offer a choice of Creative Commons Licenses. The license type is clearly identified on the article.

The Creative Commons Attribution License

The Creative Commons Attribution License (CC-BY) allows users to copy, distribute and transmit an article, adapt the article and make commercial use of the article. The CC-BY license permits commercial and non-

Creative Commons Attribution Non-Commercial License

The Creative Commons Attribution Non-Commercial (CC-BY-NC)License permits use, distribution and reproduction in any medium, provided the original work is properly cited and is not used for commercial purposes.(see below)

Creative Commons Attribution-Non-Commercial-NoDerivs License

The Creative Commons Attribution Non-Commercial-NoDerivs License (CC-BY-NC-ND) permits use, distribution and reproduction in any medium, provided the original work is properly cited, is not used for commercial purposes and no modifications or adaptations are made. (see below)

Use by commercial "for-profit" organizations

Use of Wiley Open Access articles for commercial, promotional, or marketing purposes requires further explicit permission from Wiley and will be subject to a fee.

Further details can be found on Wiley Online Library
http://olabout.wiley.com/WileyCDA/Section/id-410895.html

Other Terms and Conditions:

v1.10 Last updated September 2015

Questions? customercare@copyright.com or +1-855-239-3415 (toll free in the US) or +1-978-646-2777.

Copyright permission for Figure 1.2

Copyright Clearance Center Marketplace™

Annual Reviews, Inc. - License Terms and Conditions

This is a License Agreement between Oğuzhan Tarman ("You") and Annual Reviews, Inc. ("Publisher") provided by Copyright Clearance Center ("CCC"). The license consists of your order details, the terms and conditions provided by Annual Reviews, Inc., and the CCC terms and conditions.

All payments must be made in full to CCC.

Order Date	26-Nov-2020	Type of Use	Republish in a thesis/dissertation
Order license ID	1080078-1		
ISSN	1545-326X	Publisher	ANNUAL REVIEWS
		Portion	Chart/graph/table/figure

LICENSED CONTENT

Publication Title	Annual review of medicine	Rightsholder	Annual Reviews, Inc.
Date	01/01/1950	Publication Type	e-Journal
Language	English	URL	http://arjournals.annualreviews.org/loi/med
Country	United States of America		

REQUEST DETAILS

Portion Type	Chart/graph/table/figure	Distribution	Worldwide
Number of charts / graphs / tables / figures requested	1	Translation	Original language of publication
		Copies for the disabled?	No
Format (select all that apply)	Print, Electronic	Minor editing privileges?	No
Who will republish the content?	Academic institution	Incidental promotional use?	No
Duration of Use	Life of current edition	Currency	USD
Lifetime Unit Quantity	Up to 499		
Rights Requested	Main product		

NEW WORK DETAILS

Title	INVESTIGATION OF RESISTANCE MECHANISMS IN RESPONSE TO PIK3CA INHIBITION IN BREAST CANCER	Institution name	Bilkent University
		Expected presentation date	2020-12-09
Instructor name	Onur Çizmecioğlu		

ADDITIONAL DETAILS

Order reference number	N/A	The requesting person / organization to appear on the license	Oğuzhan Tarman

REUSE CONTENT DETAILS

Title, description or numeric reference of the portion(s)	The PI3K/AKT Pathway as a Target for Cancer Treatment	**Title of the article/chapter the portion is from**	The PI3K/AKT Pathway as a Target for Cancer Treatment
Editor of portion(s)	N/A	**Author of portion(s)**	Ingrid A. Mayer, Carlos L. Arteaga
Volume of serial or monograph	67, 2016	**Issue, if republishing an article from a serial**	N/A
Page or page range of portion	11-28	**Publication date of portion**	2016-01-01

CCC Republication Terms and Conditions

1. Description of Service; Defined Terms. This Republication License enables the User to obtain licenses for republication of one or more copyrighted works as described in detail on the relevant Order Confirmation (the "Work(s)"). Copyright Clearance Center, Inc. ("CCC") grants licenses through the Service on behalf of the rightsholder identified on the Order Confirmation (the "Rightsholder"). "Republication", as used herein, generally means the inclusion of a Work, in whole or in part, in a new work or works, also as described on the Order Confirmation. "User", as used herein, means the person or entity making such republication.

2. The terms set forth in the relevant Order Confirmation, and any terms set by the Rightsholder with respect to a particular Work, govern the terms of use of Works in connection with the Service. By using the Service, the person transacting for a republication license on behalf of the User represents and warrants that he/she/it (a) has been duly authorized by the User to accept, and hereby does accept, all such terms and conditions on behalf of User, and (b) shall inform User of all such terms and conditions. In the event such person is a "freelancer" or other third party independent of User and CCC, such party shall be deemed jointly a "User" for purposes of these terms and conditions. In any event, User shall be deemed to have accepted and agreed to all such terms and conditions if User republishes the Work in any fashion.

3. Scope of License; Limitations and Obligations.

   3.1. All Works and all rights therein, including copyright rights, remain the sole and exclusive property of the Rightsholder. The license created by the exchange of an Order Confirmation (and/or any invoice) and payment by User of the full amount set forth on that document includes only those rights expressly set forth in the Order Confirmation and in these terms and conditions, and conveys no other rights in the Work(s) to User. All rights not expressly granted are hereby reserved.

   3.2. General Payment Terms: You may pay by credit card or through an account with us payable at the end of the month. If you and we agree that you may establish a standing account with CCC, then the following terms apply: Remit Payment to: Copyright Clearance Center, 29118 Network Place, Chicago, IL 60673-1291. Payments Due: Invoices are payable upon their delivery to you (or upon our notice to you that they are available to you for downloading). After 30 days, outstanding amounts will be subject to a service charge of 1-1/2% per month or, if less, the maximum rate allowed by applicable law. Unless otherwise specifically set forth in the Order Confirmation or in a separate written agreement signed by CCC, invoices are due and payable on "net 30" terms. While User may exercise the rights licensed immediately upon issuance of the Order Confirmation, the license is automatically revoked and is null and void, as if it had never been issued, if complete payment for the license is not received on a timely basis either from User directly or through a payment agent, such as a credit card company.

   3.3. Unless otherwise provided in the Order Confirmation, any grant of rights to User (i) is "one-time" (including the editions and product family specified in the license), (ii) is non-exclusive and non-transferable and (iii) is subject to any and all limitations and restrictions (such as, but not limited to, limitations on duration of use or circulation) included in the Order Confirmation or invoice and/or in these terms and conditions. Upon completion of the licensed use, User shall either secure a new permission for further use of the

Work(s) or immediately cease any new use of the Work(s) and shall render inaccessible (such as by deleting or by removing or severing links or other locators) any further copies of the Work (except for copies printed on paper in accordance with this license and still in User's stock at the end of such period).

3.4. In the event that the material for which a republication license is sought includes third party materials (such as photographs, illustrations, graphs, inserts and similar materials) which are identified in such material as having been used by permission, User is responsible for identifying, and seeking separate licenses (under this Service or otherwise) for, any of such third party materials; without a separate license, such third party materials may not be used.

3.5. Use of proper copyright notice for a Work is required as a condition of any license granted under the Service. Unless otherwise provided in the Order Confirmation, a proper copyright notice will read substantially as follows: "Republished with permission of [Rightsholder's name], from [Work's title, author, volume, edition number and year of copyright]; permission conveyed through Copyright Clearance Center, Inc. " Such notice must be provided in a reasonably legible font size and must be placed either immediately adjacent to the Work as used (for example, as part of a by-line or footnote but not as a separate electronic link) or in the place where substantially all other credits or notices for the new work containing the republished Work are located. Failure to include the required notice results in loss to the Rightsholder and CCC, and the User shall be liable to pay liquidated damages for each such failure equal to twice the use fee specified in the Order Confirmation, in addition to the use fee itself and any other fees and charges specified.

3.6. User may only make alterations to the Work if and as expressly set forth in the Order Confirmation. No Work may be used in any way that is defamatory, violates the rights of third parties (including such third parties' rights of copyright, privacy, publicity, or other tangible or intangible property), or is otherwise illegal, sexually explicit or obscene. In addition, User may not conjoin a Work with any other material that may result in damage to the reputation of the Rightsholder. User agrees to inform CCC if it becomes aware of any infringement of any rights in a Work and to cooperate with any reasonable request of CCC or the Rightsholder in connection therewith.

4. Indemnity. User hereby indemnifies and agrees to defend the Rightsholder and CCC, and their respective employees and directors, against all claims, liability, damages, costs and expenses, including legal fees and expenses, arising out of any use of a Work beyond the scope of the rights granted herein, or any use of a Work which has been altered in any unauthorized way by User, including claims of defamation or infringement of rights of copyright, publicity, privacy or other tangible or intangible property.

5. Limitation of Liability. UNDER NO CIRCUMSTANCES WILL CCC OR THE RIGHTSHOLDER BE LIABLE FOR ANY DIRECT, INDIRECT, CONSEQUENTIAL OR INCIDENTAL DAMAGES (INCLUDING WITHOUT LIMITATION DAMAGES FOR LOSS OF BUSINESS PROFITS OR INFORMATION, OR FOR BUSINESS INTERRUPTION) ARISING OUT OF THE USE OR INABILITY TO USE A WORK, EVEN IF ONE OF THEM HAS BEEN ADVISED OF THE POSSIBILITY OF SUCH DAMAGES. In any event, the total liability of the Rightsholder and CCC (including their respective employees and directors) shall not exceed the total amount actually paid by User for this license. User assumes full liability for the actions and omissions of its principals, employees, agents, affiliates, successors and assigns.

6. Limited Warranties. THE WORK(S) AND RIGHT(S) ARE PROVIDED "AS IS". CCC HAS THE RIGHT TO GRANT TO USER THE RIGHTS GRANTED IN THE ORDER CONFIRMATION DOCUMENT. CCC AND THE RIGHTSHOLDER DISCLAIM ALL OTHER WARRANTIES RELATING TO THE WORK(S) AND RIGHT(S), EITHER EXPRESS OR IMPLIED, INCLUDING WITHOUT LIMITATION IMPLIED WARRANTIES OF MERCHANTABILITY OR FITNESS FOR A PARTICULAR PURPOSE. ADDITIONAL RIGHTS MAY BE REQUIRED TO USE ILLUSTRATIONS, GRAPHS, PHOTOGRAPHS, ABSTRACTS, INSERTS OR OTHER PORTIONS OF THE WORK (AS OPPOSED TO THE ENTIRE WORK) IN A MANNER CONTEMPLATED BY USER; USER UNDERSTANDS AND AGREES THAT NEITHER CCC NOR THE RIGHTSHOLDER MAY HAVE SUCH ADDITIONAL RIGHTS TO GRANT.

7. Effect of Breach. Any failure by User to pay any amount when due, or any use by User of a Work beyond the scope of the license set forth in the Order Confirmation and/or these terms and conditions, shall be a material breach of

the license created by the Order Confirmation and these terms and conditions. Any breach not cured within 30 days of written notice thereof shall result in immediate termination of such license without further notice. Any unauthorized (but licensable) use of a Work that is terminated immediately upon notice thereof may be liquidated by payment of the Rightsholder's ordinary license price therefor; any unauthorized (and unlicensable) use that is not terminated immediately for any reason (including, for example, because materials containing the Work cannot reasonably be recalled) will be subject to all remedies available at law or in equity, but in no event to a payment of less than three times the Rightsholder's ordinary license price for the most closely analogous licensable use plus Rightsholder's and/or CCC's costs and expenses incurred in collecting such payment.

8. Miscellaneous.

8.1. User acknowledges that CCC may, from time to time, make changes or additions to the Service or to these terms and conditions, and CCC reserves the right to send notice to the User by electronic mail or otherwise for the purposes of notifying User of such changes or additions; provided that any such changes or additions shall not apply to permissions already secured and paid for.

8.2. Use of User-related information collected through the Service is governed by CCC's privacy policy, available online here:https://marketplace.copyright.com/rs-ui-web/mp/privacy-policy

8.3. The licensing transaction described in the Order Confirmation is personal to User. Therefore, User may not assign or transfer to any other person (whether a natural person or an organization of any kind) the license created by the Order Confirmation and these terms and conditions or any rights granted hereunder; provided, however, that User may assign such license in its entirety on written notice to CCC in the event of a transfer of all or substantially all of User's rights in the new material which includes the Work(s) licensed under this Service.

8.4. No amendment or waiver of any terms is binding unless set forth in writing and signed by the parties. The Rightsholder and CCC hereby object to any terms contained in any writing prepared by the User or its principals, employees, agents or affiliates and purporting to govern or otherwise relate to the licensing transaction described in the Order Confirmation, which terms are in any way inconsistent with any terms set forth in the Order Confirmation and/or in these terms and conditions or CCC's standard operating procedures, whether such writing is prepared prior to, simultaneously with or subsequent to the Order Confirmation, and whether such writing appears on a copy of the Order Confirmation or in a separate instrument.

8.5. The licensing transaction described in the Order Confirmation document shall be governed by and construed under the law of the State of New York, USA, without regard to the principles thereof of conflicts of law. Any case, controversy, suit, action, or proceeding arising out of, in connection with, or related to such licensing transaction shall be brought, at CCC's sole discretion, in any federal or state court located in the County of New York, State of New York, USA, or in any federal or state court whose geographical jurisdiction covers the location of the Rightsholder set forth in the Order Confirmation. The parties expressly submit to the personal jurisdiction and venue of each such federal or state court.If you have any comments or questions about the Service or Copyright Clearance Center, please contact us at 978-750-8400 or send an e-mail to support@copyright.com.

v 1.1